

SOUTHAMPTON OCEANOGRAPHY CENTRE

CRUISE REPORT No. 39

RRS CHARLES DARWIN CRUISE 135

24 OCT - 18 NOV 2001

ATSR validation cruise:
Seychelles - Durban

Principal Scientist
R W Pascal

2002

Ocean Engineering Division
Southampton Oceanography Centre
University of Southampton
Waterfront Campus
European Way
Southampton
Hants SO14 3ZH
UK

Tel: +44 (0)23 8059 6138
Fax: +44 (0)23 8059 6149
Email: Robin.Pascal@soc.soton.ac.uk

DOCUMENT DATA SHEET

| | |
|--|---------------------------------|
| AUTHOR PASCAL, R W et al | PUBLICATION DATE 2002 |
| TITLE RRS <i>Charles Darwin</i> Cruise 135, 24 Oct-18 Nov 2001. ATSR validation cruise: Seychelles - Durban. | |
| REFERENCE Southampton Oceanography Centre Cruise Report, No. 39, 78pp. | |
| ABSTRACT <p>This report describes RRS <i>Charles Darwin</i> Cruise 135, an ATSR satellite validation cruise which took place in October-November 2001. The cruise was divided into two legs: Leg 1 primarily focussed on ATSR satellite validation and Leg 2 was planned around the recovery of Netherlands Institute of Sea Research (NIOZ) moorings. Throughout the cruise real-time measurements of the air-sea fluxes of momentum, sensible heat, latent heat and CO₂ were made, in addition to the usual mean meteorological parameters.</p> <p>The main aim of Leg 1 (Seychelles to Seychelles) was to achieve as many ATSR satellite overpass validations as possible with the SISTeR radiometer. In addition 5 APEX floats were deployed in support of the ARGO Programme and two XBT equatorial sections were made.</p> <p>During Leg 2 (Seychelles to Durban) the key objective was to recover an array of seven moorings, on a section across the Mozambique Channel roughly at its narrowest part, which had been previously deployed by NIOZ. Further ATSR overpass validations were achieved and two more XBT sections were made.</p> | |
| KEYWORDS APEX FLOATS, ARGO, ATSR, CHARLES DARWIN, CRUISE 135 2001, INDIAN OCEAN, INDTWMOZ, METEOROLOGICAL MEASUREMENT, MOORINGS, MOZAMBIQUE CHANNEL, RADIOMETERS, RADIOSONDE BALLOONS, SISTER, SURFACE FLUXES, XBTs | |
| ISSUING ORGANISATION Southampton Oceanography Centre Empress Dock European Way Southampton SO14 3ZH UK | |
| Copies of this report are available from: National Oceanographic Library, SOC Tel: +44(0)23 80596116 Fax: +44(0)23 80596115 Email: nol@soc.soton.ac.uk PRICE: £21.00 | |

CONTENTS

| | |
|--|-----------|
| Scientific personnel | 7 |
| Ship's personnel | 8 |
| List of Tables | 9 |
| List of Figures | 9 |
| Acknowledgements | 10 |
| 1. Introduction | 11 |
| 2. Narrative (Cruise Diary) | 12 |
| 3. Meteorological Instrumentation (Berry) | 18 |
| 4. AutoFlux Data Acquisition And Processing (Berry) | 18 |
| 4.1 Mean met results (leg 1) | 19 |
| 4.2 Mean met results (leg2) | 20 |
| 4.3 Navigation results (Legs 1 and 2) | 21 |
| 5. Visual Cloud Observations (Josey / Berry) | 22 |
| 6. Expendable Bathythermograph (XBT) Surveys (Josey) | 23 |
| 6.1 Initial Results | 23 |
| 7. Longwave Parameterisation Study (Josey) | 23 |
| 8. VMADCP – Vessel Mounted Acoustic Doppler Current Profiler (Stuart-Menteth) | 24 |
| 8.1 ADCP Operational Modes | 24 |
| 8.2 ADCP Calibration | 25 |
| 8.3 ADCP Processing | 26 |
| 9. ARGO Floats (Stuart-Menteth) | 27 |
| 10. Sea Surface Temperature (SST) Measurements (Stuart-Menteth) | 27 |
| 10.1 The Diurnal Cycle of SST | 29 |
| 10.2 Conclusions | 29 |
| 11. ATSR-2 Validation (Nightingale) | 30 |

| | |
|--|-----------|
| 12. Radiosonde Atmospheric Profiles (Marshall) | 31 |
| 13 Mooring Recovery Deck Operations (Waddington, Scott) | 33 |
| 14 Mooring recovery (Ridderinkhof) | 34 |
| 14.1. Introduction | 34 |
| 14.2. Recovery of the moorings | 34 |
| 14.3. Functioning of the instruments | 36 |
| 14.4. First results | 36 |
| 15. References | 37 |
| 16. Tables | 38 |
| 17. Figures | 53 |

Scientific personnel

AutoFlux group

| | From: | Role: |
|-----------------------|--------------|--------------------------|
| PASCAL, Robin | SOC | Principal Scientist |
| JOSEY, Simon | SOC | Surface fluxes |
| BERRY, Dave | SOC | Surface fluxes |
| STUART-MENTETH, Alice | SOC | Sea Surface Temperatures |

ATSR Validation

| | From: | Role: |
|------------------|--------------|-------------------|
| NIGHTINGALE, Tim | RAL | SISTeR Radiometer |
| MARSHAL, Glenn | UL | Radiosondes |

UKORS Scientific Support

| | From: | Role: |
|-----------------|--------------|--------------------|
| WADDINGTON, Ian | SOC | Mooring technician |
| SHORT, Jon | SOC | ITG Support |
| SCOTT, Jason | SOC | Mech Support |

Moorings

| | From: | Role: |
|----------------------|--------------|---------------------|
| SCHILLING, Jack | NIOZ | Mooring technician |
| LAAN, Martin | NIOZ | Electronics |
| HILLEBRAND, Theo | NIOZ | Mooring instruments |
| RIDDERINKHOF, Herman | NIOZ | Scientist |

Key

NIOZ: Netherlands Institute for Sea Research

RAL: Rutherford Appleton Laboratory

SOC: Southampton Oceanography Centre

UL: University of Leicester

Ship's personnel

| Name: Initials | Rank / Rating: |
|-----------------------|-----------------------|
| LONG, G.M. | Master |
| NEWTON, P.W. | Chief Officer |
| MITCHELL, J.W. | Second Officer |
| McALEA, K. | Third Officer |
| MOSS, S.A. | Chief Engineer |
| HOLT, J.M. | Second Engineer |
| CLARKE, J.R.C. | Second Engineer |
| BELL, S.J. | Third Engineer |
| BAKER, J.G.L. | ETO |
| POOK, G.A. | CPO(D) |
| LEWIS, T.G. | PO(D) |
| CRABB, G. | Seaman |
| DALE, J.E. | Seaman |
| MILLS, R.J. | Seaman |
| JOHNSON, R. | Seaman |
| PRINGLE, K. | POMTR |
| PERRY, C.K. | SCM |
| LYNCH, P.A. | Chef |
| KUJAWIA, A. | M/S |
| MINGAY, G.M. | Steward |
| SMYTH, R.I | Steward |

List of Tables

- Table 1. The mean meteorological sensors.
- Table 2. The fast response sensors
- Table 3. The navigation instruments.
- Table 4. The mean values of the observations for leg1 and the mean differences between the sensors.
- Table 5. Radiosonde LOG SHEET 1
- Table 6. XBT LOG SHEET 1
- Table 7. XBT LOG SHEET 2
- Table 8. XBT LOG SHEET 3
- Table 9. XBT LOG SHEET 4
- Table 10. XBT LOG SHEET 5
- Table 11. VMADCP Water Track Configuration File
- Table 12. Log of ADCP 'zig-zag' calibration track
- Table 13. ADCP Log
- Table 14. ARGO Float Log for Leg 1
- Table 15. Summary of the SST sensors
- Table 16. SST statistics for the four SST sensors
- Table 17. Results from SST comparison in rough weather
- Table 18. ATSR-2 overpass analysis for the first leg of CD135.
- Table 19. ATSR-2 overpass analysis for the second leg of CD135.
- Table 20. Summary of mooring activities during cruise CD135
- Table 21. Mooring Information ACS11-ACS17

List of Figures

- Figure 1. The ship track.
- Figure 2a. Schematic of the instrument locations.
- Figure 2b. Schematic plan view of the foremast platform.
- Figure 3. The difference in the longwave radiation from the two pyrgeometers.
- Figure 4. The difference in the longwave radiation from the two pyrgeometers plotted against SW
- Figure 5. The daily mean of the differences in the incoming short-wave.
- Figure 7. The daily mean differences in the wet bulb air temperatures measured by psychrometers.
- Figure 9. The difference in the longwave radiation from the two pyrgeometers plotted against SW
- Figure 10. The daily mean of the differences in the incoming short-wave .
- Figure 11. The daily mean differences in the dry bulb air temperatures measured by psychrometers.
- Figure 12. The daily mean differences in the wet bulb air temperatures measured by psychrometers.

Figure 13. The 1 minute averages of the difference between the ships heading measured by the AutoFlux KVH Gyrotrac Fluxgate compass and the ships gyro.

Figure 14. The daily averages of the differences between the ships latitude measured by the AutoFlux system and the ships navigation system.

Figure 15. The daily averages of the differences between the ships longitude measured by the AutoFlux system and the ships navigation system.

Figure 16. Time series of the total cloud amount recorded at each observing hour.

Figure 17. Variation of Temperature with Depth Along the N-S Cross-Equatorial Section 2.

Figure 18. Variation in Zonal Geostrophic Velocity with Depth at 1.5N, 58E

Figure 20. Hourly averaged SST for the four SST sensors during leg 1

Figure 21. Intercomparison of the 4 SST sensors for Leg 1 using hourly averaged data

Figure 22. Intercomparison of 3 SST sensors during rough weather (Jdays 310 & 311)

Figure 23. SST measurements during Leg 1 from all sensors

Figure 24. Examples of diurnal warming

Figure 25. Maximum diurnal SST amplitude for each sensor for days with strong warming

Figure 27. SISTeR calibration, 22nd October 2001

Figure 28. The availability of SISTeR data and the positions of the nine ATSR-2 overpasses for leg 1.

Figure 29. The availability of SISTeR data and the positions of the nine ATSR-2 overpasses for leg 2.

Figure 31. Time series of 15 minute averages of the mean meteorological variables during Leg 1

Figure 32. Time series of 15 minute averages of the mean meteorological variables during Leg 2

Figure 33. Time series of the calculated surface fluxes for Leg 1

Figure 34. Time series of the calculated surface fluxes for Leg 2

Figure 35. Location of the ACSEX moorings in the Mozambique Channel

Figure 36. Cross section of the mooring array including the type and position of the instruments

Figure 37. Current speed and direction of a current meter in mooring ACS15

Figure 38. Low pass filtered currents from 2 current meters from mooring ACS15.

Figure 39. Low pass filtered currents from current meters at mooring ACS15 (top) and ACS14 (bottom).

Acknowledgements

Thanks are due to the officers and crew of the RRS *Charles Darwin* for their contribution to a successful cruise, particularly as this was my first time as principal scientist. I would also like to express thanks to Dave Hosom and Co. from Woods Hole Oceanographic Institute for the loan of their sea surface temperature system.

1. Introduction

The ERS-2 platform is nearing the end of its operational life and the health of some parts is declining. In order both to test the current state of the ATSR-2 calibration and algorithm, and to confirm the continuity of sea surface temperature (SST) measurements between ATSR-2 on ERS-2 and AATSR on ENVISAT, it was necessary that at least one ATSR-2 validation cruise be undertaken. The cruise provided a particularly good opportunity for validation measurements, given the fine weather and low cloud cover that typify the northeast monsoon season in the Indian Ocean. A significant validation dataset will give the maximum confidence in ATSR-2 data at the end of its life. Skin SSTs were measured with a SISTeR radiometer which can operate in a marine environment and return SSTs to high accuracy. In combination with the air-sea flux and bulk SST measurements, the skin measurements will also give useful insights into the behaviour of the air-sea interface. In particular the data can be used to test the performance of existing skin SST models.

The cruise also provided a timely opportunity to improve our understanding of air-sea interaction in the tropics by taking advantage of recent advances in flux measurement methods. In particular, the downwelling atmospheric longwave flux is a key component of the net heat exchange between the ocean and the atmosphere but it remains poorly parametrized in climatological studies (Josey et al., 1997). We are in the process of developing a new empirical formula for the longwave flux in terms of routine observations of the air temperature, specific humidity and cloud cover (Josey et al., 2002). The longwave measurements were made using a radiometer fitted with a circuit that allows corrections for heating of the instrument dome (Pascal and Josey, 2000). The improvement in sensor accuracy is significant, of order 10 Wm^{-2} in the daily mean. A large number of measurements at mid-high latitudes had already been obtained with the modified sensor but this was the first opportunity to use it in the tropics. Such measurements are vital to our understanding of large scale energy exchanges, and thus ocean heat transport, as the existing formulae for the longwave flux are thought to be biased by up to 20 Wm^{-2} in regions of low cloud cover in the tropics (Tragou et al., 1999). Measurements of the downwelling atmospheric longwave flux were made throughout both legs of the cruise. When combined with routine meteorological measurements and visual cloud observations, these measurements will allow a new long wave parameterization to be developed.

In addition to the longwave flux, the turbulent fluxes of heat, momentum and moisture were obtained continuously throughout the cruise, using a number of fast response sensors. Data from these sensors and from the mean meteorological sensors were all logged using the SOC "AutoFlux" system (AutoFlux group, 1996; Pascal et al., 2000).

As a collaborative project we recovered an array of moorings, on a section across the Mozambique Channel roughly at its narrowest part, which were previously deployed by the Netherlands Institute of Sea Research (NIOZ).

Finally, as part of the UK Argo programme 5 Argo floats were deployed in the northwest Indian Ocean and additional data on water column physical properties were obtained by launching a series of expendable bathythermographs (XBTs).

2. Narrative (Cruise Diary)

DAY 297 (24/10)

Darwin sailed from port Victoria, Seychelles at 0900L hrs on the 24th of October (day 297 at 0500 GMT) and we were able to perform the first satellite validation approximately an hour and a half after sailing (06:52 GMT). The weather was generally sunny and calm, but there were a few small cumulus clouds which made overpass conditions not quite ideal. A test XBT was launched successfully at 1250hrs, ahead of the first equatorial XBT section which started at 2220hrs.

DAY 298 (25/10)

XBTs were launched every 3 hrs throughout the day as we steamed north, and the first radiosonde was successfully launched in the morning and the resultant TEMP message sent back to the U.K. Met Office. The good weather continued throughout the day, but just prior to the satellite overpass (18:10hrs) rain clouds appeared, forcing the SISTeR radiometer to be shut down. Once the last XBT of the section was completed it was decided to leave the area early, as we could get no useful overpass data, and head for the next overpass position.

Day 299 (26/10)

In the morning it was discovered that the AutoFlux air-sea interaction system (Section 4) was set to the incorrect date and hence was giving the wrong Julian Day. The data acquisition was halted so that the year could be corrected and files renamed etc., after which the system was rebooted and logging restarted.

Day 300 (27/10)

During the morning radiosonde launch the radiosonde receiver terminated the flight after approximately 10 minutes due to an error which occurred while processing the first stage of the TEMP message. This problem has been encountered on other cruises, but remains unresolved even after a number of communications to Vaisala, the manufacturer of the equipment. After a short delay the system was restarted so that at least PTU data could be acquired for the remainder of the flight.

Much of the day was spent on the automated Autoflux processing which was not yet fully working. Some problems were encountered with the number of variables which required some program modifications, after which the system functioned without problems.

The second radiosonde of the day was launched and tracked without any problems although it produced poor wind data and was finally lost at around 200 mbar.

Unfortunately the day turned out to be mostly overcast with many large rain clouds, so again we were unable to get any good satellite overpass data.

Day 301 (28/10)

Again the hoped-for clear skies failed to appear as we were greeted with 8/8ths cloud cover. The Dartcom satellite imaging system was used to successfully download a recent image. This duly showed the

ships location to be covered by thick cloud, but more importantly it gave us the best direction in which to attempt to find clear skies for the next overpass.

Again another radiosonde launch failed due to the aborted TEMP message, but we managed to restart the system into Research mode so that wind data could still be logged.

Late in the day as we approached overpass time we found a reasonable hole in the cloud so slowed the ship down to 3 or 4 knots trying to maintain a clear sky view. At overpass time only a few small clouds remained so we are hopeful of a good result. With time to spare before departing the area for the next overpass position a cross pattern survey was performed centred on the current overpass position.

Day 302 (29/10)

The day started with quite a lot of cloud which increased as we steamed north, eventually producing rain squalls with winds as high as 10m/s, so again the SISTeR radiometer had to be shut down.

The AutoFlux GPS receiver was investigated as it had been giving spurious data at non standard intervals resulting in the logging program losing some data. This was eventually attributed to an excessive number of message types being sent at too high a data rate, causing problems with the receiver. Once the message types were reduced to only those needed, the receiver was able to deliver the data at the required rate, allowing the acquisition program to run more smoothly.

The ship arrived at the most northerly position of 10° N almost 12 hrs early and the first ARGO float was deployed followed shortly by three XBT's. In an attempt to gain more time for the return leg. and in order to look for clearer skies for the evening satellite overpass, the ship steam south from the 10° N position.

Later in the day the ship was stopped for half an hour while the towed thermistor ('soap'), which measures the bulk SST, was calibrated against the ship's thermosalinograph (TSG). Then the AutoFlux heading sensor (fluxgate compass) was calibrated by having the ship slowly steam in circles to allow it to perform a self-calibration. This greatly reduced the compasses error when compared with the ship's gyro compass.

In the late afternoon the cloud conditions improved dramatically so that we hoped to get some good overpass data, but unfortunately 30 minutes before the overpass the ship found a small patch of cloud, resulting in suspect data.

Day 303 (30/10)

The day again started generally cloudy as we headed east towards the next overpass position which was 24 hrs away. At approximately 1400 hrs local time we seemed to get a pulse of the NE monsoon, with the wind shifting from the NW to the NE and increasing to over 10m/s. The air also became much drier, but after an hour or so the wind dropped again, shifted back to the NW and became more humid.

As we approached the satellite overpass position the clouds had more or less dispersed leaving only some high Cirrus so that we hope to get some useful data.

Day 304 (31/10)

Clearer skies again give hope for good data during the satellite overpass due later that morning, the pervasive cirrus layer of the previous evening having cleared to leave only scattered cumulus. Venus and Mercury were observed close together (less than 1 degree apart) on the eastern horizon in the pre-dawn sky prior to the second Argo float deployment.

As the overpass time approached a large bank of cloud was seen ahead so the decision was made to alter course and return the way we had come and so remain in relatively clear skies. After the overpass the ship resumed its original course.

The ADCP system finally began logging to the ship's computing level C.

Day 305 (1/11)

Another day of clear skies with no wind at all became very hot, with the SST sensors showing a marked diurnal increase in sea temperature.

Unfortunately once the ADCP system was fully operational it showed bit errors and little penetration, resulting in such bad data that the system was turned off. The third Argo float was also deployed in the early morning at 4° 30" N and the trailing thermistor ("soap") measured a maximum sea temperature of over 31 degrees. The high sea temperatures also caused problems with the ship's engine cooling system and the ship had to slow down to 8 knots throughout the afternoon.

Day 306 (2/11)

The day started again with an early deployment of the fourth Argo float which was followed by the start of the second XBT equatorial section, deploying as many XBT's as possible to improve the section resolution. Although there was initially some cloud it was burnt away by mid morning, producing another very hot day with rising sea temperatures.

It was noted that the AutoFlux daily script had not been working properly for the last two days as the script for day 304 was still running. The 'old' script was trying to delete a core file but did not have the correct permissions.

Again the ship had to reduce speed in the afternoon, so after a discussion with the Captain about our ETA for the Seychelles, it was decided that it would be necessary to cut time spent on the XBT section. This was achieved by ending the section early and reducing the number of deep XBT's which require the ship to slow during deployment.

Day 307 (3/11)

Continued with the XBT section and performed another early launch for the last Argo float at 0530 hrs. The rescheduled section appeared to be going well and put us back on track for the ETA at Mahe in the Seychelles the following day. The ADCP started showing signs of life as we neared the Seychelles, indicating that the problems were probably due to the lack of back scatterers in the water. The last satellite overpass for leg1 was due at 0630 hrs, but with 2/8ths cloud cover of small Cu the data may not be that good. However, the cloud reduced the amount of surface heating so that the ship was able continue at full speed. In preparation for arrival at Mahe, the towed Echo sounder fish and towed thermistor (soap) were

brought onboard. The ADCP had begun working all the time and switched into bottom track mode while the ship was over the shelf.

Day 308 (4/11)

Arrived in Victoria Mahe on time but were given very limited dock space. This required the ship to be put on the end of the dock, with only the aft end along side, and the bow was tied off to a buoy. Once securely along side both the SOC and Dutch mooring teams arrived on board and their containers were soon loaded onboard and the winch installed. While in port we took the opportunity to back up to Exabyte tape both of the AutoFlux Unix workstations.

Day 309 (5/11)

With all personnel onboard and the winch systems installed, the ship departed from Mahe at 0615 local time. As soon as possible the ADCP was turned on and put into bottom track mode and it appeared to be giving good data. The trailing thermistor was also deployed. Once off the shelf the Echo Sounder fish was re-deployed and the ADCP put into water track mode.

Day 310 (6/11)

After leaving the Seychelles the weather deteriorated with the strongest winds of the cruise so far at about Force 5 with a lumpy sea. A section of the good quality bottom track ADCP data was sent back to SOC in order to verify the quality of the data. However, due to the size of the email there were some problems with the email's reception at SOC.

Day 311 (7/11)

It was noted that the Orbcomm transmitter was not receiving messages from the AutoFlux system. Both the transmitter and the AutoFlux Orbcomm program were restarted: this cured the problem. The ADCP also started showing signs of bit errors again but this may have been due to the bad weather. During the morning the wind continued to increase to Force 6 to 7, but by late afternoon the sea state improved as we moved into the lee of Madagascar.

Day 312 (8/11)

Back to flat calm seas and low wind speeds and with another overpass due at 0720 hrs we just managed to sail out of the cloud cover in time, leaving a big bank of cloud behind and more or less clear skies ahead.

During the bad weather the port psychrometer HS1020's dry bulb (pdp1) failed, so the sensor was replaced with psychrometer IO2003, which immediately gave good agreement with starboard psychrometer IO2002. Both the shortwave and longwave sensors were cleaned, and fortunately none showed any signs of bird mess on the domes. The ADCP was still showing bit errors even with the calm weather, so again it must have been due to the lack of back scatterers in the water.

Day 313 (9/11)

Most of the day was spent sailing down the Mozambique channel close to the Madagascar coast in calm winds and seas. A few birds and dolphins were seen but none came close, although the ship did become festooned with a swarm of large dragonflies.

By mid afternoon we had arrived at the first of the Dutch moorings (ACS17), contact was made with the mooring and an XBT was deployed at the mooring location. The mooring was then recovered without any problems and the complete operation was finished by late afternoon.

With the mooring on board the ship headed off towards the next mooring with further XBTs deployed half way and another at the second mooring site. For the remainder of the night the ship lay head to wind waiting for daylight so that mooring operations could resume.

Day 314 (10/11)

Moorings operations were restarted at first light with the second mooring (ACS16) being successfully interrogated and the release command was sent at 0300 hrs. The mooring was almost immediately on the surface and the recovery was soon completed taking only 2 hrs. The ship then headed for the 3rd mooring (ACS15) again deploying an XBT halfway between the two moorings positions and again at the 3rd mooring site.

The 3rd mooring gave us our first problem by failing to respond to the acoustic commands sent from the ship. In an attempt to locate the mooring the ship set off in a search pattern in case the mooring had drifted from its deployment location, but with no success. We continued the search for the rest of the day and evening, but eventually headed on towards the next site at 2300 hrs local so that we would arrive at the next site at first light.

Day 315 (11/11)

Another early start for the 4th mooring (ASC14), and with another satellite overpass expected the day started quite cloudy with both large Cu and Cirrus. This time the releases responded, with even an old set left on the site replying too, although it did require both sets of releases to be commanded before the mooring surfaced. Once the mooring was on board we moved off to the 5th mooring (ASC13), again doing XBT's on the way. Unfortunately the 5th mooring failed to respond at all, although again two old releases left from an old mooring replied, indicating that the release deck unit was working. After a number of failed attempts at releasing the mooring the decision was made to move on to the next mooring site, as this was unlikely to be located quickly. This allowed us to attempt to recover the rest of the moorings and then return during the evening/night to try and find the 5th mooring.

On arrival at the 6th mooring site (ASC12) the mooring was soon located to much relief and was soon recovered, but unfortunately the ADCP was found to be flooded. Once the mooring was on deck we headed for the 7th and last mooring, arriving with just enough daylight to do the recovery. The mooring released without problems but arrived on the surface twisted, making the recovery much harder than expected. We then headed back to the 5th mooring site during the night and performed an acoustic survey until the morning.

During the late afternoon and evening the overcast skies cleared giving more promising conditions for the satellite overpass.

Day 316 (12/11)

As daylight arrived there was still no response from the mooring and we started to prepare to drag for it, but without any signal from the mooring we were not very hopeful. By midday the dragging gear had been attached to the main warp and had been paid out for about 1 hour. A fax was then received from NIOZ with an ARGOS position of a mooring on the surface. This was identified as ACS15, the 3rd mooring which we had failed to recover. Dragging was immediately abandoned and the gear recovered, after which we headed towards the last ARGOS position of the surfaced mooring, approximately 30 miles due east. As we approached the mooring's last known position the it was seen on the surface a mile or so off the starboard bow. After a quick investigation the mooring was seen to be intact and was immediately recovered and was onboard by 1700L. On completion of the mooring recovery the ship headed due south to start an XBT section through an eddy feature at 21°S 40.5°E.

Day 317 (13/11)

The weather was still clear and calm as we headed south with all systems working well, although the ADCP still had bit errors and a penetration of only 200 to 250 m. In the early evening we arrived at the start point for the XBT section and started deploying XBT's.

Day 318 (14/11)

The XBT section continued. Over night we had been fighting against a current of about 1 knot, but this appeared to reverse and we had about a 1.5 knots current with us by the morning indicating that we had crossed some interesting features. During the morning we had another satellite overpass, but conditions, although improving, were still not that good with 2/8ths Cu cloud. There was also a second satellite overpass in the evening with much improved cloud conditions so that many stars could be seen.

Day 319 (15/11)

At 0630 we completed the XBT section and altered course and headed for 30° S 38° E so we could do a last XBT section as we approached Durban, at right angles to the coast.

We reduced speed to 6 knots in an attempt to improve the ADCP data and performed a 'zig-zag' calibration with a knot or so of current setting to the west.

Day 320 (16/11)

With both a barbeque and a satellite overpass due that evening we woke up to 25 –30 knot winds and a developing sea, with overcast skies and rain. By midmorning we had arrived at the start of the XBT section and altered course heading directly towards Durban, making the ship much more comfortable with the wind and sea behind us rather than beam on. Needless to say with the poor weather the barbeque was cancelled and there will be no good satellite data.

Day 321 (17/11)

With the ship making very good time towards Durban we had to slow down and hove-to so as not to move out of the satellite swath for the overpass due that day. Once the satellite had flown over at 07:35 hrs we resumed course at full speed. A problem was found with the non-toxic water supply, which appeared to have been turned off over night, but was soon restarted.

At 1500 GMT all logging systems, including the AutoFlux system, were turned off and data backups were then started. The last XBT was finished at 2130 GMT.

Day 322 (18/11)

Data backups were completed to both Exabyte and DLT tapes. We finally arrived off Durban and picked up the pilot at 09:00 local time. With the seas still quite rough and with the wind blowing 30 knots, the pilot was delivered by helicopter. The ship tied up at around 10:30L.

3. Meteorological Instrumentation (Berry)

The RRS *Charles Darwin* was instrumented with a variety of meteorological sensors and a GPS navigation system for cruise CD135 by the Southampton Oceanography Centre (SOC) Meteorology Team. The air temperature and humidity, sea surface temperature, air pressure, incoming shortwave (300 – 3000 nm) radiation and incoming longwave (4 – 50 micron) radiation were measured by the mean meteorological sensors (Table 1). The measurements from the fast response instruments (Table 2) were used to calculate the surface fluxes of momentum, heat, CO₂ and moisture. In addition to the momentum flux estimates, the HS sonic anemometer provided the mean wind speed and direction. The data from the GPS instrumentation (Table 3) were used to correct the meteorological data for the ships speed and heading.

The majority of the instruments were mounted on the foremast, as indicated in Figure 2b, to obtain the best exposure. The psychrometers, HS sonic anemometer, IFM H₂O/CO₂ sensor and shortwave radiation sensors were all located on the foremast platform whilst the longwave sensors were mounted at the top of the foremast. The heights of the instruments relative to the ship's waterline were: sonic anemometer, 15.0 m; IFM sensor, 14.15 m; psychrometers, 14.95 m; shortwave sensors, 14.5 m and longwave sensors, 17.2 m.

The Woods Hole hull contact sensor was located in the engine room on the port side, about 1.0 m below the water line. The sea surface temperature 'soap' (trailing thermistor) was trailed over the port side of the bow (Figure 2a).

4. AutoFlux Data Acquisition And Processing (Berry)

All the SOC instruments (Section 3) were logged by the AutoFlux system (Pascal *et al.*, 2000; Yelland and Pascal, 2000). The AutoFlux system was based on one UNIX workstation named "Southerly" (SO), with a backup of the system installed on a second identical workstation ("South-easterly", SE). Both workstations were networked and set up in stand-alone mode, independent of the ship's systems, with the two workstations cross-mounted to allow the easy transfer of files between the two. This also allowed the sharing of the devices installed on either workstation.

The 14 channels from the mean meteorological sensors (Table 1) were acquired and logged once every 10 seconds by the AutoFlux logging system and stored in hourly files. At the end of every hour, the

calibration of the instruments were applied to the raw data, the long-wave radiation calculated (from the 3 channels output by the Epply LW sensors) and basic quality control criteria applied. The processed data were then stored in a new hourly file. Data from the WHOI sst sensor were acquired and logged every 30 seconds with basic quality control and processing carried out once every hour.

The fast response HS sonic anemometer and the IFM H₂O/CO₂ sensor were logged at a rate of 20 Hz and 10 Hz respectively into hourly files. Every hour, 64 sections (or 32 for the IFM sensor) of data were obtained, each section consisting of 1024 data samples, and at the end of every hour the data were processed to provide spectra and quality control parameters. The mean wind speed, wind direction, H₂O and CO₂ were also recorded, with the processed data stored in new hourly files (one for each instrument).

The navigation data were provided by a KVH Gyrotrac Fluxgate compass and an LGBX Pro GPS receiver. The data streams from these two instruments were logged continuously at a rate of 0.5 Hz. The data were then processed every hour and easterly and northerly speed and heading components calculated. The course made good and speed made good were also calculated every hour.

The data from the five data streams mentioned above (mean met, WHOI sst, HS sonic anemometer, IFM H₂O/CO₂ and the navigation data) were logged into individual hourly files for each stream. The files were then merged into one file after the processing at the end of every hour (with the mean meteorological and navigation data averaged and the WHOI sst data interpolated). The surface fluxes and true wind speeds and direction were also calculated at the end of every hour and stored in the merged file. The hourly processed files were then merged at the end of every day and a daily file created, and the previous day's hourly files were deleted.

4.1 Mean met results (leg 1)

On initial comparison of the results for the first leg of the cruise, the two pyrgeometers (LW1, 31170, and LW2, 27225) show good agreement with each other. The daily mean long wave measurements in general agree to within 2 W m⁻² of each other, with a standard deviation of the mean (standard error) between 0.04 W m⁻² and 0.50 W m⁻². This is shown in Figure 3, where the differences in the longwave radiation from the two pyrgeometers have been averaged daily. However, when the differences in the longwave measurements are plotted against the incoming short-wave radiation a trend is clearly visible. At lower short-wave values LW1 under estimates the down welling longwave radiation relative to LW2 by about 4.5 W m⁻². At higher short-wave values the trend has reversed, with LW1 over estimating the down welling longwave by 4.5 W m⁻². This can be seen in Figure 4, which shows the differences in the longwave values averaged into 100 W m⁻² shortwave bins.

In addition to biases due to the heating of the instruments, it has been observed that sea birds (usually red footed boobies) would occasionally land on one of the sensors before moving to the next. An example of this can be seen in Figure 26, where the time series of the mean meteorological parameters have been plotted for Jday 307. The effect of the booby can be clearly seen just after 1600h GMT (Jday = 307.67), with a sharp increase in the LW measured by one sensor followed by a sharp increase in the other

as the bird has swapped sensors. Overall, the LW sensors agree well with each other for the first leg, with a mean difference of -0.35 W m^{-2} (s.d. 0.065).

A comparison of the Kipp & Zonen short-wave sensors (SW1 and SW2) with each other showed that the sensors were in good agreement. The daily mean differences in the measured short-wave values were below 5 W m^{-2} for 60 % of the time and below 20 W m^{-2} for 80 % of the time. However, both short-wave sensors were prone to shadows from the foremast and from the psychrometers, blocking out the sunlight at different times for each sensor, resulting in some of the larger differences. Due to the effect of the shadows on the short-wave measurements it is recommended to use the maximum of the two sensors. Figure 5 shows a plot of the daily differences in the measurements from both instruments, with the good agreement between the sensors for days 297 to 305 evident. The larger differences for days 305 and 307 can also be seen. Overall, for the first leg, the two short-wave sensors show a good agreement, with a mean difference of 12 W m^{-2} (s.d. 0.906).

With the exception of the first day of leg 1, day 297, both sets of dry bulb air temperatures, pdp1 (IO2002) and pds2 (HS1020), agree well with each other. The mean daily differences in the measured air temperatures, excluding day 297, are all below 0.1 degrees C and with all but two of the days below 0.05 degrees C. Figure 6 shows the daily mean in the differences of the dry bulb air temperature measurements. In contrast, the wet bulb measurements show that the wet bulb on psychrometer 2 is consistently biased high by about 0.15 degrees C, suggesting that the wet bulb for psychrometer 2 is not being wetted properly. Incorrect calibration values could also cause this problem. This constant bias can be seen in Figure 7, a plot of the differences averaged daily. The mean differences for the wet and dry bulbs on the two sensors during the first leg were 0.10 deg C (s.d. 0.0126) and -0.02 deg C (s.d. 0.012) respectively. When the data for day 297 is excluded the mean differences become -0.03 deg C (s.d. 0.001) and -0.15 deg C (s.d. 0.0003) respectively for leg 1.

In summary, throughout the first leg of the cruise the different sets of instruments have been in good agreement with each other except for pwp1 and pws1, with a mean difference of -0.15 deg C between these sensors. The mean values of the incoming radiation (long- and short-wave) and air temperature (wet and dry bulb) are given in Table 4. The mean differences in the measurements are the standard deviations of the mean are also given.

4.2 Mean met results (leg 2)

The initial results for second leg are similar to those of the first, with a good agreement between the sensors. Over the second leg, the mean difference in the downwelling longwave radiation measured by the two pyrgeometers was 0.015 W m^{-2} (s.d. 0.0619). When the longwave radiation is plotted against the shortwave radiation a trend similar to that seen in the first leg is visible. At the lower shortwave values LW1 under estimates the downwelling longwave radiation by up to 5 W m^{-2} relative to LW2. At the higher shortwave values the longwave is over estimated by up to 5 W m^{-2} . Figures 8 and 9 show the longwave

differences averaged on a daily basis and into 100 W m^{-2} short-wave bins, with the good agreement between the sensors, on a daily-averaged basis, clearly visible.

On the second leg the results from the two shortwave sensors generally agree with each other better than they did on the first leg. The average difference in the measured shortwave for the second leg was 5.5 W m^{-2} (s.d. 0.712) compared with 12 W m^{-2} (s.d. 0.906) for the first leg. On the second leg there were still problems caused by shadows from the foremast and psychrometers and so it is recommended the maximum of the two shortwave values for any particular moment in time should be used. Over the second leg there is also a drift in the differences between the shortwave sensors (SW1 – SW2) from about 25 W m^{-2} on day 309 to -25 W m^{-2} on day 318. This can be seen in Figure 10.

The dry bulb measurements from the two psychrometers show a good agreement over the first day and a half of the second leg, up until the dry bulb on the starboard psychrometer (pds2) stops working in the evening (just after 1900h GMT) of day 310. Up until the failure of the dry bulb, the mean difference between the two dry bulbs is -0.002 deg C (s.d. 0.002). Over the same period there is a bias present in the measurements made by one of the wet bulbs. The measurements made by the starboard psychrometer (pws2) are biased high by an average of 0.116 deg C (s.d. 0.0004) compared to the port psychrometer (pwp2). However, after the broken psychrometer was replaced on day 312 (the psychrometer was not replaced before then due to inclement weather) the mean difference between the port psychrometer and the new starboard psychrometer decreased to -0.061 deg C (s.d. 0.0047). This decrease in the bias between days 312 and 313 is clearly visible in Figure 12, a plot of the daily mean differences. After the replacement of the broken psychrometer the mean difference in the dry bulb temperature becomes 0.03 deg C (s.d. 0.004).

4.3 Navigation results)

During the first five days of the cruise (days 297 – 302) there is a poor agreement between the navigation data from the AutoFlux system and the ship's navigation systems. During this period the mean difference between the KVH Gyrotrac Fluxgate compass used by AutoFlux and the ship's gyro compass was -58.5 degrees (s.d. 1.5). Due to the large errors seen in the KVH Gyrotrac compass heading the compass was re-calibrated during day 302 between 0900h and 1200h GMT by having the ship perform a number of complete turns. This resulted in a major improvement in the AutoFlux navigation data, with the mean difference between the AutoFlux heading and the ship's gyro heading reduced to 0.5 degrees (s.d. 0.1) between days 302.5 and 322. However after day 313 the KVH Gyrotrac compass began to drift, with differences between the headings from the two navigation systems of up to $\pm 30 \text{ degrees}$ towards the end of the cruise (day 322). The mean difference for this period (days 313 – 322) was 1.0 degrees (s.d. 0.2). Figure 13 shows the 1 minute averages of the differences in the headings from the AutoFlux navigation data and the ship's navigation data. The poor agreement before and the good agreement after the calibration of the KVH Gyrotrac compass can be seen in this figure, with a poor agreement between the two sets of

data before day 302.5 and a good agreement after. The drift in the KVH Gyrotrac compass after day 313 can also be seen. This drift in the compass coincided with the approach to Madagascar and entering the Mozambique channel, suggesting that the compass needs to be re-calibrated whenever the geographical/geological surroundings change.

Before the AutoFlux KVH Gyrotrac compass was re-calibrated on day 302 the latitude and longitude from the two navigation systems were in poor agreement with each other. Between days 297 and 302 the mean difference in the latitude measured by the AutoFlux system and that measured by the ship's navigation system was -0.187 degrees (s.d. 0.018). The mean difference in the longitude for this period was 9.458 degrees (s.d. 10.551). After the compass was re-calibrated the mean differences for the latitude and longitude were reduced to 0.001 degrees (s.d. 0.000) and -0.008 degrees (s.d. 0.004) respectively. Figures 14 and 15 show the differences for the latitude and longitude respectively averaged into daily bins.

In summary, after the KVH Gyrotrac compass used by AutoFlux was re-calibrated on day 302 the navigation data from the AutoFlux system were in good agreement with the data from the ship's navigation systems. After day 302 the ship's heading from the AutoFlux system and from the ship's navigation system agreed to within 0.5 degrees (s.d. 0.1). During this period the ships location from the two systems agreed to within 0.001 degrees (s.d. 0.000) latitude and -0.008 degrees (s.d. 0.004) longitude of each other. However, after the ship approached the African continental shelf the KVH Gyrotrac compass used by AutoFlux began to drift, suggesting that the compass needs to be re-calibrated whenever the geographical/geological surroundings change. This drift in the KVH Gyrotrac compass did not noticeably affect the accuracy of the longitude and latitude measured by the AutoFlux system.

5. Visual Cloud Observations (Josey / Berry)

Visual cloud observations were made every daylight hour (typically from 0600 – 1800 LST) by Josey throughout both legs of the cruise. In addition, an independent set of observations was made by Berry typically starting at 1000 LST and continuing through to 1800LST. For each observation the amount of low, medium and high cloud and the total cloud cover was recorded in octas. A time series of the total cloud amount recorded at each observing hour is shown in Figure 16, and shows that a wide range of cloud conditions were experienced during the cruise. The cloud observations will be used as part of an ongoing project aimed at parameterising the downwelling longwave radiation in terms of routinely reported meteorological variables for use in climatological analyses. Initial results of this project are discussed in Section 7.

6. Expendable Bathythermograph (XBT) Surveys (Josey)

Several XBT surveys were carried out during the cruise. The various aims of these surveys included:

- a.) an investigation of the Equatorial Undercurrent,
- b.) determination of the depth of the 4° C isotherm at 10° N,
- c.) sections across the mooring deployment and further south in the Mozambique Channel,
- d.) a survey of an eddy centred on 23.4° S 42.1° E.

In addition, the information collected in the upper 10m has been utilised as part of the study of diurnal variations in SST (Section 10). The XBTs for these analyses were supplied by the Hydrographic Office and comprised 55 Sippican T7s (with a depth capability of 760m) and 36 deeper range T5s (which operate to 1830m). The details of the individual drops for the various XBT deployments are given in Tables 6-10. No major problems were encountered with the deployments although the XBT processing software on the PC in the plot crashed during processing on 3 occasions, necessitating additional deployments as the data could not be recovered. In addition, on several occasions there appeared to be offsets of order 20-40m in the T profiles from neighbouring, closely spaced XBTs. It is not yet clear whether these offsets are an artefact of the XBT processing or represent real spatial variations.

6.1 Initial Results

Analysis of the XBT data during the cruise focused on the high resolution N-S section across the Equator with the aim being to determine whether the Equatorial Undercurrent is present in late October to early November. Previous studies indicate that it is only a reliable feature from January through to March in response to the prolonged wind forcing associated with the NE monsoon. The variation of temperature with depth and latitude along the section is shown in Figure 17. Despite the offsets noted above there appears to be some doming of the isotherms at a depth of order 150 m between 0.5 to 1.5° N which is characteristic of the undercurrent. A preliminary calculation of the geostrophic velocity profile using station data at 1.0 and 2.0° N is shown in Figure 18. The undercurrent is evident at depths of between approximately 140 to 220m as an eastward reversal, of up to 1.8 cm s⁻¹, of the predominantly westward flow. Subsequent analysis will focus on obtaining a better definition of the undercurrent characteristics by combining data from various station pairs.

7. Longwave Parameterisation Study (Josey)

The hourly observations of cloud amount made throughout the cruise were combined with measurements of the atmospheric longwave flux, air temperature and humidity to evaluate the performance of various simple longwave parameterisations of the type used in ship based climatological analyses (e.g the SOC climatology, Josey et al., 1999, for which the formula of Clark (1974) was used). This study is of particular importance as these parameterisations have yet to be properly tested using high quality measurements of the longwave flux in the Tropics and it is possible that a significant fraction of the global heat flux imbalance found in many climatological studies is due to a bias in the adopted longwave formula.

Estimates of the longwave flux at the time of each cloud observation were obtained using the formulae of Clark (1974) and Bignami et al. (1995), and compared with the measured longwave flux averaged over a ten minute interval centred on the observing time. The results of this comparison for Leg 1 and Leg 2 (as far south as 20° S) are shown in Figure 19. While reasonable agreement is obtained with the Bignami formula the Clark formula is found to be biased by over 10 Wm⁻². The Bignami formula is known to perform poorly at higher latitudes from a study carried out in the North Atlantic (Josey et al., 1997) and a new formula is being developed (Josey et al., 2002) in which the atmospheric longwave flux, Q_{LA} , is estimated using an adjustment, ΔT_a , to the measured air temperature, T_a , in deg K, which is latitude dependent as follows,

$$Q_{LA} = \sigma_{SB}(T_a + \Delta T_a)^4$$

where σ_{SB} is the Stefan-Boltzmann constant ($5.67 \times 10^{-8} \text{ W m}^{-2} \text{ K}^{-4}$).

A preliminary least square fit to the data collected from Leg 1 was used to determine the following expression for ΔT_a ,

$$\Delta T_a = an^2 + bn + c$$

where $a=11.03$, $b=-2.35$, $c=-10.80$ and n is the fractional total cloud cover. Estimates obtained with this formula for Legs 1 and 2 are also shown in Figure 19. The new formula is found to perform well when tested using the Leg 2 data, the overall bias being 3.1 Wm⁻². Some problems are encountered with the representation of high cloud but these probably reflect the lack of overcast high cloud cover conditions in the Leg1 dataset used to develop the formula.

8. VMADCP – Vessel Mounted Acoustic Doppler Current Profiler (Stuart-Menteth)

RRS Charles Darwin has an RDI 150 kHz broadband ADCP mounted in the hull. The ADCP operates in two modes: water track mode or bottom track mode. The bottom track mode was only used in shallow regions when we reached continental shelves. It was hoped that these bottom track periods would be used as a post-calibration test for the ADCP.

8.1 ADCP Operational Modes

There were several problems with the ADCP during the cruise. At first the ADCP did not read in the navigation and heading data. There were also problems with the configuration files provided by Brian King from the SOC because they were set for the RRS James Clark Ross and not the RRS Charles Darwin. The configuration files had to be altered, although the main requested changes were still kept. The configuration file was set, as requested, with:

64 x 8 m bins

pulse length 8 m
blank beyond transmit of 8 m
2 minute ensembles
1 second ping rate

The direct command menu (DC) was set to FH00004 during bottom track mode (implying a ratio of four water track pings for each single bottom track ping). The original configuration file had been set with a heading offset of 45 degrees for the James Clark Ross, which was set to zero for the Charles Darwin after checking what the offset was with the UKORS staff. See Table 11 for a complete list of the configuration settings.

Once the configuration file was accepted by the ADCP the instrument appeared to work well. However, BIT errors messages were noted and the ADCP often only showed data to 250 m or shallower, rather than the expected 450 m. The error message displayed: 'bit error on beam 1, 2, 3, 4 sig, spw, freq'. One explanation was that it might be due to the extreme water temperatures as SST reached up to 31.5 °C. Brian King suggested that it might be due to the water quality. The water was so clear that the pings were not being returned to the ADCP. This explanation seemed the most plausible as the water was very clear. The ADCP was regularly observed during leg 2 to check for the BIT errors and they were observed every day. Frequently the BIT showed OK but the depth of the data was shallow implying that there was still some problem with the return signal.

8.2 ADCP Calibration

There are two methods that can be used to calibrate the ADCP. One is to use the bottom track data and compare the absolute speeds with the speed of the ship. The other is to make a zig-zag shaped path when in water track mode. The ADCP was switched onto bottom track mode several times (see Table 13) and on day 319 a deep water 'zig-zag' track was carried out. The zig-zag track started at 12h00. The ship was on a heading of 230° and moved through a 45° angle at 12h00, to a heading of 275°. The ship maintained a steady speed of 6 knots throughout the zig-zag track. Six turns were carried out in total, with the last one ending at 14h00. After this time, the ship returned to its original heading and speed. The ADCP was monitored carefully during the calibration track and the maximum depth of good data, percentage of good data and whether BIT errors were present was recorded for every two minute bin. Table 12 summarises the track and its turns. The calibration data will be processed back at the SOC after the cruise.

8.3 ADCP Processing

The ADCP data were processed using the standard pstar programs. Pstar was only set up on one workstation and so the executables had to be split up. The ADCP programs did not append a new day's data; the programs had to be re-run with all the data. Therefore, the ADCP data was processed every other day. The data was not processed with `adpexec1`, which corrects for any drift in the ADCP's clock. since this was automatically corrected for by the ADCP. The executables required navigation data, which was processed daily (see Section 4.3), in order to correct the current measurements for any heading error. Small drifts and biases in the gyro headings were corrected using the Ashtech heading measurements. The data were first 'data-pupped' from the RVS data stream, using the UNIX script, `adcprvs0`, and then processed using the following pstar programs:

| | |
|-----------------|--|
| adpexec0 | Conversion of ADCP data from the RVS data stream to pstar format. Output: <code>adp13501</code> , <code>bot13501</code> |
| adpexec2 | Correction of ADCP data for gyro heading error. The data is merged with the ASHTECH master file. Output: <code>adp13501.true</code> , <code>bot13501.true</code> |
| adpexec3 | Velocity profiles corrected for transducer misalignment and signal amplitude error. Output: <code>adp13501.cal</code> , <code>bot13501.cal</code> |
| adpexec4 | Velocity profiles (relative to the ship) merged with the BESTNAV position fixes to produce absolute velocities. Output: <code>adp13501.abs</code> , <code>bot13501.abs</code> |

The data were separated into two files for the first (01) and second (02) legs of the cruise. The filename format indicates the cruise ID number, 135, and the leg number, 01 or 02. A 12-hour sample of the level C data from `adpexec0` was sent back to the SOC to check the quality of the data. The data were confirmed to be good. The data sent back were sampled from one of the only good days when the ADCP was working correctly during the final approach to the Seychelles at the end of leg 1.

Table 13 lists the ADCP's operational log and any switches between water and bottom track modes.

9. ARGO Floats (Stuart-Menteth)

Five ARGO floats were deployed during the first leg of the cruise, starting at 10° N. They were then deployed at regular intervals of 2.5° to 3° latitude (see Table 14) as the ship travelled south towards the Seychelles. Dive times were calculated before the deployment to ensure that the floats would be at the surface transmitting data when the largest number of satellites were available. The floats could be activated six hours prior to the dive time and needed to be deployed in the water before the estimated dive time. After each deployment, the details of the ARGO float were emailed back to the SOC, where they checked that the ARGO float was transmitting properly. All the floats were deployed successfully.

10. Sea Surface Temperature (SST) Measurements (Stuart-Menteth)

Five different instruments measured SST during the cruise: the SISTeR radiometer, the 'soap' thermistor, a hull-contact sensor from WHOI, the ship's thermosalinograph (TSG) and the Expendable Bathy Thermograph's (XBTs). Each sensor measured SST at a different depth. Table 15 summarises the instruments and their measurements.

As Table 15 indicates, the depth of the 'soap' thermistor was variable. Most of the time the ship was steaming at 10 knots. However the ship was often slowed down to deploy deep XBTs (T5s) and ARGO floats, which caused the soap to sink to approximately 5 m. The ship frequently slowed down completely during the days of the mooring recoveries and in these cases the soap was raised as high as possible. In these circumstances the soap tended to be positioned about 2-3m below the surface and would gradually float up to the surface over an hour.

Two types of XBTs were used: T7 and T5 (Section 6). Data from the top 10 m of each XBT profile were analysed to provide a further comparison with the other SST sensors. The XBTs measure temperature at regular intervals of 0.6 m to 0.7 m (depending on XBT type) from a depth of 0.7 m onwards. At first the XBTs were deployed from the back of the ship, where the water is likely to be well mixed by the ship's wake. Mid-way through leg 2 the XBTs were deployed off the starboard side of the ship to try and avoid the mixed water. The mixing effect might also vary between the two XBT types since the ship slowed down for T5s.

Figure 20 shows the hourly averaged SST data for the four main sensors for leg1. The data has been despiked to remove any bad data. This was done by first rejecting SST data outside a threshold (22-32°C). However most of the spikes still remained. They were caused by the soap either sinking or being brought on deck. The temperatures were still within the threshold but created obvious spikes, so these data were removed manually. The temperature cycle has a very strong diurnal signal which reflects the calm, sunny conditions experienced during most of the cruise. Two-minute averaged SST data were used to compare the different SST sensors, though only the hourly averages are shown in the figures for visual reasons. There is a lot of small-scale variability in the signal, although this is not visible in the hourly plots because it has been averaged out. This variability (on timescales of minutes) was detected by nearly all the

sensors, implying that it must be a real feature. The variability is most likely due to natural patchiness caused by warming and wind effects. Only the WHOI-hull sensor failed to capture the same fine variability and this is most likely due to its time lag in recording the SST, making it smooth out any rapid changes in SST.

Figure 20 shows that the hull sensor, at 1 m depth, is consistently the warmest followed by the TSG and then the soap. These results are surprising given the conditions were so calm and warm. Therefore it is likely that some of the sensors have an offset. The SISTeR data is always cooler than the other measurements but this is expected as it is measuring the skin temperature of the ocean.

In order to inter-compare the sensors, only night-time data is considered since the daily warming produces a lot of scatter. This can be seen in Table 16 by comparing day and night standard deviations. The Table summarises the results of the intercomparison based on the two minute averaged data. The results are separated into day and night bins.

Figure 21 shows the temperature difference between the sensors for leg 1 and focuses on night-time conditions. The top figure show the differences in the hourly averaged data for leg 1 and reveals offsets between the instruments. The WHOI sensor has the greatest offset but this was expected from previous cruise experience. The sensor is affected by the heat of the ship's engine, producing warmer SSTs. The scatter plots compare the different sensors for night-time only. The hull sensor still experiences some scatter which is probably related to the instrument's lagged thermal response. The TSG and soap correlate very well.

In order to truly compare the sensors to establish if there is an offset between the soap and the TSG, data was analysed for two very rough days at the start of leg 2 (days 310 and 311). The winds were over 10 m/s so it was assumed that the upper 5 m would be well mixed and hence of a uniform temperature. The results, shown in Figure 22 and Table 17, confirm that an offset does exist between the TSG and soap. It was decided that the TSG was likely to be the most accurate because it was the superior sensor. Furthermore it had been calibrated at the start of the year. Therefore data from the soap and hull sensors were both adjusted to the TSG values: the soap was corrected by 0.1 °C and the WHOI hull sensor by – 0.41°C.

The corrected data were then compared with XBT data for the top 10 m. The XBT data were averaged into 1 m, 3 m, 5 m, 7 m and 10 m bins. The first four XBTs have a cold bias at the surface because they were stored in the air conditioned main lab and so were cooler than the SST. This caused the upper readings to be cool-biased as the XBT responded to the sudden increase in temperature. The 5th XBT onwards was stored outside, in the lab annexe, so that these XBTs were at the outside air temperature. Figure 23 shows the corrected hourly averaged SST data for leg 1 and most of leg 2. SISTeR data is not shown for leg 2 because it was not available at the time of processing. It will be looked at a later stage. All the sensors agree very well now except when the surface layer is warmed during the day. The soap tends to have the highest temperatures and sometimes peaks before the other sensors. Agreement between the XBT and other SST sensors is varied. In general the XBT data is cooler than the other sensors, which may be a

direct reflection of the mixing caused by the ship's wake. In some cases the 1m averaged XBT data is the coolest, so perhaps there is still some thermal lag effect even from XBTs stored at ambient air temperature.

10.1 The Diurnal Cycle of SST

Further analysis was carried out on the SST data to look at the diurnal cycle. Figure 24 shows some examples of days when there was a strong diurnal signal (Jdays 312, 314, 315 and 317). The peak of the warming occurs around 15h00 Local although in some cases the soap heats up earlier and reaches its maximum around midday. The soap can be up to 2°C warmer than the hull and TSG sensors at the peak of the cycle.

Figure 25 shows the diurnal SST amplitude (Tmax-Tmin) for days with an obvious signal. The local time for Tmax (daily maximum SST) was checked to make sure that it occurred during the afternoon and therefore was likely to be a diurnal signal. In a couple of cases, Tmax was observed during the night, which must be related to a change in water mass. Figure 25a shows the diurnal amplitude for the soap, hull and TSG sensor data. In almost every case, the soap has the largest range as one would expect since it is the closest to the surface. The TSG, at a depth of 5 m, still has quite a strong signal. Figure 25b shows that the soap also has the highest daily temperatures, although in some cases all three sensors have identical readings. At night (figure 25c) the minimum values are similar between the sensors.

Figure 26 shows the diurnal cycle in the XBT data. The example shown here is for day 315, when an XBT line was carried out across the Mozambique Channel from the Madagascan continental shelf to the Mozambique shelf. The XBTs were deployed from the starboard side of the ship, rather than from the back, to try and sample undisturbed water. The data were then averaged to produce mean SSTs for depths at 1 m, 3 m, 5 m, 7 m and 10 m. A mean value was computed for each depth and from that the SST anomaly over the diurnal cycle was calculated for each level. The different depths all follow a similar SST evolution; warming between 10h00 to 13h00. In this case, SST peaks around midday at all depths which is in contrast to the results from Figure 25. In Figure 25 although the soap peaks at midday the other sensors do not reach their maximum until around 15h00. This is not observed in the XBT data. Further analysis on these differences and the evolution of the diurnal cycle will be carried out back at the SOC using all the data.

10.2 Conclusions

- WHOI – Hull contact sensor is warm biased by 0.41°C
- The Soap has a cool bias of 0.1 °C
- The Soap and the TSG data correlate very well and reveal a lot of small-scale variability
- SISTeR's skin SST is cooler than the bulk SST measurements except during some extreme warming conditions.

- The XBT data has mixed agreement with the other SST data (further investigation is required)
- There is a very clear diurnal cycle during calm, sunny conditions.
- A thermal lag is sometimes noted between the different sensors, related to the depth of the measurement.

11. ATSR-2 Validation (Nightingale)

The ATSR-2 SST sensor on the ESA ERS-2 platform is now nearing the end of its operational life and will be superseded by AATSR on the ENVISAT platform at the beginning of 2002. The end-of-life validation of the ATSR-2 SST products is an important part of the ATSR-2 programme and is required to demonstrate both the consistency of the SST products and their continuity with those from the new AATSR instrument.

The RAL SISTeR (Scanning Infrared Sea surface Temperature Radiometer) instrument is a chopped, self-calibrating filter radiometer designed specifically to make in-situ measurements of the sea surface in support of the ATSR instruments. SISTeR S/N “Alice” was operated during CD135.

Immediately after unpacking on the 22nd October, SISTeR was calibrated against a CASOTS portable black body (Donlon *et al*, 1998) in the Darwin’s main laboratory. The CASOTS black body consists of a thin-walled copper cavity immersed in a water bath. The bath temperature was monitored with a Thermometrics AS125 thermistor, S/N 2228 and a Hart Scientific 1504 bridge S/N A14282. The combined accuracy of the thermistor and bridge was approximately 3 mK at room temperature. The water in the CASOTS water bath was circulated with a 50 W immersible pump, which doubled as a water heater, giving a temperature rise of approximately 3 K every hour. The deviation of the brightness temperature recorded by the SISTeR from the thermometric temperature of the water bath is shown in Figure 27. A straight-line fit to the difference data showed a deviation of order 5 mK and no significant gradient over the measurement interval. The noise temperature associated with each 0.8 s radiance sample recorded by SISTeR was 28 mK.

The SISTeR was mounted on the handrails on the port quarter of the Darwin’s foremast platform, immediately inboard of the access ladder and facing outwards over the bow about 40° from the centre line. The SISTeR scan mirror was stepped out from the ship at small angular increments and the first clear view to the sea was identified at approximately 22° from nadir. A sea view at 25° was chosen for the standard scanning sequence, along with sky views at 50°, 25° and 0° from zenith.

The first leg of CD135, north of the Seychelles, was planned to give the maximum number of opportunities for ATSR-2 validation measurements. The ATSR-2 swath was calculated from a reference orbit supplied by Berthyl Dusemann of ESA for a 501 orbit, 35 day repeat cycle and an ascending node-crossing time of 10:30:00 at 0.1335° E for the first orbit of the cycle. An IDL tool was written to plot the orbits and to overlay a ship’s track and calculate waypoint times. This tool was used both in the planning stages and during the cruise to modify the track in the light of local conditions.

The first leg departed the Seychelles on the 24th November and returned on the 3rd December. A total of nine overpasses were obtained during this leg. These are shown in Figure 28 and summarised in Table 18. The weather was generally good and the cloud cover low. Two ATSR-2 overpasses (2 and 3) could be ruled out through either rain or cloud while the remainder had either sparse cumulus “fluff balls” (1, 4, 7 and 8), or local cloud (5, 6 and 9) with the possibility of validations a short distance away from the immediate overpass point. Twenty GPS sondes, supplied by the UK Met Office, were released at the 6 am and 6 pm synoptic times during the first leg. These in general coincided quite closely with the ATSR-2 overpass times.

There were a further eight coincidences during the second leg, departing the Seychelles on the 5th December and arriving in Durban on the 18th December. These are shown in Figure 29 and summarised in Table 19. The weather was variable for the first four days, with occasional rain and heavier seas towards the end of this period. SISTeR was not operated for the majority of this time and overpass 10 was missed through bad weather. The final four days were characterised by increasing winds (30 knots and more approaching Durban) along with big seas and occasional rain. SISTeR was operated for the majority of this period, but the final overpass was most likely cloudy. Of the remainder, one was cloudy (12), and the others (11, 13 – 16) were clear overhead but characterised by “fluff balls” and nearby cloud.

The high seas at the end of CD135, combined with the very limited time available for derigging, precluded a second calibration before SISTeR was packed for return to the UK.

12. Radiosonde Atmospheric Profiles (Marshall)

Twenty Vaisala RS80-15G radiosondes were provided by the U.K. Met Office to be launched during the first leg of the cruise at 05:15 and 17:15 GMT daily. The radiosondes measured the temperature and water vapour structure of the atmosphere and also (intermittently) wind speed and direction. At the end of each flight, typically two hours after launch, a TEMP message was sent to the Met Office to be incorporated into their forecasting models. Data were acquired via an RS232 connection from a PC to a DigiCORA MW15 GPS receiver with “TEMP Grabber” and “GPS Sonde” used during each flight to produce a real-time display and to log files of PTU (pressure, temperature and humidity), raw wind data and to produce an averaged profile file.

Out of twenty radiosonde flights, three resulted in no TEMP message being sent. This appears to have been a problem associated with the DigiCORA receiver but it is unclear why the receiver rejected some flight profiles when others, which looked very similar, were accepted. All that could be done was to reset the receiver and go into Research mode. Although this did not provide a TEMP message it did allow the data from the remainder of the flight to be logged (PTU, raw). As there were only 20 radiosondes available no repeat flights were undertaken (see Table 5).

When undertaking the ground check to calibrate the radiosondes, one radiosonde showed a relative humidity of 35% when it should have read close to zero. It is believed that the receiver may have been

reading the calibration tape incorrectly since after a second calibration of the original radiosonde, the humidity was shown as 1%. During the flight some of the humidity data plotted on-screen was not logged. There were also discrepancies between the data shown on-screen and what data was actually logged. Occasionally the “GPSonde” program indicated that no data was being collected when the data could clearly be seen being logged in the “TEMP Grabber” window. Care must be taken when quitting “GPSonde”: use the “quit” button and don’t simply close the window as this may result in the program hanging.

The balloons were inflated in a specially designed restrainer which held them securely even in the strongest winds. Launches taking place during relatively wind free conditions did not require the ship to change course but it was deemed necessary on occasions when high winds may have blown the radiosonde and balloon dangerously close to the A-frame on the aft deck of the ship. Eighteen of the 20 radiosondes got above 70 mbar and all, except one, recorded wind data. In general, wind data was recorded intermittently but there was enough data to allow interpolation of the missing values.

The data were logged into a PC before being transferred to a SUN station where they were converted into PSTAR format. It was then relatively straightforward to obtain plots of temperature, specific humidity, wind speed and direction as a function of pressure. The data were then despiked and interpolated at 5 mbar intervals and contour-plotted for distance run versus altitude and latitude versus altitude.

The sonde profiles were incorporated into radiative transfer models to compare the calculated top of the atmosphere (TOA) radiances with those obtained from the ATSR-2 instrument on ERS-2. Most of the work onboard was associated with RTTOV6 but the profiles were also incorporated into the RFM at a later date. RTTOV6 is a fast radiative transfer model derived from GENLN2. Unfortunately, there was little coincidence between clear skies and ATSR-2 overpasses so comparisons of near real time brightness temperatures (BTs) with actual measured SSTs or RTTOV-derived brightness temperatures were limited. Subsequently the SSTs, as derived from the predicted ATSR-2 brightness temperatures obtained from the model, were compared with ship-measured SSTs. The model produced SSTs that were consistently within 0.1C of the actual measured SSTs.

RTTOV6 was believed to have been very sensitive to the specific humidity profile used but it appears that the importance of having a rigorous specific humidity profile was exaggerated with widely differing profiles resulted in similar (within 0.1C) predicted BTs. Conversion from BTs to SSTs is dependent upon the viewing angle and location within the overpass swath. The lack of strong overpass candidates resulted in an averaged SST being used for comparisons with the measured SSTs. The lack of sonde measurements at the higher levels (up to 0.1 mbar) required for the input file resulted in extrapolated values being used. The model is not very sensitive to the values at the higher levels and, providing the extrapolated values were sensible, there was little impact on the obtained BTs. What, unsurprisingly, had a large impact on the model output was the assumption that the emissivity of the ocean was 1. Calculating the emissivity for the various viewing angles gives a range of emissivities from 0.965-0.99. Using the corrected values for the emissivities gives good agreement between the calculated SSTs and observation (see fig 30).

From this short investigation, it appears that RTTOV6 is a fast and effective model with which to calculate TOA radiances and subsequently SST.

13 Mooring Recovery Deck Operations (Waddington, Scott)

The NIOZ ACSEX moorings were all coated wire moorings with lengths varying from 2200 m to 30 m, all buoyed by glass spheres from the top of the moorings and with no back up buoyancy. A scheme for recovery had been arranged at SOC, prior to the cruise, which utilised the recently revised OED Double Barrel Capstan (DBC) winch system with associated reelers to permit rapid recovery of the moorings with minimal winding-off time between moorings. The DBC system was set up to operate with one reeler equipped with either steel or wooden drums and a second reeler unit positioned as a standby unit as required. The system used operates from the ship's hydraulic supply and was assembled and tested prior to departure from the Seychelles.

Discussions were held prior to the recovery of the first mooring as to who would be included as part of the recovery team as well as recovery and instrument procedures. This team then operated as planned throughout all the mooring operations. Radio communications were maintained during all operations with the ship's Bridge Officers in order to adjust the ship's speed and the wire angle. Mooring release was initiated by NIOZ and a combined NIOZ, OED and Ship's team then recovered the moorings.

The mooring, once sighted on the surface, was brought alongside by manoeuvring the ship so that recovery of the mooring could be initiated by grappling from midships and attaching the (buoyant) winch recovery rope to the floating mooring recovery line. The mooring was then passed astern to be hauled onboard by the DBC, hauling through a wide throat sheave attached to the stern mounted starboard EFFER crane. Periodically the mooring was stopped off to allow the removal of buoyancy and instrumentation by the use of a deck mounted chain and BOSS hook. Before hauling the long strings of buoyancy onboard the floating rope was removed from the winch and replaced by steel wire rope. This reduced the spring in the line and provided increased strength which improved the safety factor while lifting the buoyancy overhead. The long strings of glass buoyancy were recovered in sections, stopping off to remove sections as necessary. This involved control of both the ship's crane and winch to optimise positioning of the glass spheres. Instrumentation was recovered by conventional SOC stopping off procedures .

On only one mooring, ACS11, were problems encountered. This short mooring comprising marker float, ADCP float and acoustic releases surfaced with the mooring wire entangled. By stopping off parts of the wire under low load, using a rope stopper, it was possible to disconnect the marker and ADCP buoyancy and to haul several parts of the wire onto the DBC to recover the acoustic releases.

The recovered mooring wire was stored either directly onto steel reeler drums or wound off to wooden drums . For the longer moorings this involved changing drums on the reeler whilst the mooring was stopped off. This procedure took around 5 minutes .

Some minor modifications will be required to the winch system for future operations and a report has been submitted to OED regarding these items.

14 Mooring recovery (Ridderinkhof)

14.1. Introduction

The Agulhas Current Sources Experiment (ACSEX) is a joint research programme from the Institute for Marine and Atmospheric Research of Utrecht University (IMAU), the Netherlands Institute for Sea Research (NIOZ) and the University of Cape Town (UCT). The purpose of ACSEX is to study the current field in Mozambique Channel. In the past hardly any observations in this region, which might be an important source region for the Agulhas Current, had been obtained.

In March 2000 the first ACSEX cruise was carried out during which hydrographic sections were obtained in Mozambique Channel and an array of current meter moorings was deployed at its narrowest section. During the second ACSEX cruise in March 2001 the array of current meter moorings was recovered; the instruments were serviced and the array was redeployed at the same location. Both ACSEX cruises were carried out with the Dutch RV Pelagia.

The final recovery of the current meter moorings was done with the British vessel RRS Charles Darwin during the cruise CD135. Below, first the recovery of the moorings is described, followed by some first results of the current meter observations.

Ship time for the recovery of the moorings and the opportunity to participate on the RRS Charles Darwin cruise CD135 was kindly funded and made possible by NERC. Ian Waddington and Jason Scott, both from SOC, prepared the equipment for the mooring recovery (winches etc) and participated during the cruise in leading the recovery of the moorings. Their skills, combined with the skills of the experienced crew from the RRS Charles Darwin, meant that the recovery of the moorings (if released) was very smooth and successful. Robin Pascal, chief scientist on this cruise, was very helpful before and during the cruise. Especially his patience, ‘sensitivity’ to our ‘release problems’ and willingness to allow us one extra day of ship time for a search for lost moorings was a great experience (happily we could recover one of the two lost moorings during that extra day). We thank all crew members and scientists on cruise CD135 for a pleasant stay.

14.2. Recovery of the moorings

Figure 35 shows the position of the moorings at the narrowest cross-section in the Mozambique Channel. RRS Charles Darwin arrived at the first mooring to be recovered, ACS17 (see figure 35), on Friday November 9th, after roughly 4.5 days of transit from the port of Victoria at the Seychelles. Mooring ACS17 was recovered successfully in the late afternoon. In the evening of the same day, the RRS Charles Darwin sailed to mooring ACS16 where contact was made with both acoustic releases. Early in the

morning of Saturday November 10th, mooring ACS16 was released and the mooring was recovered successfully. On the same day, at noon, RRS Charles Darwin arrived at the deployment position of mooring ACS15. Here, there was no response from both acoustic releases. The remainder of the day, until midnight, was used to carry out an acoustic survey around the deployment site. A transect with a length of roughly 10 nm was made in all directions with an ‘acoustic station’ at about every 2 nm. No response from the releases was obtained. At midnight this acoustic survey was finished and on Sunday November 11th, at sunrise, RRS Charles Darwin arrived at the location of mooring ACS14. The releases of mooring ACS14 were released successfully and the recovery of this mooring was finished early in the morning. Later in the morning we arrived at mooring ACS13. The releases of ACS13 did not give a response. RRS Charles Darwin continued on and arrived at mooring ACS12 by early afternoon. This mooring was released successfully. Finally, we arrived at the location of mooring ACS11 in the late afternoon and finished the recovery of this short mooring at before sun set.

Then, RRS then Charles Darwin sailed back to the deployment position of mooring ACS13 to start an acoustic survey. This survey began just before midnight using the transducer of the ‘fish’ of the RRS Charles Darwin and the NIOZ transmission unit (this enabled continuous transmission and reception of acoustic signals). The survey started 5 nm to the north of ACS13 and headed towards the deployment position of ACS13. The main transect of this survey was from this deployment position to the SSW of ACS13 (the direction of the strongest currents) and continued to 28 nm of ACS13. Here some additional transects perpendicular and parallel to the main transect between 20 and 28 nm from the mooring were carried out. No contact with both releases could be obtained during this survey. On Monday November 12th, early in the morning, RRS Charles Darwin sailed back to the deployment position of ACS13 to dredge around the deployment site (motivated by the possibility that both acoustic releases did not function). While paying out the dredging cable a fax arrived at the Charles Darwin mentioning that the ARGOS unit from mooring ACS15 had been located at the surface. Subsequently, the dredging preparations were cancelled and RRS Charles Darwin sailed to the position where ACS15 had been located most recently. Late in the afternoon mooring ACS15 was found, with its top drifting at the surface. The recovery of mooring ACS15 was finished just before sunset and RRS Charles Darwin continued its original scientific programme by sailing southwards.

The track of the drifting mooring ACS15 and its first location after reaching the surface clearly showed that this mooring had been released at roughly 12 nm away from the position of deployment. Apparently the mooring had drifted over this distance during the period of deployment. Our conclusion is that the anchor weight of this mooring has been too small. Most presumably this is also the case for mooring ACS13 which could not be found. (Apparently the train wheels which had been bought in Cape Town for this deployment, were slightly lighter than the train wheels which were used for the first deployment period).

Table 20. summarises the activities during the recovery of the ACSEX moorings as part of the CD 135 cruise.

14.3. Functioning of the instruments

Figure 36 shows the instruments that were deployed in the mooring array. The encircled instruments (solid lines) were either lost (moorings ACS13) or did not function. One of the current meters on mooring ACS14 leaked and failed. The Data Storage Unit (DSU) of one of the other current meters of this mooring, the second one from the top, did not function normally and has a large number of suspect records. Repair of the data may be possible. The ADCP on the top of mooring ACS12 was heavily damaged when it was recovered. The damage suggests that this ADCP had ‘exploded’ during the deployment period.

Further details on the instruments can be found in Table 21.

14.4. First results

Figure 37 shows raw data from a current meter from mooring ACS15, the second one from the top which was deployed at some 400 m from the surface.

Both the current speed and direction suggest that important contributions to the time variability come both from relatively large time scales (associated with passing eddies) and relatively small time scales (tides). This is also clear from the spectra of the current speed (not shown) which show clear peaks at periods of 50-100 days and the diurnal and semi diurnal time scale. At this location the current speed due to the eddies reaches some 40 cm/s and the tidal current speed is some 10 cm/s.

Figure 38 shows low pass currents from the current meter at 400 m and at 650 m, again both from mooring ACS15. Both the low pass current speed and direction for both current meters look very similar and clearly show currents due to the passing of a large scale eddy. These currents are qualitatively similar to the currents that have been observed during the first deployment period from March 2000 to March 2001.

Finally, figure 39 shows low pass currents from the current meters which were deployed at 100 m above the bottom, from mooring ACS15 and ACS14. At mooring ACS 15, which was deployed above a ridge in the centre of the Mozambique Channel, the near bottom current is mainly in a south-west direction; the mean current speed over the entire period is some 5 cm/s. At mooring ACS14, where the near bottom current meter was deployed in the deepest part of the cross section, the near bottom current is mainly in a north-east direction, with a mean current speed of 4.5 cm/s. In this part of the cross-section North Atlantic Deep Water (NADW) was found during the previous ACSEX cruises. Thus these observations suggest that NADW flows more or less continuously towards the equator through the Mozambique Channel.

15. References

AutoFlux group, 1996: AutoFlux - an autonomous system for monitoring air-sea fluxes using the inertial dissipation method and ship mounted instrumentation. Proposal to MAST research area C - Marine Technology, 38 pp. + appendices

Bignami, F., S. Marullo, R. Santoleri and M. E. Schiano, 1995: Longwave radiation budget in the Mediterranean Sea. *J. Geophys. Res.*, **100**(C2), 2501 - 2514.

Clark, N. E., L. Eber, R. M. Laurs, J. A. Renner and J. F. T. Saur, 1974: Heat exchange between ocean and atmosphere in the eastern North Pacific for 1961 - 71. *NOAA Tech. Rep. NMFS SSRF-682*, U.S. Dept. of Commer., Washington, D.C., 108.

Donlon, C.J., Keogh, S.J., Baldwin, D.J., Robinson, I.S., Ridley, I., Sheasby, T., Barton, I.J., Bradley, E.F., Nightingale, T.J. and Emery, W., 1998: Solid state radiometer measurements of sea surface skin temperature, *Journal of Atmospheric and Oceanic Technology*, 15, 775-787.

Josey, S. A., D. Oakley and R. W. Pascal, 1997: On estimating the atmospheric longwave flux at the ocean surface from ship meteorological reports. *J. Geophys. Res.*, **102** (C13), 27961 - 27972.

Josey, S.A., E.C. Kent and P.K. Taylor: 1999 New insights into the ocean heat budget closure problem from analysis of the SOC air-sea flux climatology. *Journal of Climate*, 12, 1999, 2856-2880.

Josey, S.A., R. W. Pascal, P. K. Taylor and M. J. Yelland, 2002: A new formula for determining the atmospheric longwave flux at the ocean surface at mid-high latitudes. *Submitted to J. Geophys. Res.*

Pascal, R. W. and S. A. Josey, 2000: Accurate radiometric measurement of the atmospheric longwave flux at the sea surface. *J. Atmos. Oceanic Technol.*

Pascal, R. W., M. J. Yelland and C. H. Clayson, 2000: The AutoFlux logging system - draft handbook. *James Rennell Division, Southampton Oceanographic Centre, Southampton, U. K.*

Tragou, E., C. Garrett, R. Outerbridge, C. Gilman, 1999: The Heat and Freshwater Budgets of the Red Sea. *Journal of Physical Oceanography*, 29 (10), 2504-2522

Yelland, M.J. and R. W. Pascal, 2000: RRS "James Clark Ross" Cruise, 11 Sep-17 Oct 2000. AutoFlux trials cruise, UK to Falklands Passage, *Southampton Oceanography Centre Cruise Report*, No.

16. Tables

| Sensor | Channel, variable name | Address | Serial No. | Calibration $Y = C0 + C1*X + C2*X^2 + C3 *X^3$ | Sensor position | Parameter (accuracy) |
|---------------------------------|------------------------|---------|---------------|---|---|---|
| Psychrometer | 1 pdp1 | \$ARD | IO2002 DRY | C0 -11.03127 C1 4.117637E-2 C2 -1.773013E-6 C3 1.595187E-9 | Foremast platform, to port of HS sonic | Wet and dry bulb air temperatures and humidity (0.05°C) |
| Psychrometer | 2 pwp1 | \$ERD | IO2002 WET | C0 -10.70357 C1 4.104128E-2 C2 -1.631621E-6 C3 1.527643E-9 | | |
| Psychrometer to day 312 0600h | 3 pds2 | \$VRD | HS1020 DRY | C0 -1.405749 C1 3.85345E-2 C2 1.848178E-6 C3 4.793964E-11 | Foremast platform, to stbd. of HS sonic | Wet and dry bulb air temperatures and humidity (0.05°C) |
| Psychrometer to day 312 0600h | 4 pws2 | \$WRD | HS1020 WET | C0 -1.443511 C1 3.93881E-2 C2 6.668183E-7 C3 5.882345E-10 | | |
| Psychrometer from day 312 0600h | 3 pds2 | \$VRD | IO2003 | C0 -10.90536 C1 4.055126E-2 C2 -9.616976E-7 C3 1.271695E-9 | Foremast platform, to stbd. of HS sonic | Wet and dry bulb air temperatures and humidity (0.05°C) |
| Psychrometer from day 312 0600h | 4 pws2 | \$WRD | IO2003 | C0 -10.78525 C1 4.120784E-2 C2 -1.935707E-6 C3 1.718843E-9 | | |
| SST "soap" | 5 soap sst | \$XRD | PD0010 / 53 | C0 55.33283 C1 -8.80405E-2 C2 9.854325E-5 C3 -8.722052E-8 | Trailing over port side of foredeck | Sea surface temperature (0.1°C) |
| Epply LW Dome | 6 Td1 | \$HRD | 31170 | C1 1 | Top of foremast platform, forwards position | Incoming longwave radiation |
| Body | 7 Ts1 | \$BRD | 31170 | C1 1 | | |
| Thermopile | 8 E1 | \$2RD | 31170 | C1 1 | | |
| Epply LW Dome | 9 Td2 | \$QRD | 27225 | C1 1 | Top of foremast platform, aft position | Incoming longwave radiation |
| Body | 10 Ts2 | \$6RD | 27225 | C1 1 | | |
| Thermopile | 11 E2 | \$CRD | 27225 | C1 1 | | |
| Kipp and Zonen SW1 | 12 SWp | \$1RD | 902836 | C1 0.2203 | Foremast platform, port side | Incoming shortwave radiation |
| Kipp and Zonen SW2 | 13 SWs | \$3RD | 903289 | C1 0.2045 | Foremast platform, stbd side | Incoming shortwave radiation |
| Vaisala Pressure | 14 press | N/A | | 1 | Scientific plot | Air pressure |
| WHOI hull sst | 15 sstMEAN | N/A | | N/A | Port side of engine room | Sea surface temperature |

Table 1. The mean meteorological sensors. The columns show, from left to right; sensor type, channel number, Rhopoint address, serial number of instrument, calibration applied, position on ship and the parameter measured (after Yelland and Pascal, 2000).

| Sensor | Program | Location | Data Rate | Sections | Derived flux |
|---|---------|-------------------------------------|-----------|----------|--------------------------------------|
| Gill Horizontally Symmetrical (HS) Research Ultrasonic Anemometer | Gillhs | Starboard side of foremast platform | 20 Hz | 64 | Momentum and heat |
| IFM IR H ₂ O/CO ₂ sensor | Ifmhs | Starboard side of foremast platform | 10 Hz | 32 | H ₂ O and CO ₂ |

Table 2. The fast response sensors

| Instrument | Acquisition Program | Position | Sampling Rate | Parameters |
|-----------------------------|---------------------|--|---------------|---|
| CSI LGBX – PRO GPS receiver | gps6 | Aerial on port railing of wheel house deck | 1 or 0.5 Hz | GPS time, lat, lon, sog, cog and QC information |
| KVH fluxgate compass | gps6 | Scientific plot | 1 Hz | Ship's heading (magnetic) |

Table 3. The navigation instruments.

| Measurement (units) | Mean (units) | Standard deviation of mean | Mean difference between sensors | Standard deviation of mean |
|-------------------------------------|------------------|----------------------------|---------------------------------|----------------------------|
| LW radiation (W m ⁻²) | 411 | 0.084 | -0.35 | 0.065 |
| SW radiation (W m ⁻²) | 504 ¹ | 4.066 | 12 | 0.906 |
| Dry bulb (deg C) | 27.52 | 0.006 | 0.10 | 0.013 |
| Wet bulb (deg C) | 24.06 | 0.005 | -0.02 | 0.012 |
| Dry bulb (deg C), excluding day 297 | 27.54 | 0.004 | -0.03 | 0.001 |
| Wet bulb (deg C), excluding day 297 | 24.04 | 0.003 | -0.15 | 0.000 |

Table 4. The mean values of the observations for leg1 and the mean differences between the sensors.

¹ The maximum short-wave readings from the two sensors have been used to calculate this value.

| Flight | JDay | Launch time (GMT) | Filename | Latitude (N/S) | Longitude E | Pressure (Bridge-sonde) | Temp (GC-sonde) | Hum (sonde) | Cap On | Burst Pressure | Comments |
|--------|------|-------------------|----------|----------------|-------------|-------------------------|-----------------|-------------|--------|----------------|--|
| 1 | 298 | 05:15 | 2980515 | 0°21.6 S | 55°27.6 | -0.3 | -0.1 | 2 | Y | 31.8 | |
| 2 | 298 | 17:26 | 2981726 | 1°57.2 N | 55°30.0 | -0.1 | -0.2 | 1 | Y | 34.1 | |
| 3 | 299 | 05:26 | 2990526 | 2°17.8 N | 57°22.3 | 0.0 | 0.0 | 1 | Y | 49.7 | |
| 4 | 299 | 17:22 | 2991722 | 2°16.0 N | 59°20.1 | 0.2 | 0.0 | 1 | Y | 217.9 | |
| a | 300 | 05:28 | 3000528 | 3°34.4 N | 60°00.5 | 0.3 | 0.1 | 1 | Y | 50 | Rain. No TEMP message. |
| 6 | 300 | 17:15 | 3001715 | 5°02.4 N | 60°53.4 | 0.3 | -0.2 | 1 | Y | 185 | |
| 7 | 301 | 05:23 | 3010523 | 6°38.9 N | 61°40.1 | 1.2 | 0.0 | 1 | N | 26.5 | No TEMP message. |
| 8 | 301 | 17:07 | 3011707 | 8°09.7 N | 61°05.2 | 0.7 | 0.0 | 1 | N | 43 | |
| 9 | 302 | 05:08 | 3020508 | 9°56.9 N | 60°19.5 | 0.1 | -0.3 | 1 | Y | 25 | |
| 10 | 302 | 16:42 | 3021642 | 8°25.8 N | 60°28.1 | 0.5 | 0.0 | 2 | Y | 62.8 | |
| 11 | 303 | 05:26 | 3030526 | 8°27.1 N | 62°26.2 | -0.1 | -0.3 | 1 | Y | 26.4 | No TEMP message. |
| 12 | 303 | 17:02 | 3031702 | 8°27.2 N | 64°25.1 | 0.6 | -0.3 | 2 | Y | 29.2 | |
| 13 | 304 | 05:06 | 3040506 | 7°09.5 N | 63°19.5 | 0.1 | -0.2 | 1 | Y | 40 | Tether didn't unwind properly. |
| 14 | 304 | 16:59 | 3041659 | 5°58.5 N | 62°05.4 | 0.3 | 0.0 | 1 | Y | 53.7 | |
| 15 | 305 | 05:02 | 3050502 | 4°32.8 N | 60°38.7 | 0.1 | 0.0 | 1 | Y | 40 | |
| 16 | 305 | 16:58 | 3051658 | 3°13.9 N | 59°15.6 | 0.0 | -0.1 | 2 | Y | 26.7 | |
| 17 | 306 | 05:02 | 3060502 | 1°45.0 N | 57°59.0 | 0.0 | -0.2 | 0 | Y | 36 | |
| 18 | 306 | 16:52 | 3061652 | 0°10.3 S | 58°00.0 | 0.0 | -0.2 | 0 | Y | 31.1 | |
| 19 | 307 | 05:21 | 3070521 | 1°59.1 S | 57°27.4 | -0.1 | 0.2 | 1 | Y | 30.4 | |
| 20 | 307 | 16:50 | 3071650 | 3°19.8 S | 55°57.6 | -0.1 | 0.0 | 0 | Y | 36 | Humidity GC error. Corrected by repeat calibration. Humidity shown on-screen but not logged. |

Table 5. Radiosonde LOG SHEET 1

| Drop No. | Day | Lat | Long | Depth (m) | Spd sog (knots) | Course cog | Wind Dir | Wind Spd (knots) | SST | Launch time(gmt) | Launch Lat | Launch Lon | Type |
|----------|-----|-----------|-----------|-----------|-----------------|------------|----------|------------------|------|------------------|------------|------------|------|
| 001 | 297 | 03 17.70S | 055 27.8E | 2500 | | | | | 28.5 | 1249 | 03 17.70S | 055 27.8E | T7 |
| 002 | 297 | 01 30.00S | 055 27.4E | 4500 | 11.0 | 002 | 040 | 3.6 | 28.0 | 2220 | 01 28.43S | 055 27.4E | T7 |
| 003 | 298 | 01 00.00S | 055 27.3E | 4500 | 10.9 | 359 | 000 | 6.7 | 28.0 | 0059 | 01 00.20S | 055 27.3E | T7 |
| 004 | 298 | 00 30.00S | 055 27.3E | 4500 | 10.9 | 000 | 023 | 5.3 | 28.1 | 0349 | 00 30.15S | 055 27.3E | T7 |
| 005 | 298 | 00 00.00N | 055 27.4E | 1000 | 11.0 | 002 | 050 | 6.0 | 28.7 | 0655 | 00 02.49N | 055 27.4E | T7 |
| 006 | 298 | 00 30.00N | 055 27.6E | 1000 | 11.0 | 358 | 040 | 7.4 | 28.9 | 0920 | 00 30.00N | 055 27.6E | T7 |
| 007 | 298 | 01 00.00N | 055 27.5E | 1000 | 11.2 | 359 | 035 | 6.7 | 29.0 | 1203 | 01 00.10N | 055 27.5E | T7 |
| 008 | 298 | 01 30.00N | 055 27.5E | 3000 | 11.0 | 000 | 060 | 8.9 | 28.4 | 1447 | 01 30.00N | 055 27.5E | T7 |
| 009* | 298 | 02 00.00N | 055 27.3E | 3000 | 9.2 | 290 | 035 | 8.9 | 28.4 | 1753 | 01 59.00N | 055 27.6E | T7 |
| 010 | 298 | 02 00.00N | 055 27.5E | 3000 | 9.2 | 290 | 035 | 8.9 | 28.5 | 1816 | 02 00.30N | 055 27.5E | T7 |
| 011 | 302 | 10 00.00N | 060 17.8E | 4000 | 2.0 | 046 | 063 | 6.0 | 28.8 | 0555 | 10 00.30N | 060 18.1E | T5 |
| 012 | 302 | 10 00.00N | 060 23.3E | 4000 | 2.0 | 090 | 070 | 5.1 | 28.6 | 0647 | 09 59.90N | 060 24.1E | T5 |
| 013 | 302 | 09 59.00N | 060 24.1E | 4000 | 5.0 | 090 | 070 | 5.1 | 28.6 | 0658 | 09 59.90N | 060 25.4E | T5 |

Notes 1) Drop 001 was a test but data is good. Only have approximate coordinates.

- 2) Drops 001-003 are likely to have a cold bias as the XBT's were initially stored in an air-conditioned lab. The box of XBT's was moved after drop 3 but drop 4 appears to have still been affected. For these drops, data is good after 5m
- 3) Drop 009 is a bad XBT. The XBT malfunctioned and the instrument didn't measure correctly. It gave a constant temperature profile. Therefore drop 010 was carried out immediately afterwards. So ignore data from drop 009.
- 4) Depths are very crude as we had to refer to a bathymetric chart. Drops 005 to 007 were around a sea mount so depth may be shallower or deeper than the depth given.
- 5) Drop 012 was incorrectly set to T7 instead of T5, data still obtained to about 800m but followed directly by repeat T5 drop.

Table 6. XBT LOG SHEET 1 for Day 298 First equator Crossing (S to N) XBT line and XBT's at 10N

| No. | XBT type | Lat | Long | Depth (m) | Spd sog (knots) | Course cog | Wind Dir (-180) | Wind Spd (knots) | SST | Time & day (gmt) | Launch Lat | Launch Lon | WHOI SST | TSG SST |
|-----|----------|---------|---------|-----------|-----------------|------------|-----------------|------------------|-------|------------------|------------|------------|----------|---------|
| 14 | T5 | 04 00 N | 60 00 E | 2000 | 10.7 | 224 | 190 | 3.2 | 30.92 | 305 1008 | 04 00 N | 60 02.37 E | - | - |
| 15 | T7 | 03 00 N | 59 00 E | 700 | 10.4 | 225 | 195 | 5.3 | 39.53 | 305 1910 | 03 00 N | 59 01.4 E | - | - |
| 16 | T5 | 02 00 N | 58 00 E | 4300 | 5.0 | 224 | 155 | 7.2 | 28.9 | 306 0350 | 01 59.8 N | 58 00 E | - | - |
| 17 | T7 | 01 45 N | 58 00 E | 4710 | 10.3 | 181 | 250 | 10.6 | 29.1 | 306 0520 | 01 45 N | 58 00 E | - | - |
| 18 | T5 | 01 30 N | 58 00 E | 4730 | 10.3 | 181 | 180 | 14.5 | 29.4 | 306 0650 | 01 30 N | 58 00 E | - | - |
| 19 | T7 | 01 15 N | 58 00 E | 4700 | 9.5 | 179 | 192 | 12.5 | 29.6 | 306 0820 | 01 15 N | 58 00 E | - | - |
| 20 | T5 | 01 00 N | 58 00 E | 4700 | 10.3 | 180 | 196 | 11.0 | 30.2 | 306 0950 | 01 00 N | 58 00 E | 30.50 | 28.83 |
| 21 | T7 | 00 50 N | 58 00 E | 4700 | 8.7 | 180 | 196 | 12.5 | 30.0 | 306 1055 | 00 50 N | 57 59.9 E | 30.39 | 29.94 |
| 22 | T5 | 00 40 N | 58 00 E | 4720 | 8.6 | 180 | 194 | 11.0 | 29.84 | 306 1205 | 00 40 N | 58 00 E | 30.22 | 29.85 |
| 23* | T7 | 00 30 N | 58 00 E | 4720 | 10.1 | 180 | 209 | 11.6 | 29.5 | 306 1315 | 00 30 N | 58 00 E | 30.03 | 29.56 |
| 23 | T5 | 00 20 N | 58 00 E | 4716 | 10.0 | 170 | 201 | 11.9 | 29.34 | 306 1407 | 00 20 N | 58 00 E | 29.82 | 29.44 |
| 24* | T7 | 00 10 N | 58 00 E | 4714 | 9.5 | 180 | 196 | 12.1 | 29.1 | 306 1510 | 00 10 N | 58 00 E | - | - |
| 24 | T7 | 00 09 N | 58 00 E | 4714 | 9.5 | 180 | 196 | 12.1 | 29.1 | 306 1520 | 00 09 N | 58 00 E | - | - |
| 25 | T5 | 00 00 N | 58 00 E | 4706 | 9.6 | 180 | 191 | 11.2 | 29.1 | 306 1620 | 00 00 N | 58 00 E | 29.56 | 29.22 |
| 26 | T7 | 00 10 S | 58 00 E | 4662 | 10.2 | 180 | 180 | 11.9 | 29.0 | 306 1720 | 00 10 S | 58 00 E | 29.45 | 29.08 |
| 27 | T7 | 00 20 S | 58 00 E | 4701 | 10.2 | 180 | 170 | 10.0 | 29.0 | 306 1817 | 00 20 S | 58 00 E | 29.46 | 29.10 |
| 28 | T7 | 00 30 S | 58 00 E | 4699 | 10.5 | 180 | 170 | 10.6 | 28.9 | 306 1915 | 00 30 S | 58 00 E | 29.41 | 29.04 |
| 29 | T7 | 00 40 S | 58 00 E | 4605 | 10.4 | 180 | 178 | 10.0 | 29.0 | 306 2012 | 00 40 S | 58 00 E | 29.50 | 29.22 |
| 30 | T7 | 00 50 S | 58 00 E | 4589 | 10.4 | 180 | 183 | 9.0 | 29.0 | 306 2109 | 00 50 S | 58 00 E | 29.49 | 29.14 |
| 31 | T5 | 01 00 S | 58 00 E | 4548 | 10.4 | 180 | 171 | 11.5 | 29.0 | 306 2210 | 01 00 S | 58 00 E | 29.51 | 29.17 |
| 32 | T7 | 01 15 S | 58 00 E | 4528 | 10.8 | 180 | 169 | 13.1 | 29.0 | 306 2335 | 01 15 S | 58 00 E | 29.52 | 29.20 |
| 33* | T5 | 01 30 S | 58 00 E | 4500 | 10.6 | 180 | 170 | 13.0 | 29.1 | 307 0103 | 01 29.5 S | 58 00 E | 29.56 | 29.24 |
| 33 | T5 | 01 30 S | 58 00 E | 4500 | 10.6 | 180 | 170 | 13.0 | 29.1 | 307 0103 | 01 30.5 S | 58 00 E | 29.56 | 29.24 |
| 34 | T7 | 01 45 S | 57 44 E | 4500 | 10.3 | 230 | 150 | 14.5 | 29.0 | 307 0325 | 01 45.2 S | 57 43.0 E | - | - |
| 35 | T5 | 02 00 S | 57 26 E | 4500 | 10.3 | 230 | 190 | 13.5 | 28.9 | 307 0535 | 02 00.2 S | 57 25.0 E | - | - |
| 36 | T7 | 02 30 S | 56 53 E | 4300 | 11.1 | 230 | 145 | 12.6 | 29.0 | 307 1010 | 02 31.0 S | 56 52.3 E | - | - |

Table 7. XBT LOG SHEET 2 for Days 305-307 Second Equator Crossing (N to S) section.

* Drop No.'s 23,24 and 33 all crashed during processing with complete loss of data. Drops 24 and 33 were repeated at the same latitude but Drop 23 was not.

| Drop No. | XBT type | Lat | Long | Depth (m) | Spd sog (knots) | Course cog | Wind Dir (-180) | Wind Spd (knots) | SST | Time & day (gmt) | Launch Lat | Launch Lon |
|----------|----------|-----------|-----------|-----------|-----------------|------------|-----------------|------------------|-------|------------------|------------|------------|
| 37 | T7 | 17 17.5 S | 043 09.6E | 410 | 10.3 | 182 | 211 | 8.3 | 28.40 | 313 1327 | 17 17.4 S | 43 09.7 E |
| 38 | T7 | 17 14.4 S | 042 59.0E | 1552 | 10.7 | 290 | 179 | 15.2 | 28.45 | 313 1535 | 17 14.1 S | 42 59.0 E |
| 39* | T5 | 17 12.0 S | 042 50.2E | 1800 | 4.3 | 293 | 179 | 10.4 | 28.58 | 313 1640 | 17 12.0 S | 42 49.9 E |
| 40 | T7 | 17 05.5 S | 042 23.0E | 2200 | 11.3 | 286 | 190 | 8.5 | 29.06 | 314 0734 | 17 05.3 S | 42 23.0 E |
| 41 | T5 | 16 58.6 S | 041 56.0E | 1988 | 12.2 | 282 | 200 | 9.2 | 29.39 | 314 0952 | 16 59.1 S | 41 55.9 E |
| 42 | T7 | 16 54.1 S | 041 34.0E | 2766 | 11.9 | 284 | 202 | 12.4 | 28.14 | 314 2331 | 16 53.5 S | 41 34.0 E |
| 43 | T5 | 16 48.7 S | 041 13.9E | 2614 | 4.0 | 280 | 160 | 7.4 | 28.70 | 315 0210 | 16 48.8 S | 41 13.9 E |
| 44 | T7 | 16 45.5 S | 041 01.0E | 2400 | 11.5 | 282 | 145 | 9.5 | 28.37 | 315 0610 | 16 45.5 S | 41 01.0 E |
| 45 | T5 | 16 41.9 S | 040 48.4E | 2200 | 11.1 | 276 | 158 | 8.2 | 28.62 | 315 0720 | 16 42.3 S | 40 48.4 E |
| 46 | T7 | 16 38.8 S | 040 30.3E | 1970 | 11.4 | 282 | 165 | 10.5 | 30.48 | 315 0920 | 16 37.9 S | 40 30.1 E |
| 47 | T7 | 16 30.6 S | 040 16.6E | 1600 | 10.8 | 280 | 195 | 7.0 | 29.60 | 315 1035 | 16 35.3 S | 40 16.7 E |
| 48 | T7 | 16 32.8 S | 040 07.5E | 1365 | 10.5 | 290 | 225 | 5.7 | 29.20 | 315 1307 | 16 33.4 S | 40 07.3 E |
| 49 | T7 | 16 30.6 S | 039 58.5E | 485 | 11.0 | 285 | 225 | 5.7 | 28.4 | 315 1401 | 16 30.6 S | 39 58.5 E |

- Bad drop, raw data logged but not processed.

Table 8. XBT LOG SHEET 3 for Zonal XBT Section Across Mozambique Channel Coincident with Mooring Line

| Drop No. | XBT type | Lat | Long | Depth (m) | Spd sog (knots) | Course cog | Wind Dir (-180) | Wind Spd (knots) | SST | Time & day (gmt) | Launch Lat | Launch Lon |
|----------|----------|----------|----------|-----------|-----------------|------------|-----------------|------------------|------|------------------|------------|------------|
| 50 | T5 | 21 00.0S | 40 30.0E | 2950 | 10 | 190 | 200 | 16.7 | 27.9 | 317 1436 | 21 00.0S | 40 30.0E |
| 51 | T7 | 21 15.0S | 40 33.1E | 3098 | 9.8 | 170 | 200 | 17.7 | 27.5 | 317 1615 | 21 15.0S | 40 33.5E |
| 52 | T5 | 21 30.0S | 40 37.0E | 3099 | 9.7 | 165 | 195 | 16.0 | 27.4 | 317 1756 | 21 30.0S | 40 37.5E |
| 53 | T7 | 21 45.0S | 40 41.1E | 2967 | 9.7 | 165 | 175 | 16.6 | 27.3 | 317 1936 | 21 45.0S | 40 41.2E |
| 54 | T5 | 22 00.0S | 40 44.6E | 2982 | 8.9 | 170 | 180 | 14.4 | 27.1 | 317 2122 | 22 00.0S | 40 44.6E |
| 55 | T7 | 22 15.0S | 40 45.1E | 3108 | 9.5 | 165 | 170 | 14.3 | 27.2 | 317 2305 | 22 15.0S | 40 48.4E |
| 56 | T5 | 22 30.0S | 40 52.1E | 3189 | 9.4 | 165 | 170 | 15.0 | 27.3 | 318 0045 | 22 30.0S | 40 52.0E |
| 57 | T7 | 22 45.0S | 40 55.1E | 3231 | 10.0 | 166 | 170 | 15.0 | 27.3 | 318 0223 | 22 45.0S | 40 55.9E |
| 58 | T5 | 23 00.0S | 40 59.5E | 3000 | 5.0 | 173 | 146 | 14.6 | 27.6 | 318 0400 | 23 00.4S | 40 59.4E |
| 59 | T7 | 23 15.0S | 41 03.0E | 3000 | 11.7 | 165 | 165 | 8.2 | 27.5 | 318 0523 | 23 15.0 S | 41 03.2 E |
| 60 | T5 | 23 30.0S | 41 06.7E | 3000 | 11.4 | 170 | 210 | 8.0 | 27.2 | 318 0645 | 23 30.0 S | 41 07.0 E |
| 61 | T7 | 23 45.0S | 41 11.0E | 3500 | 11.5 | 167 | 222 | 8.0 | 27.3 | 318 0805 | 23 45.0 S | 41 11.0 E |
| 62 | T5 | 24 00.0S | 41 15.0E | 3600 | 11.2 | 165 | 235 | 11.2 | 27.4 | 318 0931 | 24 00.0 S | 41 14.5 E |
| 63 | T7 | 24 15.0S | 41 18.0E | 3600 | 10.9 | 165 | 235 | 15.5 | 27.0 | 318 1101 | 24 15.0 S | 41 18.0 E |
| 64 | T5 | 24 30.0S | 41 21.5E | 3600 | 10.0 | 170 | 232 | 18.0 | 26.8 | 318 1229 | 24 29.9S | 41 22.0E |
| 65* | T7 | 24 45.0S | 41 25.5E | 3744 | 10.7 | 170 | 210 | 16.6 | 26.6 | 318 1401 | 24 45.0S | 41 25.6E |
| 66 | T5 | 24 46.0S | 41 25.8E | 3744 | 10.7 | 170 | 220 | 26.5 | 26.5 | 318 1408 | 24 46.3S | 41 25.9E |
| 67 | T5 | 25 00.0S | 41 29.5E | 3997 | 10.2 | 165 | 210 | 25.9 | 25.9 | 318 1533 | 25 00.0S | 41 29.6E |
| 68 | T7 | 25 15.0S | 41 33.3E | 4042 | 10.5 | 165 | 200 | 12.4 | 25.8 | 318 1707 | 25 15.0S | 41 33.4E |
| 69 | T5 | 25 30.0S | 41 37.2E | 4089 | 11.0 | 170 | 185 | 9.0 | 25.2 | 318 1832 | 25 30.0S | 41 37.2E |
| 70 | T7 | 25 45.0S | 41 40.0E | 4178 | 11.0 | 170 | 190 | 8.0 | 25.2 | 318 2000 | 25 45.0S | 41 40.9E |
| 71 | T5 | 26 00.0S | 41 44.6E | 4207 | 10.9 | 165 | 205 | 7.8 | 25.3 | 318 2127 | 26 00.0S | 41 44.6E |
| 72 | T7 | 26 15.0S | 41 48.5E | 4221 | 11.0 | 170 | 210 | 5.5 | 25.1 | 318 2251 | 26 15.0S | 41 48.4E |
| 73 | T5 | 26 30.0S | 41 52.0E | 4239 | 11.0 | 165 | 220 | 6.6 | 24.9 | 319 0021 | 26 30.0S | 41 52.2E |
| 74 | T7 | 26 45.0S | 41 56.0E | 4289 | 11.7 | 165 | 240 | 7.0 | 25.0 | 319 0145 | 26 45.0S | 41 56.0E |
| 75 | T5 | 27 00.0S | 42 00.0E | 4300 | 10.8 | 167 | 252 | 10.0 | 24.5 | 319 0314 | 27 00.0S | 42 00.0E |

Table 9. XBT LOG SHEET 4 for Nov 13-15 N-S XBT Section Across Eddy off Madagascar. "*" indicates a bad drop

| Drop No. | XBT type | Lat | Long | Depth (m) | Spd (m/s) | Course cog | Wnd Dir (-180) | Wind Spd (kts) | SST | Time & day (gmt) | Launch Lat | Launch Lon |
|----------|----------|----------|----------|-----------|-----------|------------|----------------|----------------|-------|------------------|------------|------------|
| 76 | T7 | 30 00.0S | 38 00.0E | 4970 | 9.6 | 230 | 240 | 20.0 | 23.44 | 320 0720 | 30 00.0 S | 37 59.7E |
| 77 | T7 | 30 00.0S | 37 30.0E | 5200 | 11.1 | 265 | 025 | 15.0 | 23.39 | 320 0946 | 30 00.0 S | 37 29.8E |
| 78 | T7 | 30 00.0S | 37 00.0E | 5000 | 10.8 | 270 | 052 | 15.0 | 23.93 | 320 1210 | 20 00.2 S | 37 00.0E |
| 79 | T7 | 30 00.0S | 36 30.0E | 2500 | 11.1 | 275 | 050 | 9.0 | 23.04 | 320 1437 | 29 29.7S | 36 30.0E |
| *80 | T5 | 30 00.0S | 36 00.0E | 2000 | 11.2 | 270 | 050 | 9.5 | 22.73 | 320 1701 | 30 00.4S | 35 59.9E |
| 81 | T7 | 30 00.0S | 35 30.0E | 2200 | 11.2 | 270 | 000 | 8.0 | 22.86 | 320 1436 | 30 00.0S | 35 30.0E |
| 82 | T5 | 30 00.0S | 35 00.0E | 2400 | 10.8 | 270 | 350 | 5.6 | 22.84 | 320 2204 | 29 59.8S | 35 00.0E |
| 83 | T7 | 30 00.0S | 34 30.0E | 2700 | 10.6 | 270 | 025 | 9.5 | 22.79 | 321 0037 | 29 59.9S | 34 30.0E |
| 84 | T5 | 30 00.0S | 34 00.0E | 2400 | 10.4 | 266 | 010 | 8.0 | 23.39 | 321 0309 | 30 00.0S | 34 00.0E |
| 85 | T7 | 30 00.0S | 33 30.0E | 2700 | 10.0 | 265 | 320 | 16.5 | 23.39 | 321 0914 | 30 00.0S | 33 30.0E |
| 86 | T5 | 30 00.0S | 33 00.0E | 2000 | 11.0 | 270 | 310 | 15.0 | 23.17 | 321 1143 | 30 00.0S | 33 00.0E |
| 87 | T7 | 30 00.0S | 32 30.0E | 1700 | 10.8 | 270 | 300 | 17.4 | 23.82 | 321 1407 | 30 00.1S | 32 30.0E |
| 88 | T7 | 30 00.0S | 32 00.0E | 1300 | 10.7 | 270 | 280 | 24.5 | 24.32 | 321 1631 | 30 00.1S | 32 00.0E |
| 89 | T7 | 30 00.0S | 31 30.0E | 1000 | 9.6 | 270 | - | - | - | 321 1850 | 30 00.1S | 31 30.2E |
| 90 | T7 | 30 00.0S | 31 15.0E | 1000 | 10.0 | 270 | - | - | - | 321 2017 | 29 58.8 S | 31 15.1E |
| 91 | T7 | 30 00.0S | 31 05.0E | 1000 | 9.7 | 270 | - | - | - | 321 2124 | 29 59.9 S | 31 05.0E |

- May have hit bottom at approximately 1800 as the profile is straight thereafter

Table 10. XBT LOG SHEET 5 for Zonal Section Along 30S into Durban

| | |
|--------------------|---|
| AD,SI,HUNDREDTHS | 120.00 Sampling interval |
| AD,NB,WHOLE | 64 Number of Depth Bins |
| AD,BL,WHOLE | 3 Bin Length |
| AD,PL,WHOLE | 8 Pulse Length |
| AD,BK,TENTHS | 8.0 Blank Beyond Transmit |
| AD,PE,WHOLE | 1 Pings Per Ensemble |
| AD,PC,HUNDREDTHS | 1.00 Pulse Cycle Time |
| AD,PG,WHOLE | 25 Percent Pings Good Threshold |
| XX,OD2,WHOLE | 5 [SYSTEM DEFAULT, OD2] |
| XX,TE,HUNDREDTHS | 0.00 [SYSTEM DEFAULT, TE] |
| AD,US,BOOLE | NO Use Direct Commands on StartUp |
| DP,TR,BOOLE | NO Toggle roll compensation |
| DP,TP,BOOLE | NO Toggle Pitch compensation |
| DP,TH,BOOLE | YES Toggle Heading compensation |
| DP,VS,BOOLE | YES Calculate Sound Velocity from TEMP/Salinity |
| DP,UR,BOOLE | NO Use Reference Layer |
| DP,FR,WHOLE | 6 First Bin for reference Layer |
| DP,LR,WHOLE | 15 Last Bin for reference Layer |
| DP,BT,BOOLE | NO Use Bottom Track |
| DP,B3,BOOLE | NO Use 3 Beam Solutions |
| DP,EV,BOOLE | YES Use Error Velocity as Percent Good Criterion |
| DP,ME,TENTHS | 150.0 Max. Error Velocity for Valid Data (cm/sec) |
| DR,RD,BOOLE | YES Recording on disk |
| DR,RX,BOOLE | YES Record N/S (FORE/AFT) Vel. |
| DR,RY,BOOLE | YES Record E/W (FORT/STBD) Vel. |
| DR,RZ,BOOLE | YES Record vertical vel. |
| DR,RE,BOOLE | YES Record error Good |
| DR,RB,BOOLE | NO Bytes of user prog. buffer |
| DR,RP,BOOLE | YES Record Percent good |
| DR,RA,BOOLE | YES Record average AGC/Bin |
| DR,RN,BOOLE | YES Record Ancillary data |
| DR,AP,BOOLE | YES Auto-ping on start-up |
| XX,LDR,TRI | 4 [SYSTEM DEFAULT, LDR] |
| XX,RB2,WHOLE | 192 [SYSTEM DEFAULT, RB2] |
| DR,RC,BOOLE | NO Record CTD data |
| XX,FB,WHOLE | 1 [SYSTEM DEFAULT, FB] |
| XX,PU,BOOLE | NO [SYSTEM DEFAULT, PU] |
| GC,TG,TRI | 1 DISPLAY (NO/GRAPH/TAB) |
| GC,ZV,WHOLE | 1 ZERO VELOCITY REFERENCE (S/B/M/L) |
| GC,VL,WHOLE | -100 LOWEST VELOCITY ON GRAPH |
| GC,VH,WHOLE | 100 HIGHEST VELOCITY ON GRAPH |
| GC,DL,WHOLE | 0 LOWEST DEPTHS ON GRAPH |
| GC,DH,WHOLE | 500 HIGHEST DEPTHS ON GRAPH |
| GC,SW,BOOLE | NO SET DEPTHS WINDOW TO INCLUDE ALL BINS |
| GC,MP,WHOLE | 25 MINIMUM PERCENT GOOD TO PLOT |
| SG,PNS,BOOLE | YES PLOT NORTH/SOUTH VEL. |
| SG,PEW,BOOLE | YES PLOT EAST/WEST VEL. |
| SG,PVT,BOOLE | YES PLOT VERTICAL VEL. |
| SG,PEV,BOOLE | YES PLOT ERROR VEL. |
| SG,PPE,BOOLE | NO PLOT PERCENT ERROR |
| SG,PMD,BOOLE | NO PLOT MAG AND DIR |
| SG,PSW,BOOLE | NO PLOT AVERAGE SP. W. |
| SG,PAV,BOOLE | YES PLOT AVERAGE AGC. |
| SG,PPG,BOOLE | YES PLOT PERCENT GOOD |
| SG,PD1,BOOLE | NO PLOT DOPPLER 1 |
| SG,PD2,BOOLE | NO PLOT DOPPLER 2 |
| SG,PD3,BOOLE | NO PLOT DOPPLER 3 |
| SG,PD4,BOOLE | NO PLOT DOPPLER 4 |
| SG,PW1,BOOLE | NO PLOT SP. W. 1 |
| SG,PW2,BOOLE | NO PLOT SP. W. 2 |
| SG,PW3,BOOLE | NO PLOT SP. W. 3 |
| SG,PW4,BOOLE | NO PLOT SP. W. 4 |
| SG,PA1,BOOLE | NO PLOT AGC 1 |
| SG,PA2,BOOLE | NO PLOT AGC 2 |
| SG,PA3,BOOLE | NO PLOT AGC 3 |
| SG,PA4,BOOLE | NO PLOT AGC 4 |
| SG,PP3,BOOLE | NO PLOT 3-BEAM SOLUTION |
| SS,OD,WHOLE | 5 OffSet for Depth |
| SS,OH,TENTHS | 0.0 OffSet for Heading |

| | |
|------------------|--|
| SS,OP,TENTHS | 0.0 OffSet for Pitch |
| SS,ZR,TENTHS | 0.0 OffSet for Roll |
| SS,OT,HUNDREDTHS | 45.00 OffSet FOR temp |
| SS,ST,HUNDREDTHS | 50.00 Scale for Temp |
| SS,SL,HUNDREDTHS | 35.00 Salinity (PPT) |
| SS,UD,BOOLE | YES Toggle UP/DOWN |
| SS,CV,BOOLE | NO Toggle concave/Convex transducerhead |
| SS,MA,TENTHS | 30.0 Mounting angle for transducers. |
| SS,SS,HUNDREDTHS | 1500.00 Speed of Sound (m/sec) |
| XX,GP,BOOLE | YES [SYSTEM DEFAULT, GP] |
| XX,DD,TENTHS | 1.0 [SYSTEM DEFAULT, DD] |
| XX,PT,BOOLE | NO [SYSTEM DEFAULT, PT] |
| XX,TU,TRI | 2 [SYSTEM DEFAULT, TU] |
| TB,FP,WHOLE | 1 FIRST BINS TO PRINT |
| TB,LP,WHOLE | 64 LAST BIN TO PRINT |
| TB,SK,WHOLE | 6 SKIP INTERVAL BETWEEN BINS |
| TB,DT,BOOLE | YES DIAGNOSTIC TAB MODE |
| DU,TD,BOOLE | NO TOGGLE USE OF DUMMY DATA |
| XX,PN,WHOLE | 0 [SYSTEM DEFAULT, PN] |
| DR,SD,WHOLE | 4 Second recording drive |
| DR,PD,WHOLE | 4 First recording drive (1=A:,2=B: ...) |
| DP,PX,BOOLE | NO Profiler does XYZE transform |
| SS,LC,TENTHS | 5.0 Limit of Knots change |
| SS,NW,TENTHS | 0.5 Weight of new knots of value |
| GC,GM,TRI | 2 GRAPHICS CONTROL 0=LO RES, 1=HI RES, 2=ENHANCED |
| AD,PS,BOOLE | YES YES=SERIAL/NO=PARALLEL Profiler Link |
| XX,LNN,BOOLE | YES [SYSTEM DEFAULT, LNN] |
| XX,BM,BOOLE | YES [SYSTEM DEFAULT, BM] |
| XX,RSD,BOOLE | NO RECORD STANDARD DEVIATION OF VELOCITIES PER BIN |
| XX,DRV,WHOLE | 1 [SYSTEM DEFAULT, DRV] |
| XX,PBD,WHOLE | 3 [SYSTEM DEFAULT, PBD] |
| TB,RS,BOOLE | NO SHOW RHPT STATISTIC |
| UX,EE,BOOLE | YES ENABLE EXIT TO EXTERNAL PROGRAM |
| SS,VSC,TRI | 0 Velocity scale adjustment |
| AD,DM,BOOLE | NO USE DMA |
| TB,SC,BOOLE | NO SHOW CTD DATA |
| AD,CW,BOOLE | NO Collect spectral width |
| DR,RW,BOOLE | NO Record average SP.W./Bin |
| DR,RRD,BOOLE | NO Record last raw dopplers |
| DR,RAA,BOOLE | YES Record last raw AGC |
| DR,RRW,BOOLE | NO Record last SP.W. |
| DR,R3,BOOLE | NO Record average 3-Beam solutions |
| DR,RBS,BOOLE | YES Record beam statistic |
| XX,STD,BOOLE | NO [SYSTEM DEFAULT, STD] |
| LR,HB,HUNDREDTHS | 0.00 Heading Bias |
| SL,1,ARRAY5 | 1 1 8 NONE 19200 PROFILER |
| SL,2,ARRAY5 | 0 1 8 NONE 1200 LORAN RECEIVER |
| SL,3,ARRAY5 | 4 1 8 NONE 4800 REMOTE DISPLAY |
| SL,4,ARRAY5 | 2 1 8 NONE 9600 ENSEMBLE OUTPUT |
| SL,5,ARRAY5 | 0 1 8 NONE 1200 AUX 1 |
| SL,6,ARRAY5 | 0 1 8 NONE 1200 AUX 2 |
| DU,1,ARRAY6 | 100.00 100.00 60.00 0.00 0.00 YES D1 |
| DU,2,ARRAY6 | -100.00 -100.00 60.00 0.00 0.00 YES D2 |
| DU,3,ARRAY6 | 200.00 200.00 60.00 0.00 0.00 YES D3 |
| DU,4,ARRAY6 | -200.00 -200.00 60.00 0.00 0.00 YES D4 |
| DU,5,ARRAY6 | 200.00 19.00 60.00 0.00 0.00 YES AGC |
| DU,6,ARRAY6 | 0.00 0.00 60.00 0.00 0.00 NO SP. W. |
| DU,7,ARRAY6 | 0.00 0.00 60.00 0.00 0.00 NO ROLL |
| DU,8,ARRAY6 | 0.00 0.00 60.00 0.00 0.00 NO PITCH |
| DU,9,ARRAY6 | 0.00 0.00 60.00 0.00 0.00 NO HEADING |
| DU,10,ARRAY6 | 0.00 0.00 60.00 0.00 0.00 NO TEMPERATURE |
| DC,1,SPECIAL | "FH00004" MACRO 1 |
| CI,1,SPECIAL | "C135" CRUISE ID GOES HERE |
| LR,1,SPECIAL | " " LORAN FILE NAME GOES HERE |

Table 11. VMADCP Water Track Configuration File

(Configuration setting DP,BT,BOOLE (Bottom Track) was set to YES when in shallow water.)

| Time GMT | Ship's heading (°) | Ship's speed (knots) | Max depth of good data (m) | % Good data | BIT errors |
|----------|--------------------|----------------------|----------------------------|-------------|------------|
| 12h00 | 275 | 6 | 150-180 | 75-90 | Yes |
| 12h20 | 185 | 6 | 60-150 | 60-75 | Yes |
| 12h40 | 275 | 6 | 125-150 | 70-80 | Yes |
| 13h00 | 185 | 6 | 125-200 | 65-75 | Yes |
| 13h20 | 275 | 6 | 100-200 | 65-75 | Yes |
| 13h40 | 185 | 6 | 100-200 | 65-80 | Yes |

Table 12. Log of ADCP 'zig-zag' calibration track

| DAY | TIME (GMT) | DETAILS |
|-----|------------|--|
| 297 | 07:28 | ADCP works using an old configuration file but headings are not being read into ADCP so data is wrong. |
| 304 | 12:00 | ADCP finally logging to level C. Correct configuration file accepted. |
| 305 | 05:44 | Beam errors observed so ADCP is switched off in case it is due to extreme SST (31.5 °C) and left to 'cool'. |
| 306 | 07:25 | ADCP switched back on but still errors. Water quality now assumed to be cause of error. Currents only plotted to 250m. |
| 307 | 04:15 | ADCP is working properly. (Near Seychelles) |
| 307 | 17:00 | ADCP is switched to bottom track mode. |
| 308 | 05:40 | ADCP switched off as ship arrives at Seychelles. |
| | | END OF LEG 1. START OF LEG 2. |
| 309 | 04:15 | ADCP switched on. (Bottom track mode) |
| 309 | 08:10 | ADCP switched to water track mode. |
| 311 | 05:30 | ADCP beam errors noted again. |
| 313 | 10:10 | ADCP switched to bottom track mode at Madagascan continental shelf. |
| 313 | 15:40 | ADCP switched back to water track mode. Beam errors still observed. Also currents only plotted to 250m. |
| 319 | 12:00 | ADCP zig-zag calibration |

Table 13. ADCP Log

| Julian Day | APEX Float no. | Decimal Argos ID | Deployment Latitude | Deployment Longitude | Deployment Time (GMT) | Estimated Dive Time | Coincident XBT |
|------------|----------------|------------------|---------------------|----------------------|-----------------------|---------------------|----------------|
| 302 | 396 | 10388 | 10 00 N | 60 18 E | 06:02 | 06:20 | XBT 11 (T7) |
| 304 | 395* | 10382 | 07 30 N | 63 41 E | 02:16 | 03:30 | |
| 305 | 375 | 10362 | 04 30 N | 60 33 E | 05:30 | 06:00 | |
| 306 | 394 | 10373 | 01 34 N | 58 00 E | 06:20 | 06:30 | |
| 307 | 376 | 10363 | 01 31 S | 58 00 E | 01:10 | 04:40 | XBT 33 (T5) |

* Bung was accidentally pushed inside the float so there was no bung present.

Table 14. ARGO Float Log for Leg 1

| Instrument | Depth of SST | Accuracy (°C) | Lag in SST response | Time of measurements | Location of sensor |
|--------------------|--------------------------|---------------|---------------------|--|------------------------|
| <i>SISTeR</i> | skin (μm 's) | | none | Continuous (stopped when rain approached) | Foremast |
| Soap | surface (~0.3m) | 0.1 | ~ 15 sec | Continuous (depth fluctuated depending on speed of ship) | Port side of fore-deck |
| WHOI – Hull | 1m | | ~ 15 min | Continuous | Engine room |
| TSG | 5m | 0.01 | ~ 10 sec | Continuous | |
| XBT | 0.7m + | 0.02 | not known | Only deployed in regions of interest | Off back/side of ship |

Table 15. Summary of the SST sensors

| LEG1 (Day 298-308) | MEAN | STD DEV. | MAX | MIN |
|---------------------|--------------|-------------|--------------|--------------|
| SISTeR (all) | 28.64 | 0.56 | 31.15 | 27.50 |
| (night) | 28.46 | 0.25 | | |
| (day) | 28.83 | 0.60 | | |
| SOAP (all) | 28.87 | 0.53 | 31.47 | 27.69 |
| (night) | 28.73 | 0.28 | | |
| (day) | 29.00 | 0.59 | | |
| HULL (all) | 29.38 | 0.41 | 31.02 | 28.61 |
| (night) | 29.24 | 0.26 | | |
| (day) | 29.46 | 0.45 | | |
| TSG (all) | 28.93 | 0.43 | 31.21 | 27.96 |
| (night) | 28.85 | 0.29 | | |
| (day) | 29.03 | 0.45 | | |

| LEG1 (Day 298-308) | MEAN | STD DEV. | MAX | MIN | r |
|------------------------|--------------|-------------|-------------|--------------|-------------|
| SIS-SOAP (all) | -0.26 | 0.13 | 1.84 | -0.65 | 0.97 |
| (night) | -0.32 | 0.11 | | | 0.94 |
| (day) | -0.23 | 0.14 | | | 0.98 |
| SOAP-HULL (all) | -0.48 | 0.22 | 1.39 | -1.80 | 0.91 |
| (night) | -0.51 | 0.12 | | | 0.95 |
| (day) | -0.46 | 0.27 | | | 0.90 |
| SOAP-TSG | -0.08 | 0.24 | 2.00 | -2.16 | 0.90 |
| (night) | -0.15 | 0.04 | | | 0.99 |
| (day) | -0.04 | 0.29 | | | 0.87 |
| HULL-TSG | 0.39 | 0.11 | 1.26 | -0.37 | 0.96 |
| (night) | 0.37 | 0.08 | | | 0.96 |
| (day) | 0.41 | 0.12 | | | 0.96 |

Table 16. SST statistics for the four SST sensors

| Rough (Day 310-311) | MEAN | STD DEV. | r |
|---------------------|--------|----------|-------|
| SOAP-HULL | -0.512 | 0.10 | 0.991 |
| SOAP-TSG | -0.104 | 0.03 | 0.999 |
| TSG-HULL | -0.415 | 0.10 | 0.99 |

Table 17. Results from SST comparison in rough weather

| Overpass | Julian Day UTC | Time UTC | Latitude | Longitude | Across Track Position (km) | Comments |
|----------|-------------------|-------------|-----------|------------|-------------------------------|----------|
| 1 | 297 | 06:52:05 | 4°21.61'S | 55°27.68'E | 180 | |
| 2 | 298 | 18:54:21 | 2°00.26'N | 55°35.16'E | 217 | Rain |
| 3 | 299 | 18:23:02 | 2°13.67'N | 59°20.12'E | 229 | Cloud |
| 4 | 301 | 06:23:16 | 6°41.49'N | 61°40.61'E | 111 | |
| 5 | 302 | 18:30:17 | 8°25.87'N | 60°35.53'E | 211 | Cloud |
| 6 | 303 | 17:58:55 | 8°28.78'N | 64°31.09'E | 216 | Cloud |
| 7 | 304 | 06:28:41 | 7°13.30'N | 63°23.55'E | 216 | |
| 8 | 305 | 18:34:36 | 3°04.13'N | 59°05.50'E | 77 | |
| 9 | 307 | 06:37:12 | 2°06.55'S | 57°19.20'E | 62 | Cloud |

Table 18. ATSR-2 overpass analysis for the first leg of CD135. The time and ship's position at overpass is listed, along with the distance of the overpass from the centre of the ATSR-2 swath and a note on the conditions at overpass. None of the first nine overpasses could confidently be declared free of cloud.

| Overpass | Julian Day UTC | Time UTC | Latitude | Longitude | Across Track Position (km) | Comments |
|----------|-------------------|-------------|------------|------------|-------------------------------|-------------|
| 10 | 310 | 19:14:18 | 9°07.81'S | 50°43.20'E | 46 | Bad weather |
| 11 | 312 | 07:23:20 | 13°20.53'S | 46°21.26'E | 185 | |
| 12 | 315 | 07:30:14 | 16°42.33'S | 40°47.92'E | 166 | Cloud |
| 13 | 315 | 19:55:22 | 16°36.91'S | 40°45.72'E | 48 | |
| 14 | 318 | 07:37:44 | 23°39.24'S | 41°09.51'E | 187 | |
| 15 | 318 | 19:58:32 | 25°44.73'S | 41°40.86'E | 32 | |
| 16 | 320 | 20:34:35 | 29°59.82'S | 35°17.87'E | 142 | |
| 17 | 321 | 07:45:32 | 30°00.08'S | 33°44.99'E | 229 | Heavy seas |

Table 19. ATSR-2 overpass analysis for the second leg of CD135. The time and ship's position at overpass is listed, along with the distance of the overpass from the centre of the ATSR-2 swath and a note on the conditions at overpass.

| Time (GMT) | Activity | Remarks |
|--------------------|---------------------------------|-----------------------------------|
| 9 Nov. 2001 13.30 | Arrival at ACS17 | |
| 9 Nov. 2001 13.37 | Release mooring ACS17 | |
| 9 Nov. 2001 14.30 | Finish recovery ACS17 | |
| | | Stay overnight at ACS16 |
| 10 Nov. 2001 02.55 | Release mooring ACS16 | |
| 10 Nov. 2001 04.55 | Finish recovery ACS16 | |
| 10 Nov. 2001 09.50 | Arrival at ACS15 | Acoustic survey around ACS15 |
| 10 Nov. 2001 21.00 | Departure from ACS15 | |
| 11 Nov. 2001 02.30 | Arrival at ACS14 | |
| 11 Nov. 2001 02.45 | Release mooring ACS14 | |
| 11 Nov. 2001 05.00 | Finish recovery ACS14 | |
| 11 Nov. 2001 07.30 | Release mooring ACS13 | No contact with releases |
| 11 Nov. 2001 11.30 | Arrival at ACS12 | |
| 11 Nov. 2001 11.40 | Release mooring ACS12 | |
| 11 Nov. 2001 12.00 | Finish recovery ACS12 | |
| 11 Nov. 2001 14.00 | Arrival at ACS11 | |
| 11 Nov. 2001 14.10 | Release mooring ACS11 | |
| 11 Nov. 2001 15.00 | Finish recovery ACS11 | |
| 11 Nov. 2001 20.00 | Start acoustic survey at ACS13 | |
| 12 Nov. 2001 07.00 | Finish acoustic survey | |
| 12 Nov. 2001 07.00 | Start preparation for dredging | |
| 12 Nov. 2001 09.00 | Finish preparation for dredging | Transit to drifting mooring ACS15 |
| 12 Nov. 2001 12.30 | Start recovery mooring ACS13 | |
| 12 Nov. 2001 14.00 | Finish recovery ACS13 | |

Table 20. Summary of mooring activities during cruise CD135

| Mooring ID | Lat | Lon | Water depth | Meas. type | Instrument type | Inst. ID | Ht above bottom | Meas. Int. | DSU No. | No. of words | First rec. (UTC) | Last rec. (UTC) | DSU/corr (sec.) | Filename | Remarks | |
|------------|-----------|-----------|-------------|------------|-----------------|----------|-----------------|------------|---------|--------------|------------------|-----------------|-----------------|-------------|---------------------|----------------------|
| ACSI11 | 16 39.62S | 39 58.52E | 526 | ADCP | WHLR 75KHz | 1431 | 26 | | | | | | | | | |
| ACSI12 | 16 34.73S | 40 16.63E | 1595 | ADCP | WHLR 75KHz | 853 | 1098 | | | | | | | | | Short batteries lost |
| ACSI12 | | | | CM | RCM_11 | 44 | 597 | 600 | 12222 | 126151 | 8/4/01;18:21 | 11/11/01;11:56 | + 3:45 | ACSI2-44 | | |
| ACSI12 | | | | CM | RCM_11 | 45 | 97 | 600 | 12223 | 126144 | 8/4/01;18:42 | 11/11/01;12:16 | + 6:26 | ACSI2-45 | | |
| ACSI12 | | | | CM | RCM_11 | 411 | 1946 | 600 | 10034 | | | | | | | not recovered |
| ACSI13 | 16 41.92S | 40 48.41E | 2199 | CM | RCM_9 | 411 | 1796 | 600 | 7318 | | | | | | | not recovered |
| ACSI13 | | | | CM | RCM_8 | 11835 | 1546 | 600 | 11118 | | | | | | | not recovered |
| ACSI13 | | | | CM | RCM_8 | 11826 | 1200 | 600 | 12228 | | | | | | | not recovered |
| ACSI13 | | | | CM | RCM_11 | 47 | 97 | 600 | 156371 | | | | | | | not recovered |
| ACSI14 | 16 48.74S | 41 13.88E | 2603 | CM | RCM_9 | 350 | 2347 | 600 | 7322 | 156371 | | | + 3:05 | | no transfer on ship | |
| ACSI14 | | | | CM | RCM_8 | 12052 | 2197 | 600 | 7320 | 59880 | 10/04/01;11:46 | | + 3:47 | | DSU sync. Prob. | |
| ACSI14 | | | | CM | RCM_8 | 14488 | 1947 | 600 | 11556 | | | | | | | Drowned, lost |
| ACSI14 | | | | Temp/Turb | NIOZ | B7 | 1605 | | | | | | | ACSI4-B7 | | |
| ACSI14 | | | | CM | RCM_11 | 36 | 97 | 600 | 12197 | 124904 | 10/04/01;14:44 | 11/11/01;05:01 | + 0:23 | ACSI4-36 | | |
| ACSI15 | 16 58.63S | 41 56.02E | 1998 | CM | RCM_9 | 341 | 1746 | 600 | 11394 | 156845 | | 12/11/01; | - 0:43 | | no transfer on ship | |
| ACSI15 | | | | CM | RCM_8 | 11829 | 1596 | 600 | 8128 | 188178 | 10/04/01;06:54 | 12/11/01, | + 3:01 | ACSI5-11829 | | |
| ACSI15 | | | | CM | RCM_8 | 11831 | 1346 | 600 | 7030 | 188148 | Record 99 | | | ACSI5-11831 | | |
| ACSI15 | | | | | | | | | | | 11/04/01;00:02 | | + 9:24 | | | |
| ACSI15 | | | | CM | RCM_11 | 35 | 96 | 600 | 12091 | 125835 | 10/04/01;09:28 | 12/11/01; | + 5:18 | ACSI5-36 | Temp. sensor prob. | |
| ACSI16 | 17 12.13S | 42 50.24E | 1815 | CM | RCM_9 | 11823 | 1565 | 600 | 11041 | 184692 | 11/04/01;22:07 | 10/11/01;04:44 | + 1:26 | ACSI6-11823 | no transfer on ship | |
| ACSI16 | | | | CM | RCM_8 | 11834 | 1415 | 600 | 11392 | 184686 | 11/01/01;22:19 | 10/11/01;04:44 | + 3:05 | ACSI6-11834 | | |
| ACSI16 | | | | CM | RCM_8 | 11487 | 1165 | 600 | 11040 | 184680 | 11/04/01;22:27 | 10/11/01;04:49 | + 3:10 | ACSI6-11487 | | |
| ACSI16 | | | | CM | RCM_11 | 49 | 96 | 600 | 12227 | 123556 | 11/04/01;22:48 | 10/11/01;05:30 | + 3:42 | ACSI6-49 | | |
| ACSI17 | 17 17.30S | 43 09.55E | 445 | CM | RCM_9 | 351 | 346 | 600 | 7321 | 156559 | | 09/11/01;15:36 | + 3:43 | | no transfer on ship | |

Table 21. Mooring Information ACSI1-ACSI17

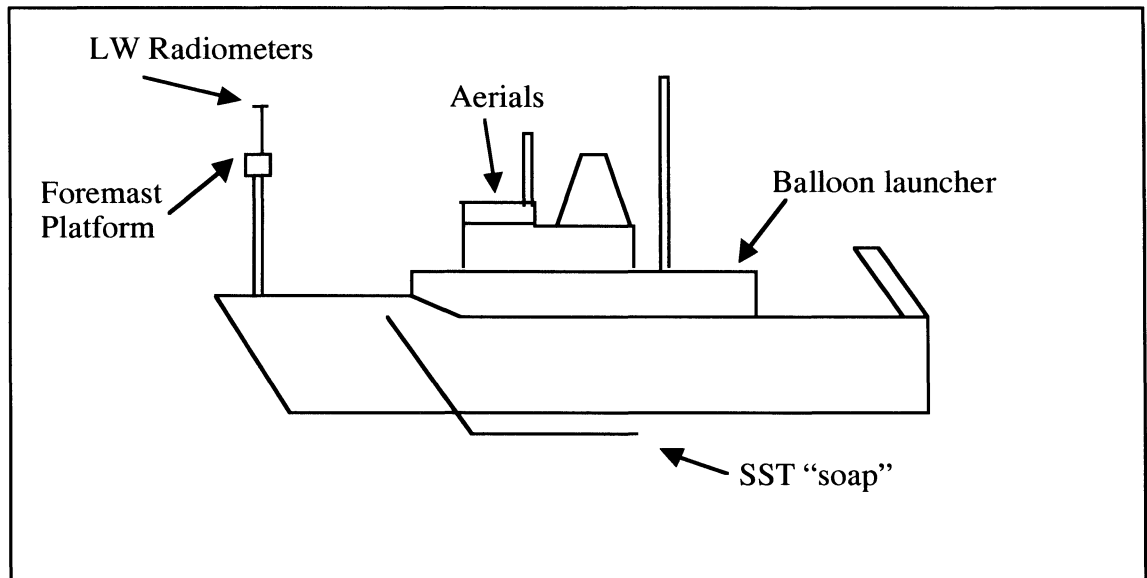


Figure 2a. Schematic of the instrument locations.

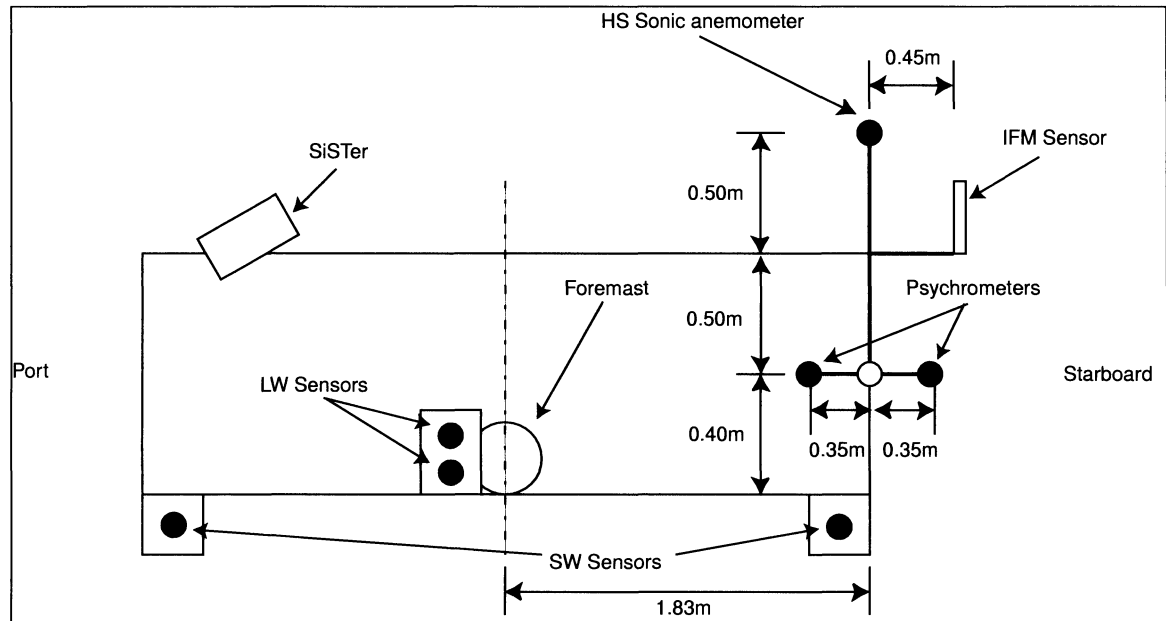


Figure 2b. Schematic plan view of the foremast platform, showing the positions of the fast response sensors in their positions. The two psychrometers are also shown (small black circles). Distances are given in m.

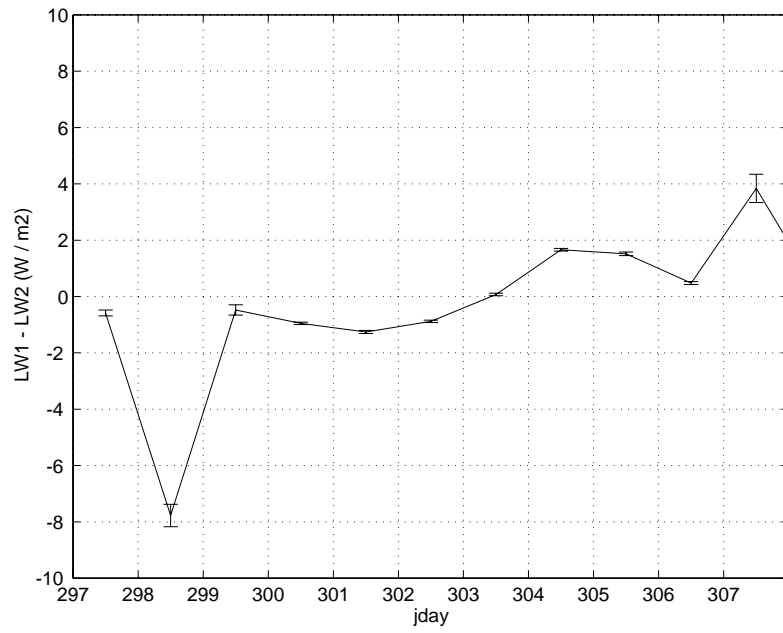


Figure 3. The difference in the longwave radiation from the two pyrgeometers. The error bars indicate the standard deviation of the mean.

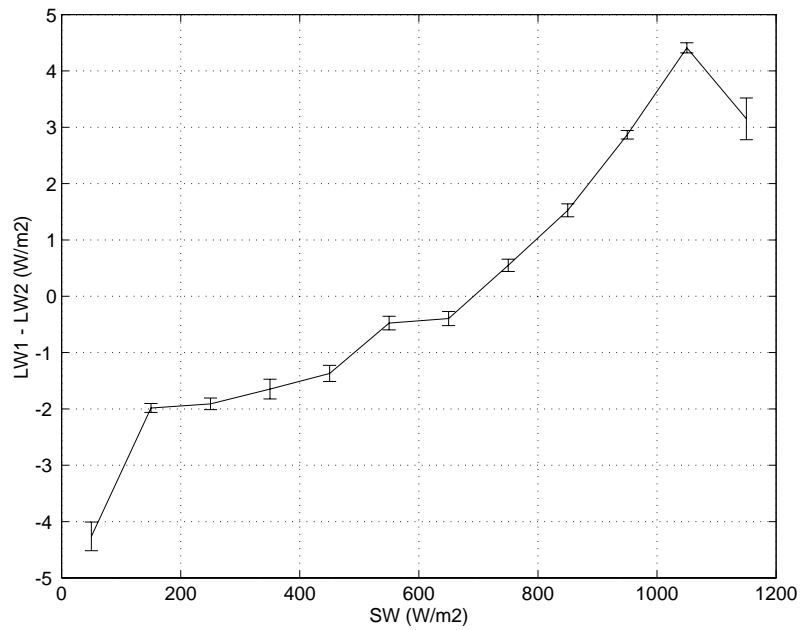


Figure 4. The difference in the longwave radiation from the two pyrgeometers plotted against SW. The difference in the longwave measurement have been averaged in 100 W m^{-2} (SW) bins and the error bars indicate the standard deviation of the mean.

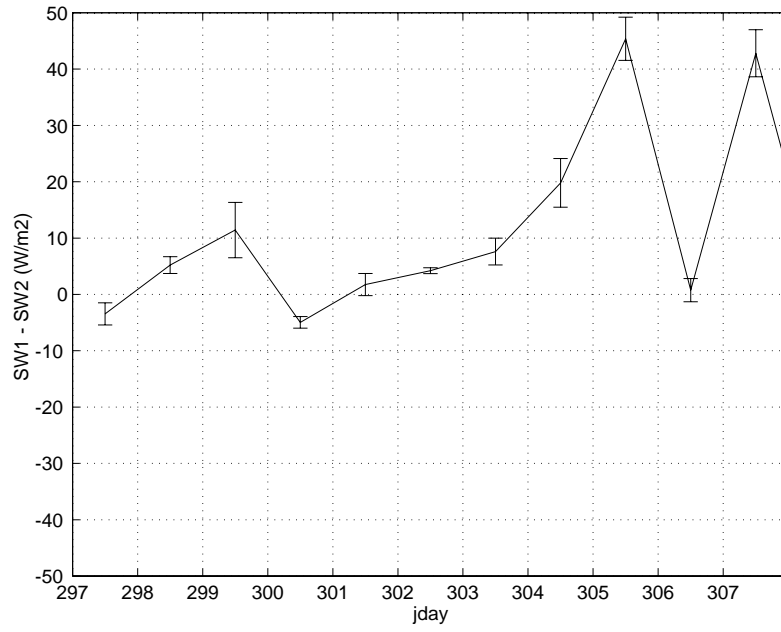


Figure 5. The daily mean of the differences in the incoming short-wave measured by sensors SW1 (902836) and SW2 (903289). The error bars indicate the standard deviation of the mean.

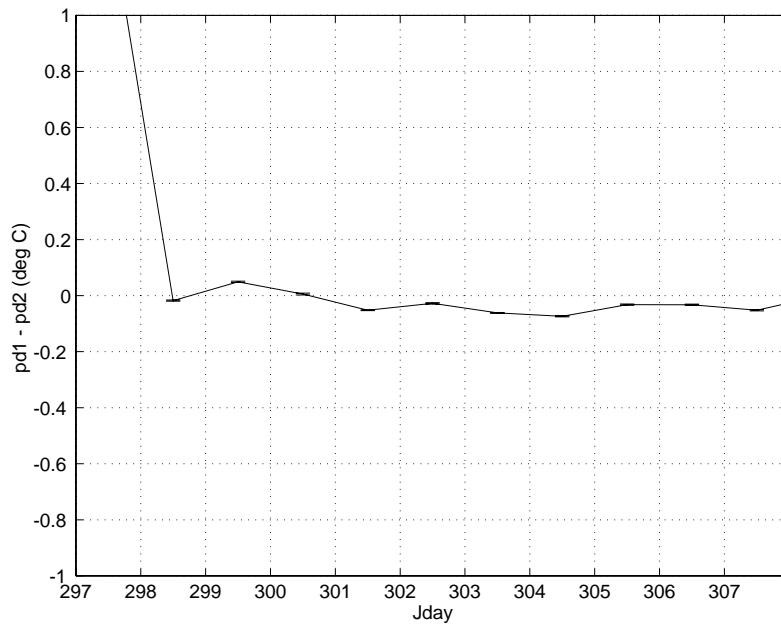


Figure 6. The daily mean differences in the dry bulb air temperatures measured by psychrometers pdp1 (IO2002) and pds2 (HS1020). The error bars indicate the standard deviation of the mean.

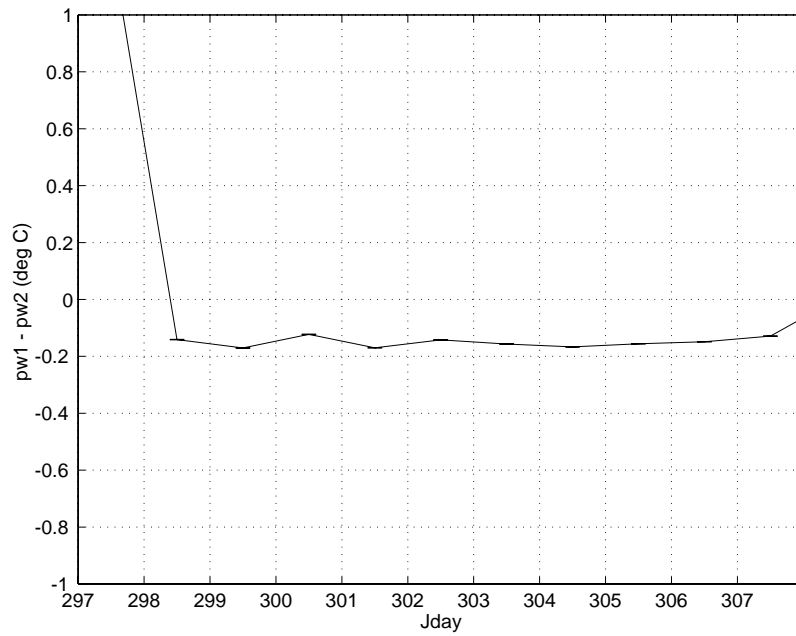


Figure 7. The daily mean differences in the wet bulb air temperatures measured by psychrometers pwp1 (IO2002) and pws2 (HS1020). The error bars indicate the standard deviation of the mean.

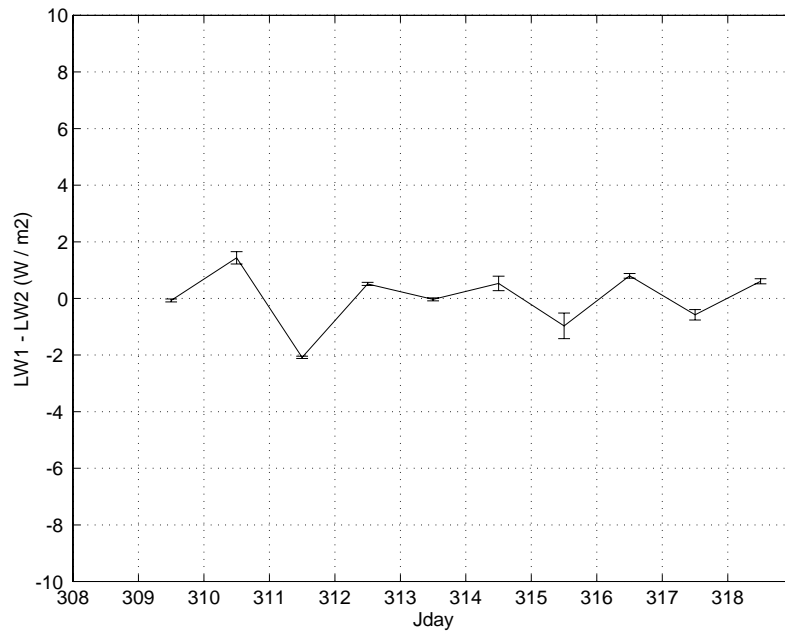


Figure 8. The difference in the longwave radiation from the two pyrgeometers averaged daily for the second leg. The error bars indicate the standard deviation of the mean.

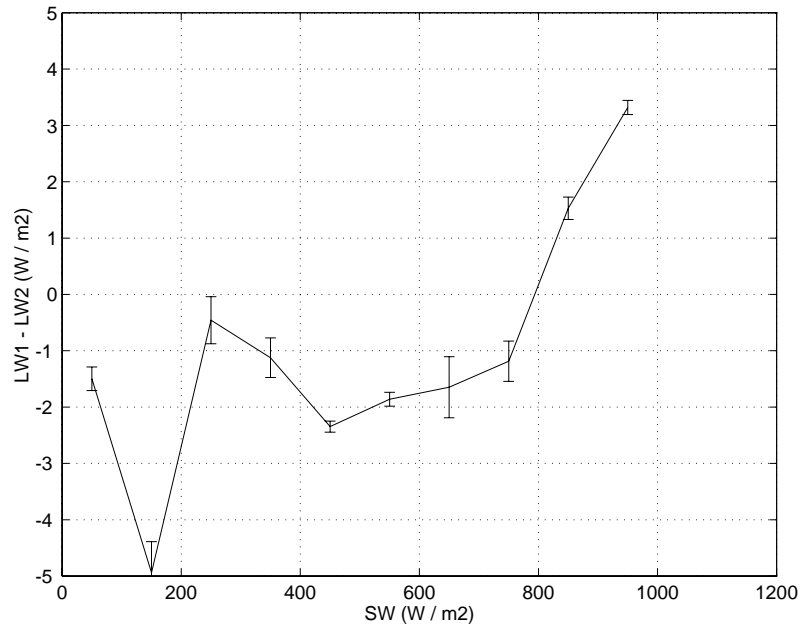


Figure 9. The difference in the longwave radiation from the two pyrgeometers plotted against SW. The difference in the longwave measurement have been averaged in 100 W m^{-2} (SW) bins and the error bars indicate the standard deviation of the mean.

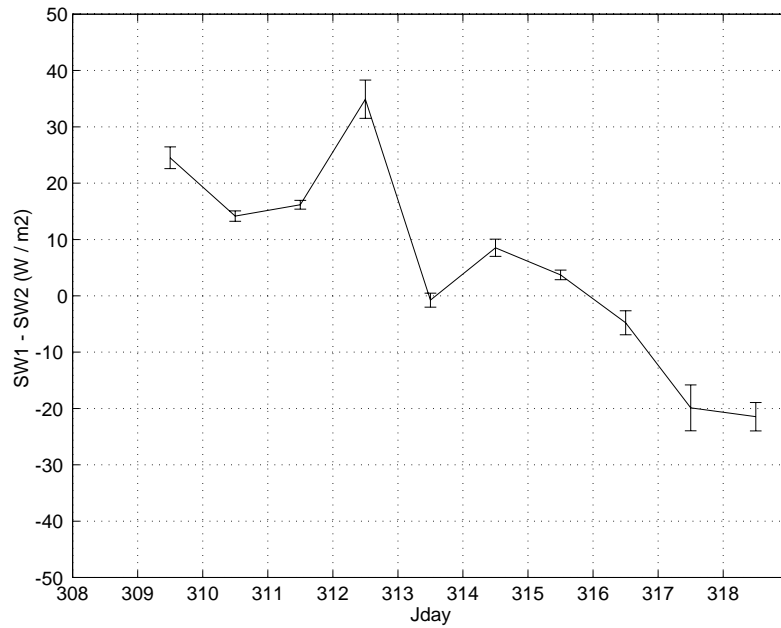


Figure 10. The daily mean of the differences in the incoming short-wave measured by sensors SW1 (902836) and SW2 (903289). The error bars indicate the standard deviation of the mean.

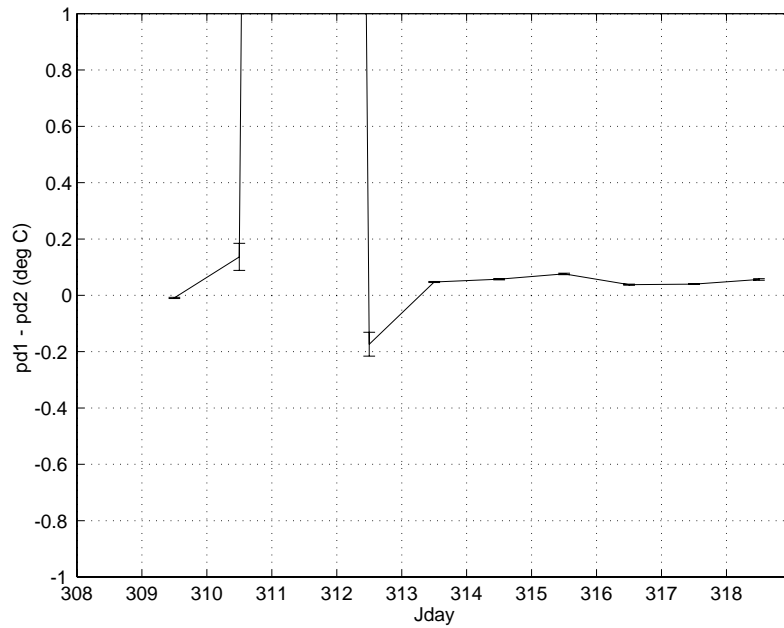


Figure 11. The daily mean differences in the dry bulb air temperatures measured by psychrometers pdp1 (IO2002) and pds2 (HS1020 before day 310, IO2003 after day 312). The error bars indicate the standard deviation of the mean.

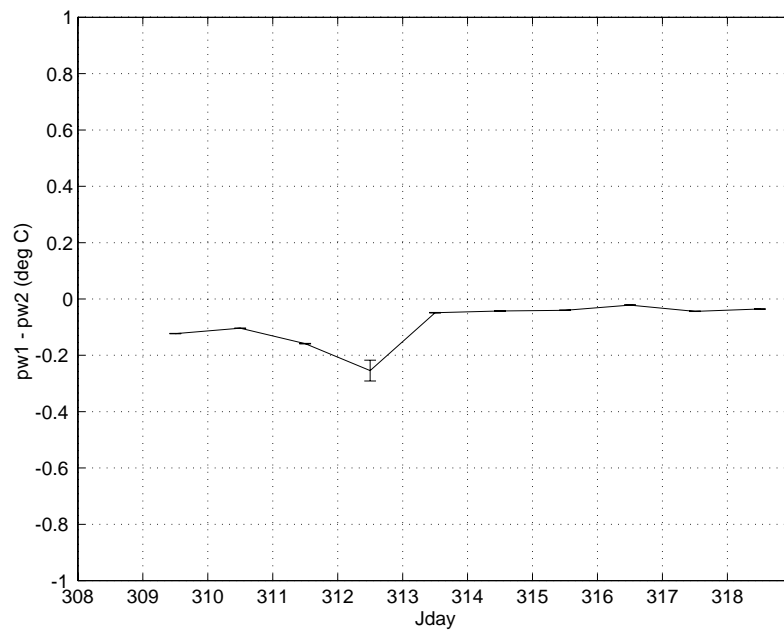


Figure 12. The daily mean differences in the wet bulb air temperatures measured by psychrometers pwp1 (IO2002) and pws2 (HS1020 before day 310, IO2003 after day 312). The error bars indicate the standard deviation of the mean.

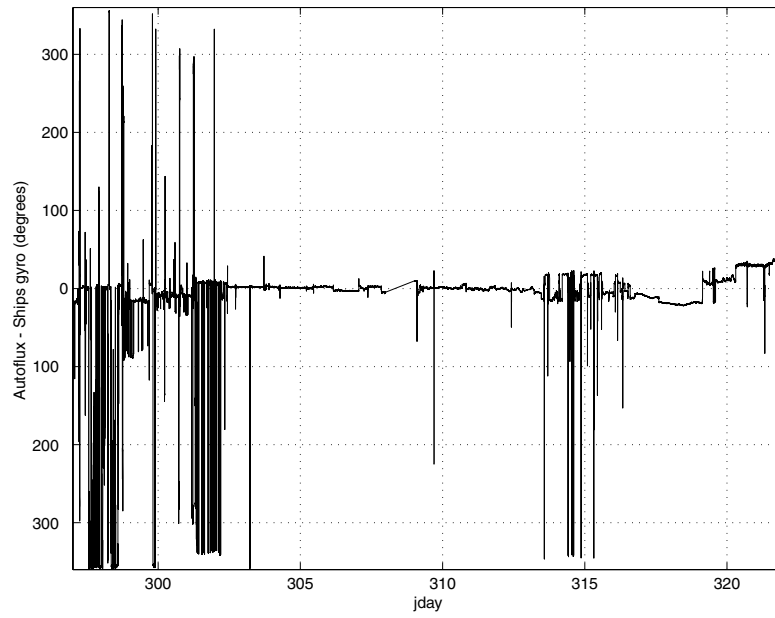


Figure 13. The 1 minute averages of the difference between the ships heading measured by the AutoFlux KVH Gyrotrac Fluxgate compass and the ships gyro.

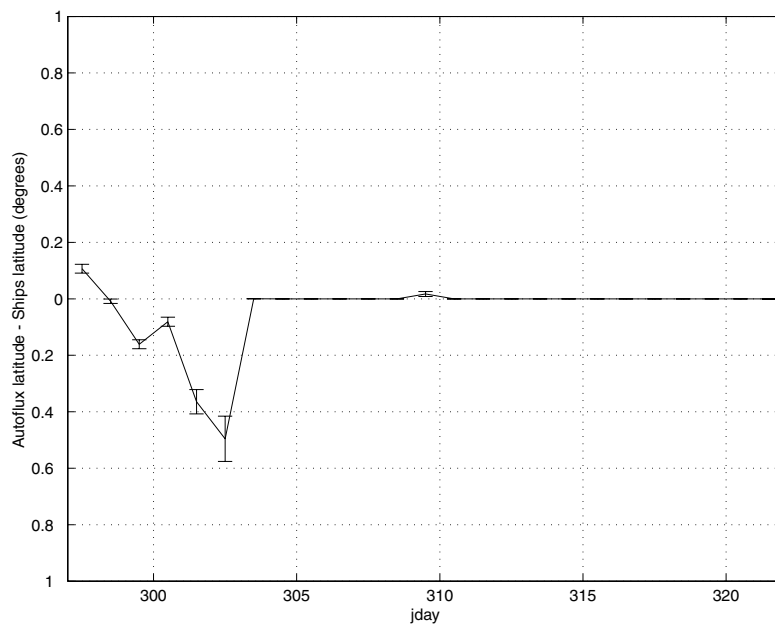


Figure 14. The daily averages of the differences between the ships latitude measured by the AutoFlux system and the ships navigation system.

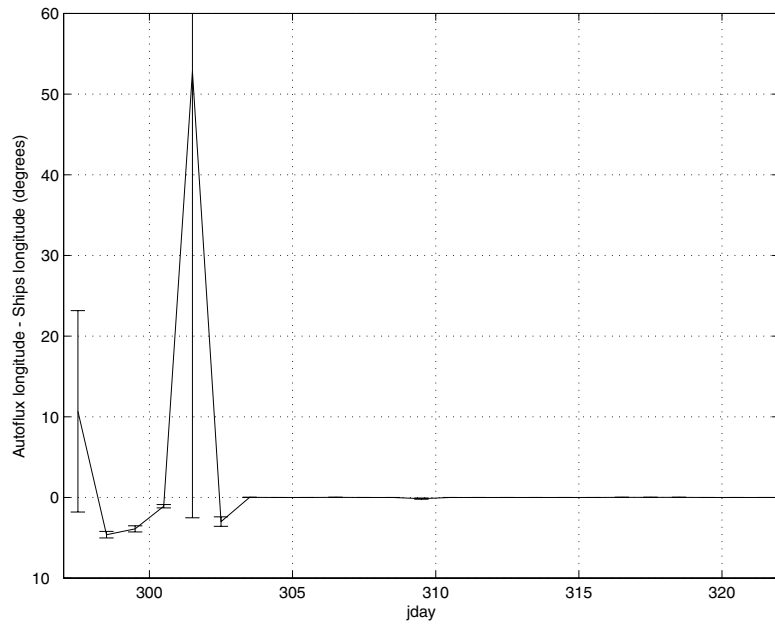


Figure 15. The daily averages of the differences between the ships longitude measured by the AutoFlux system and the ships navigation system.

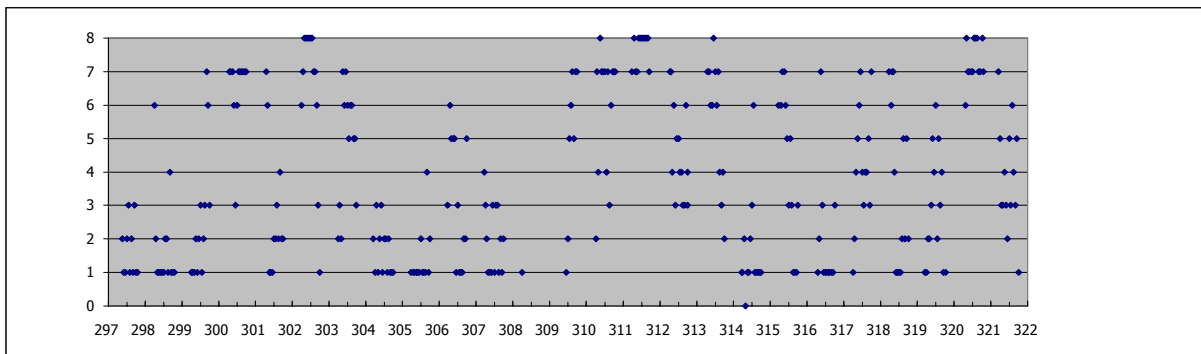


Figure 16. Time series of the total cloud amount recorded at each observing hour.

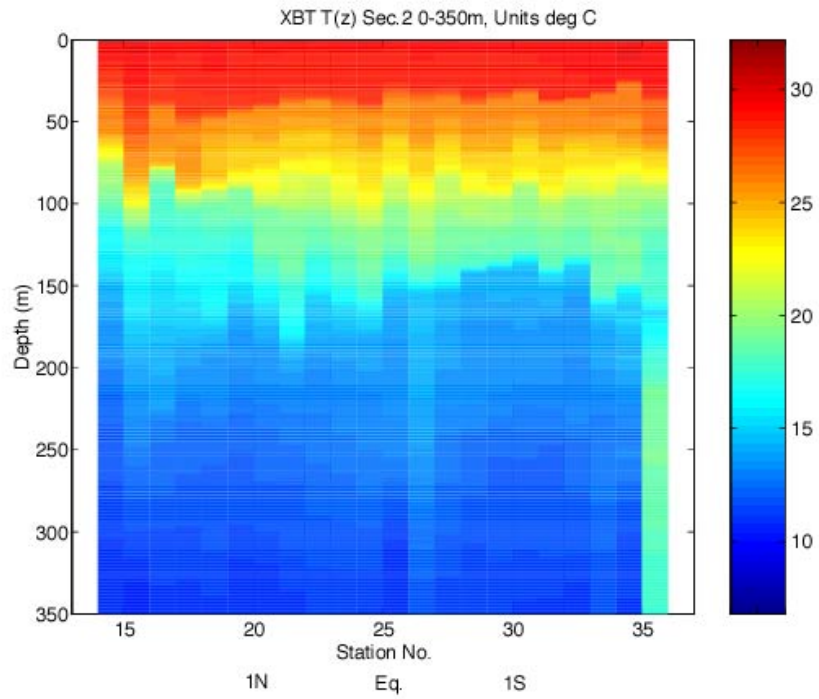


Figure 17. Variation of Temperature with Depth Along the N-S Cross-Equatorial Section 2.

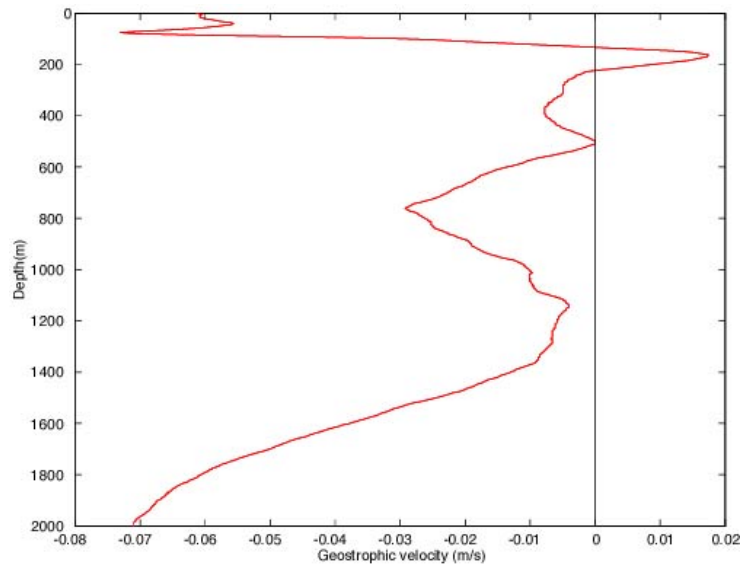


Figure 18. Variation in Zonal Geostrophic Velocity with Depth at 1.5N, 58E

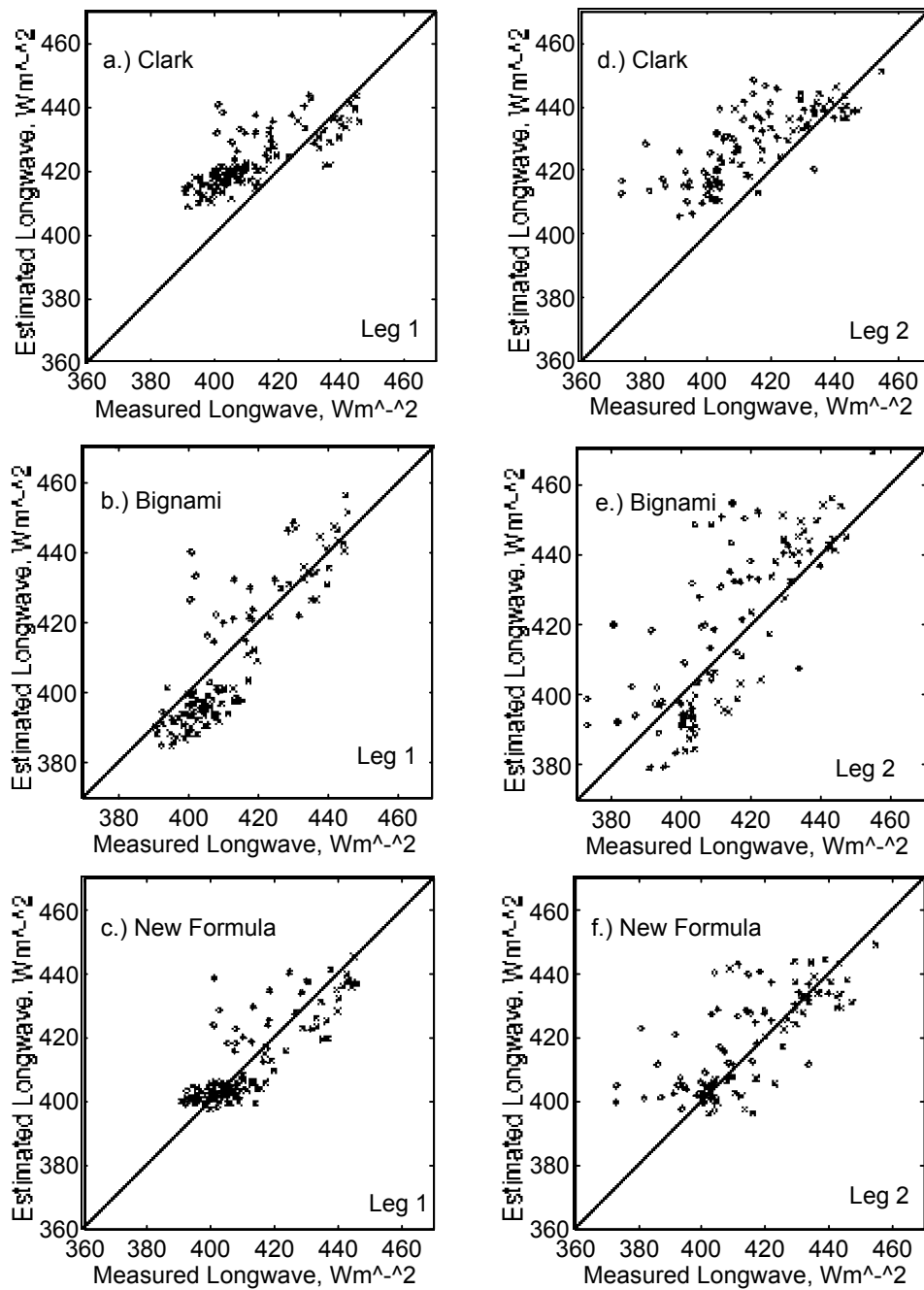


Figure 19. Estimated versus measured atmospheric longwave for CD135 Legs 1 and 2. Symbols: x, predominantly low level cloud; +, medium level ; open circle, high level

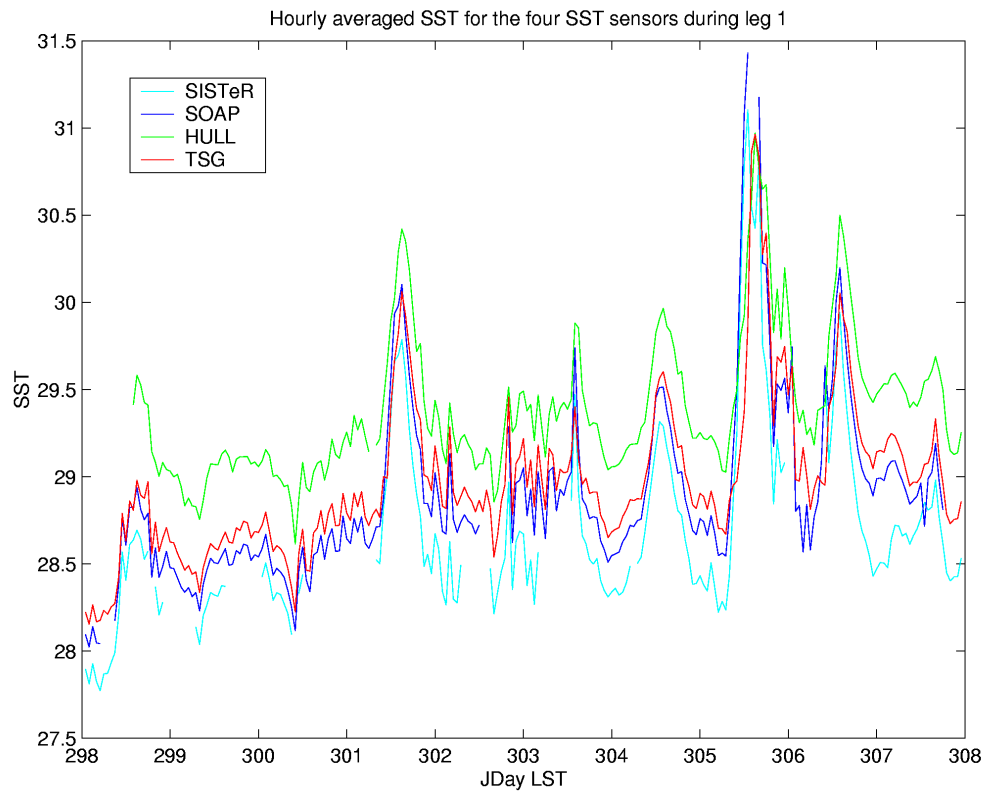


Figure 20. Hourly averaged SST for the four SST sensors during leg 1

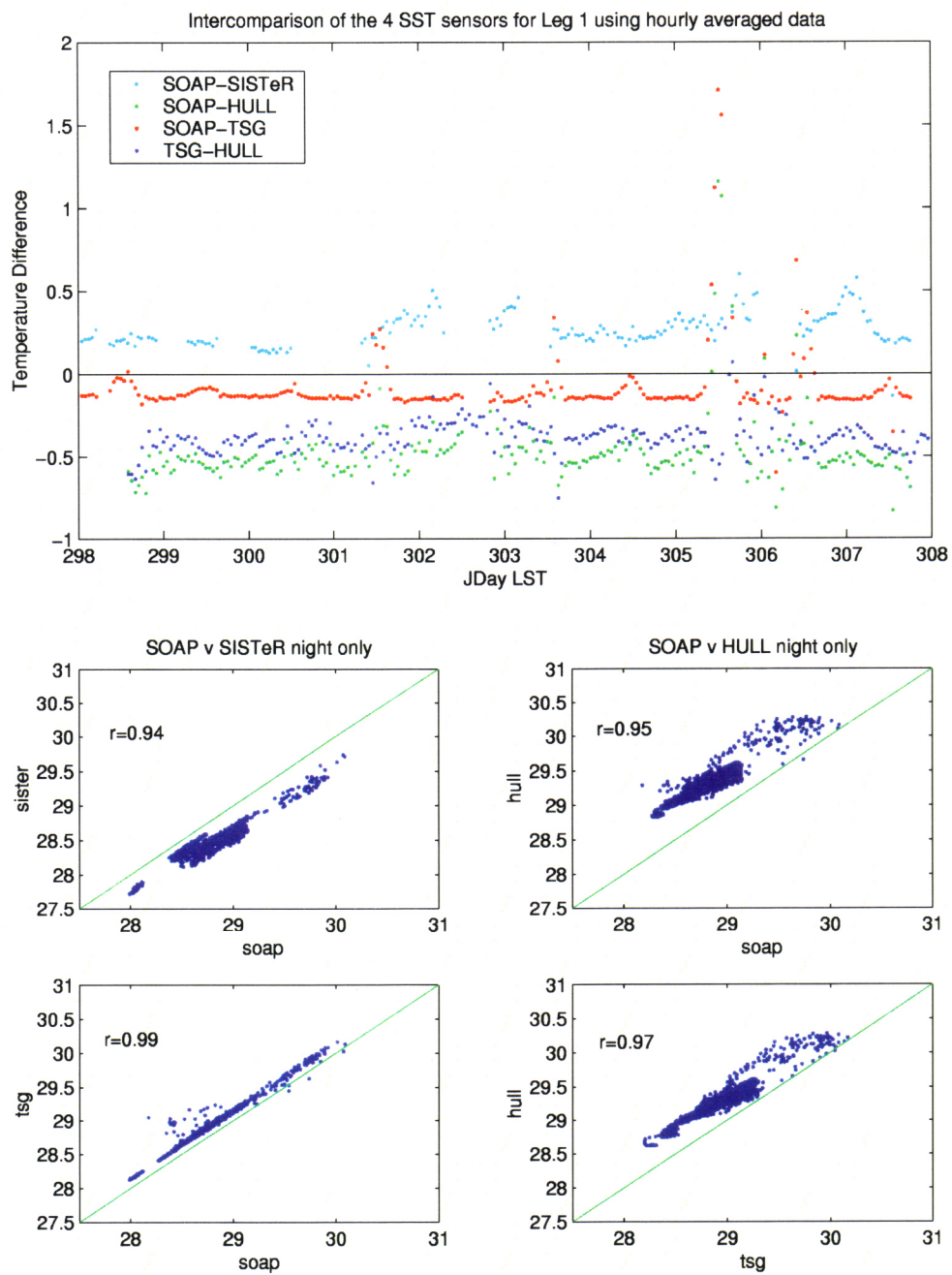


Figure 21. Intercomparison of the 4 SST sensors for Leg 1 using hourly averaged data

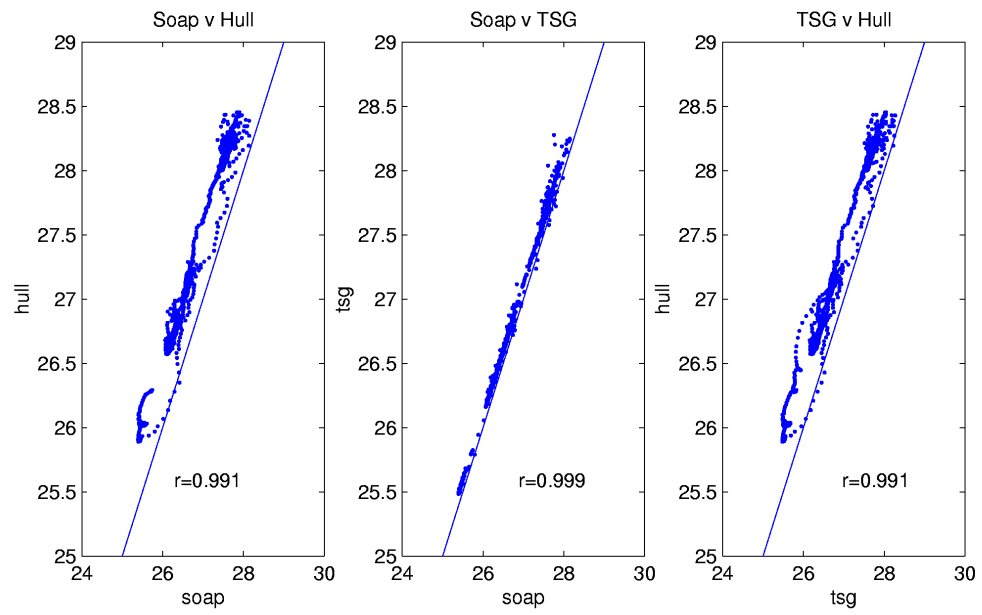
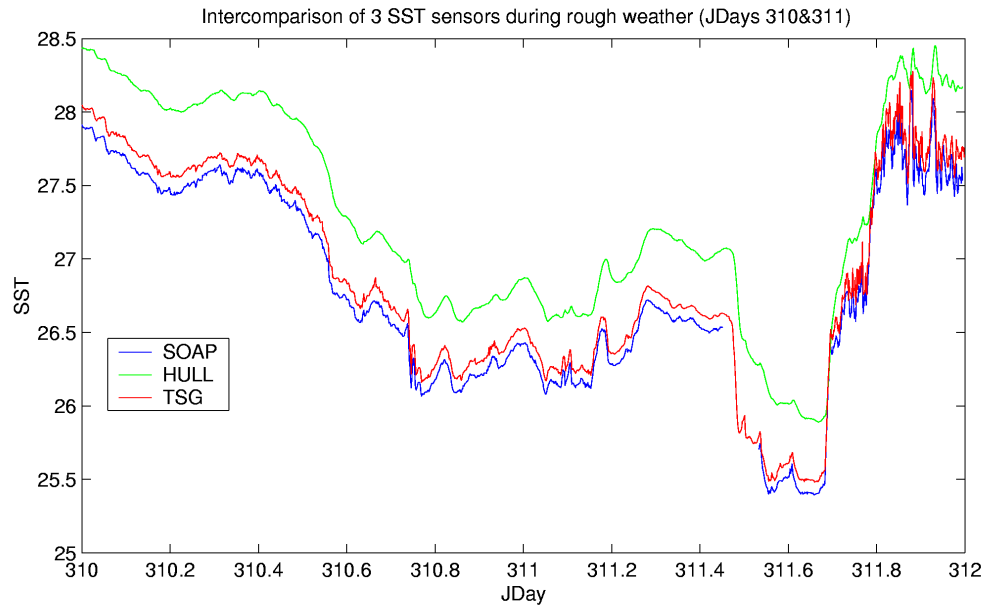


Figure 22. Intercomparison of 3 SST sensors during rough weather (Jdays 310 & 311)

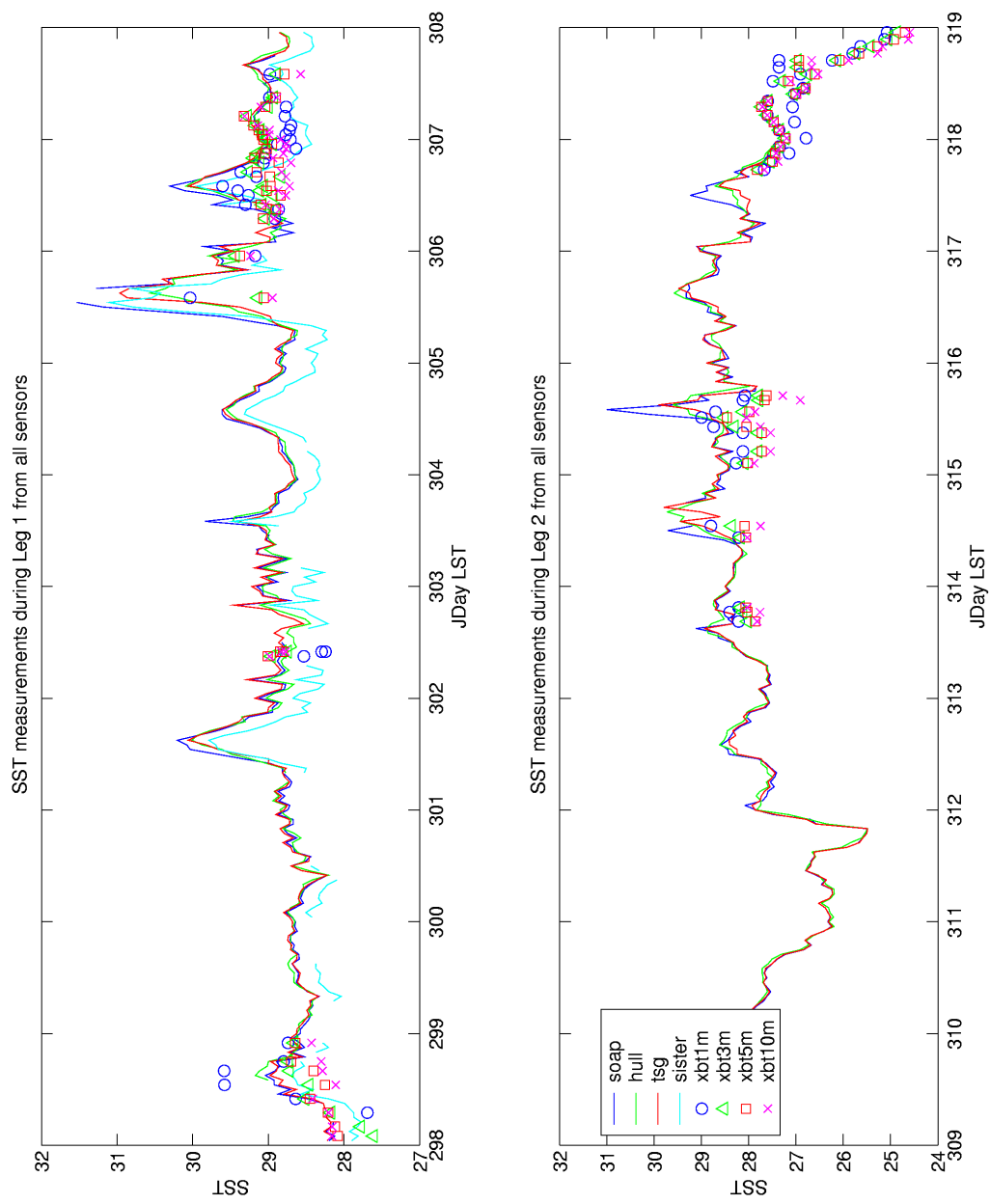


Figure 23. SST measurements during Leg 1 from all sensors

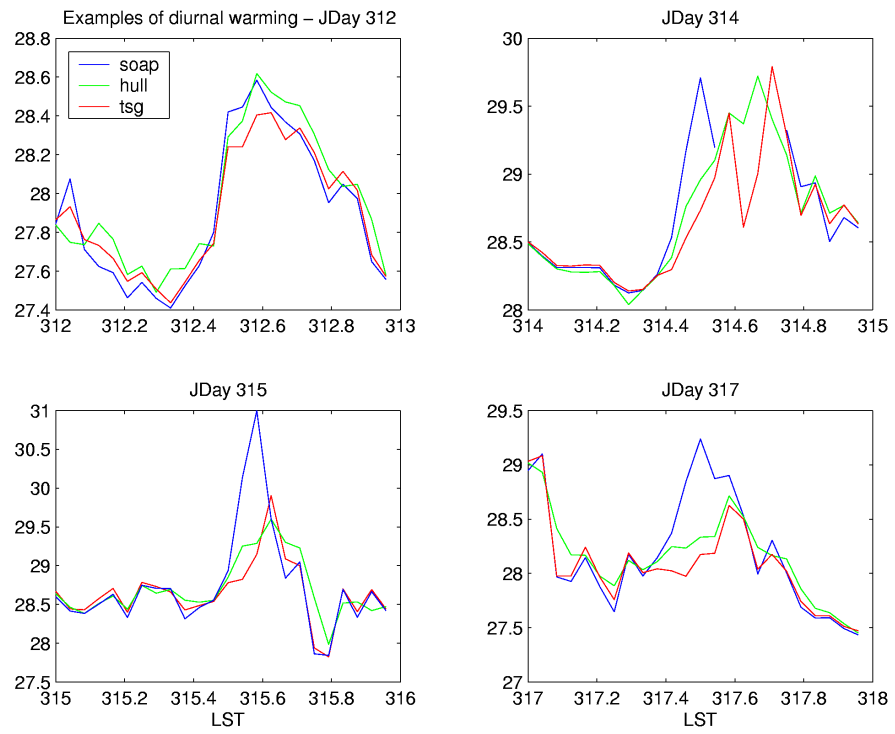


Figure 24. Examples of diurnal warming

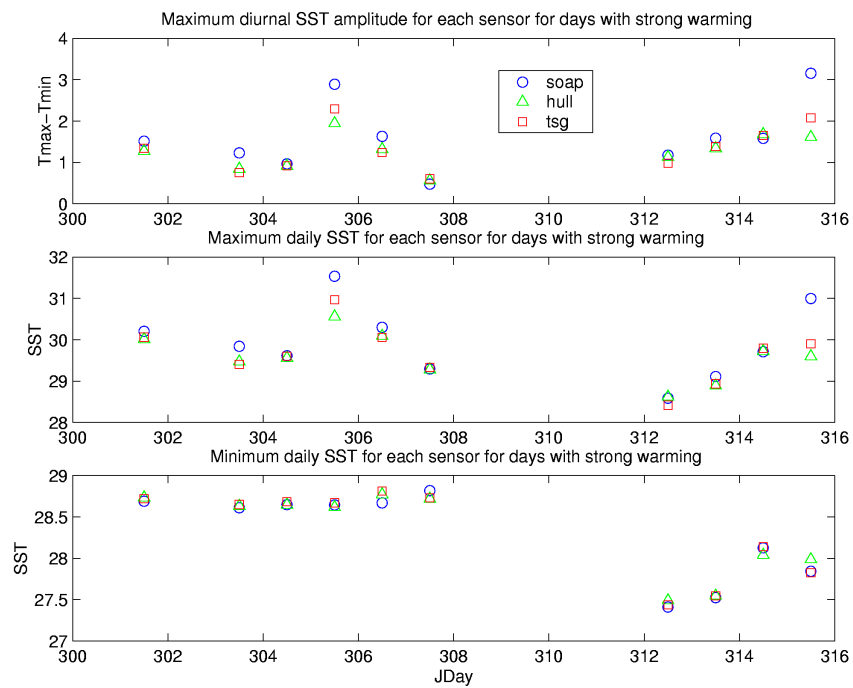


Figure 25. Maximum diurnal SST amplitude for each sensor for days with strong warming

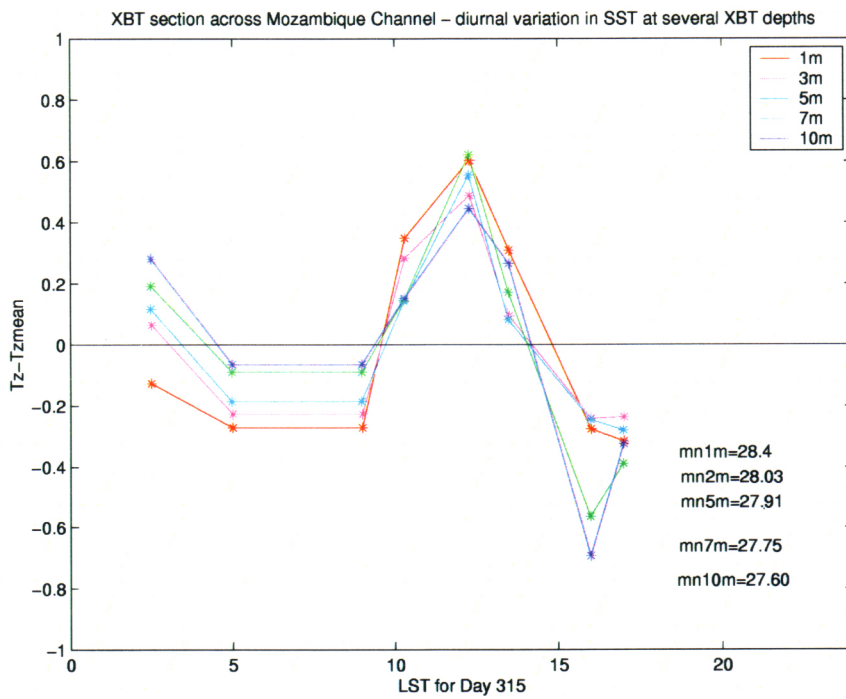


Figure 26. XBT section across Mozambique Channel – diurnal variation in SST at several XBT depths

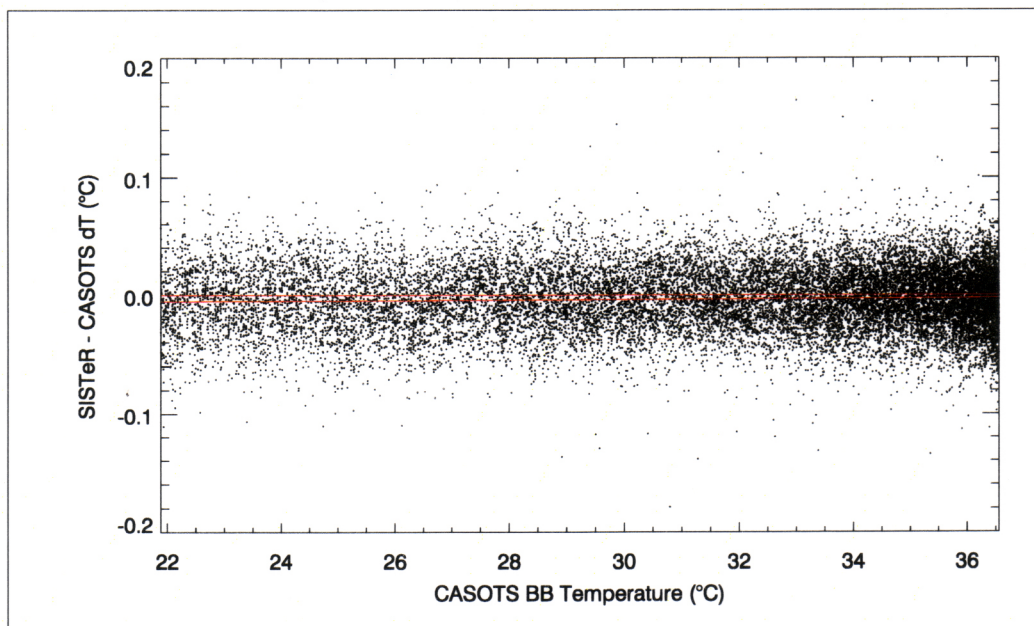


Figure 27. SISTeR calibration, 22nd October 2001, showing the deviation of the radiometric brightness temperature recorded by SISTeR from the CASOTS black body water bath temperature, as a function of the water bath temperature. Zero deviation and best fit straight lines are overlaid on the data points.

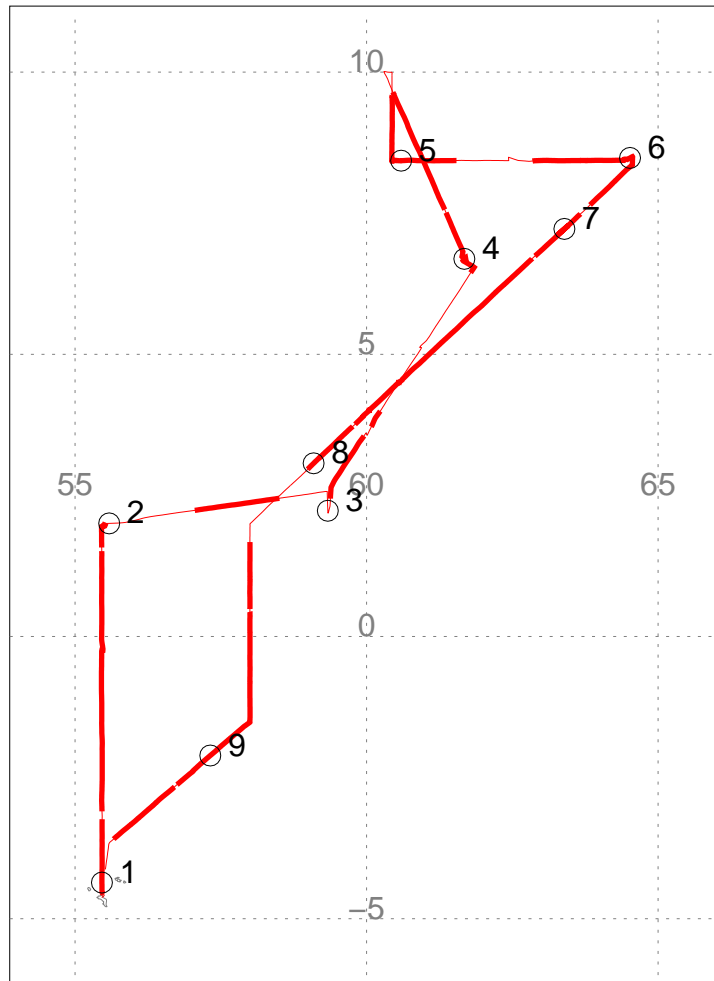


Figure 28. The first leg of CD135, starting and finishing at Mahe, Seychelles, showing the availability of SISTeR data and the positions of the nine ATSR-2 overpasses.

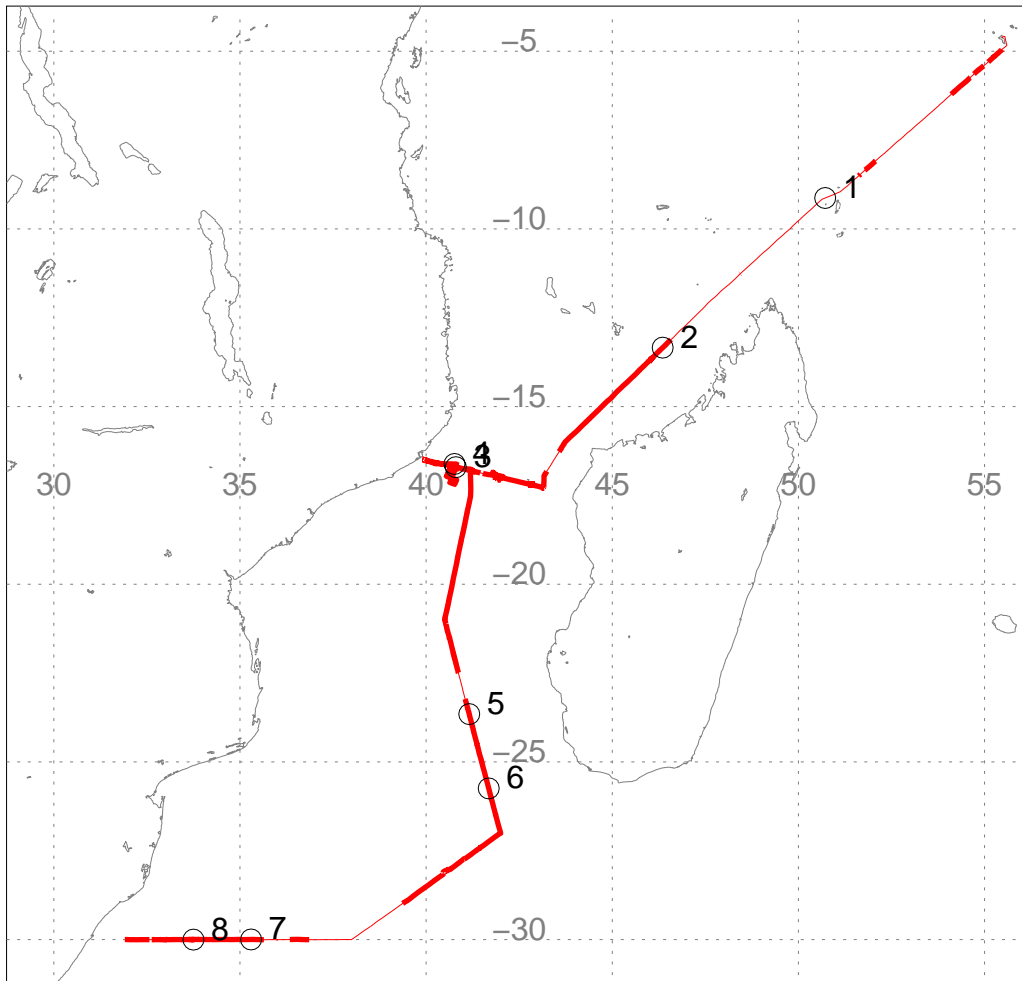


Figure 29. The second leg of CD135, starting at Mahe, Seychelles and ending in Durban, South Africa, showing the availability of SISTeR data and the positions of the nine ATSR-2 overpasses.

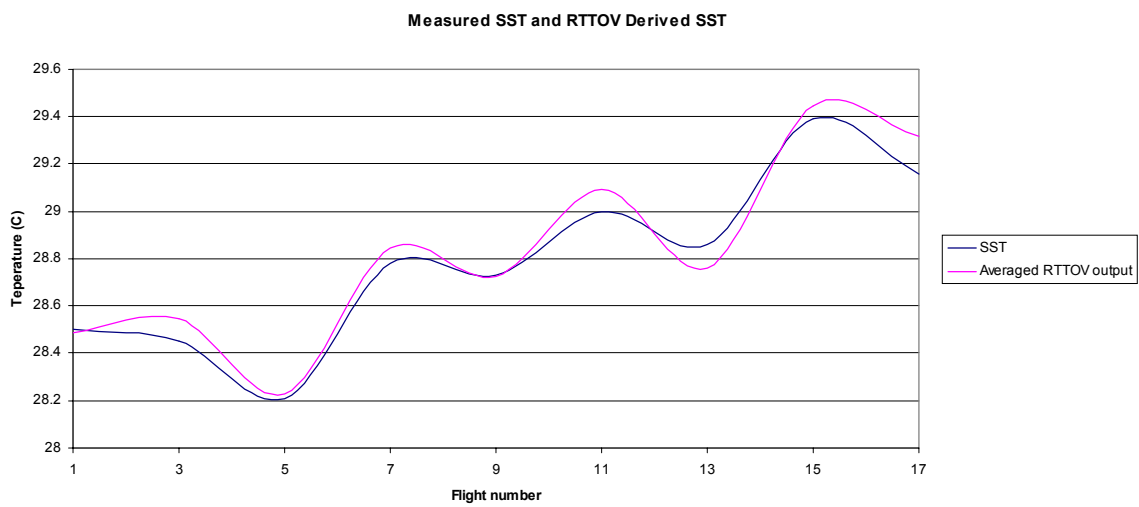


Figure 30. Measured SST and RTTOV Derived SST.

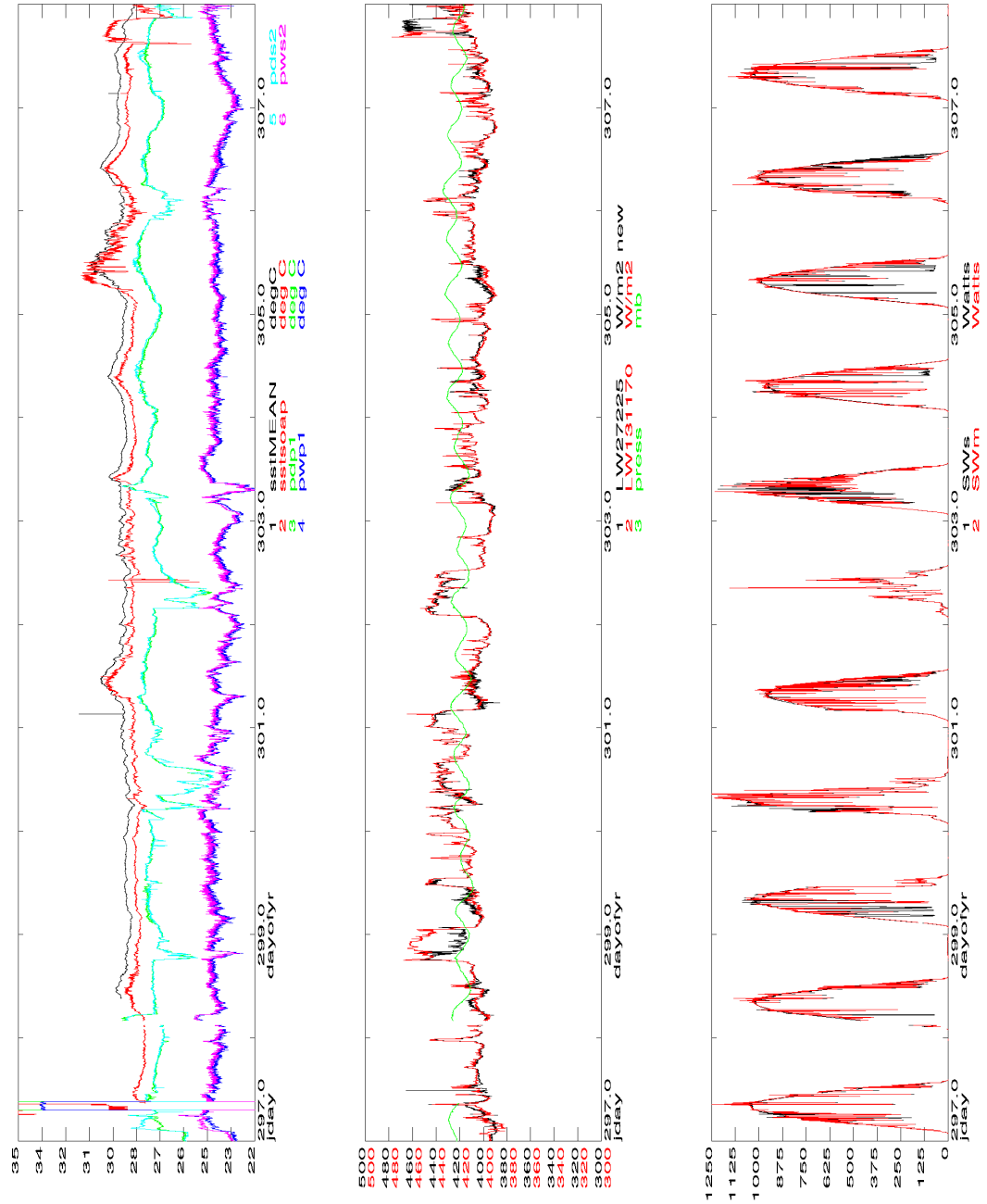


Figure 31. Time series of 15 minute averages of the mean meteorological variables during Leg 1

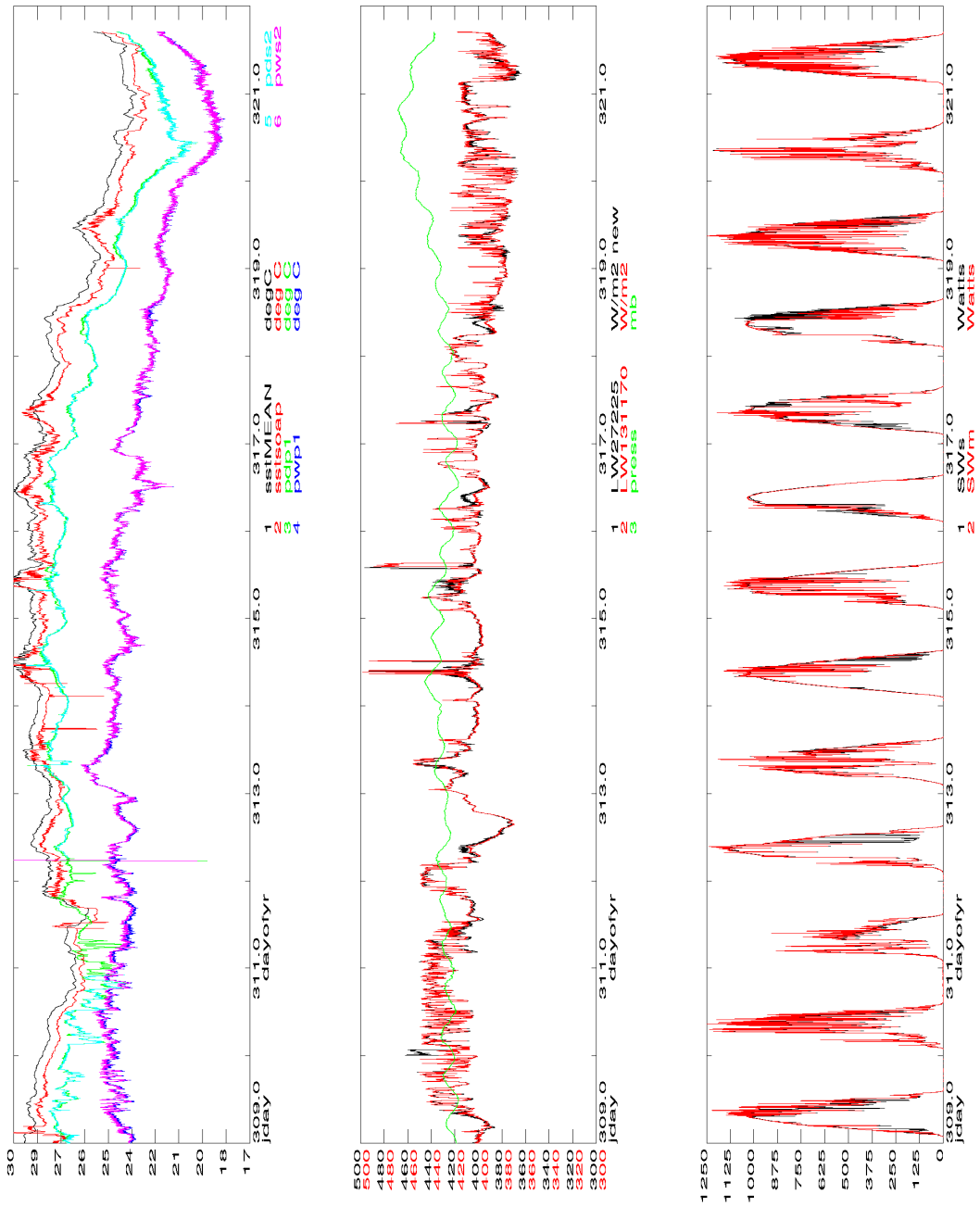


Figure 32. Time series of 15 minute averages of the mean meteorological variables during Leg 2

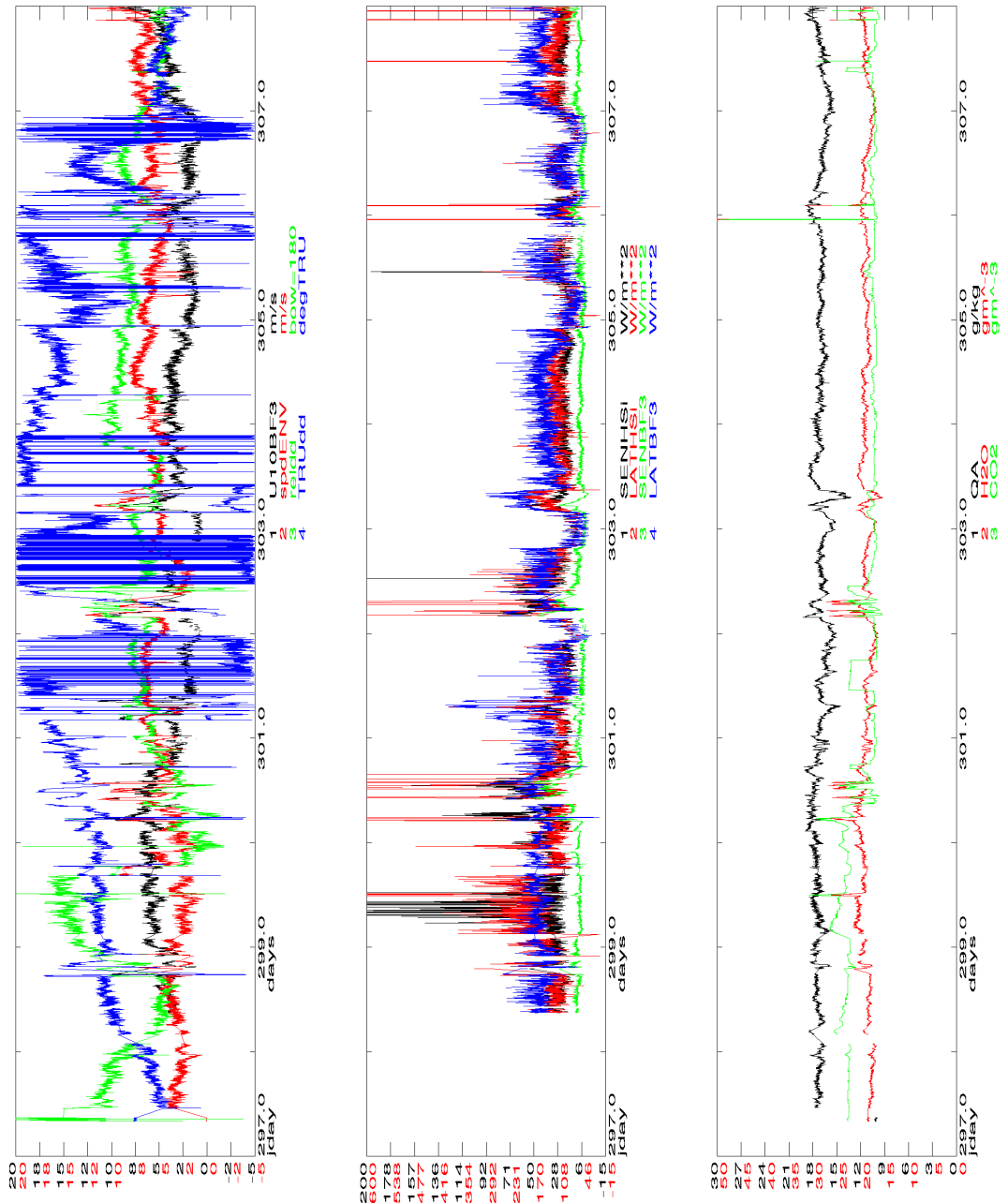


Figure 33. Time series of the calculated surface fluxes for Leg 1

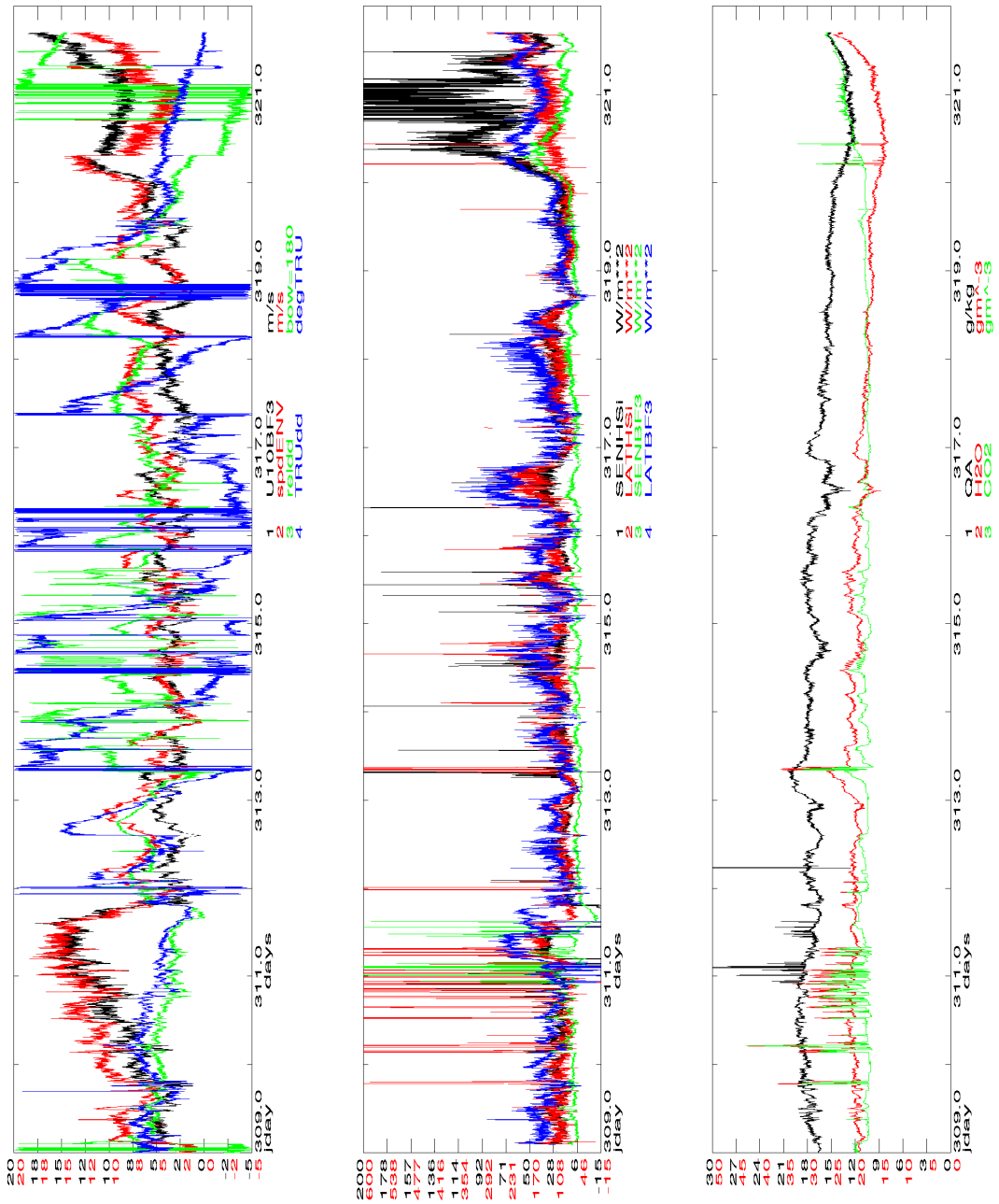


Figure 34. Time series of the calculated surface fluxes for Leg2

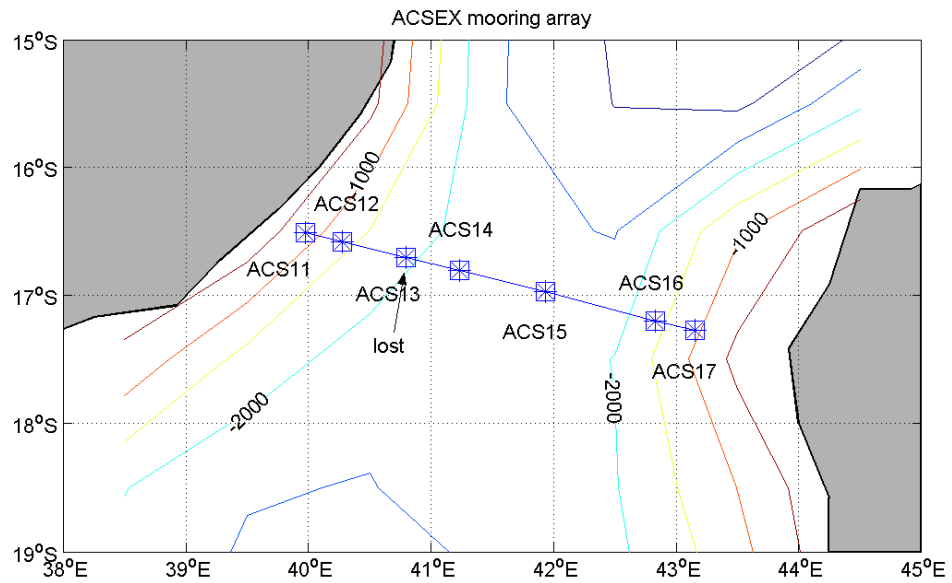


Figure 35. Location of the ACSEX moorings in the Mozambique Channel

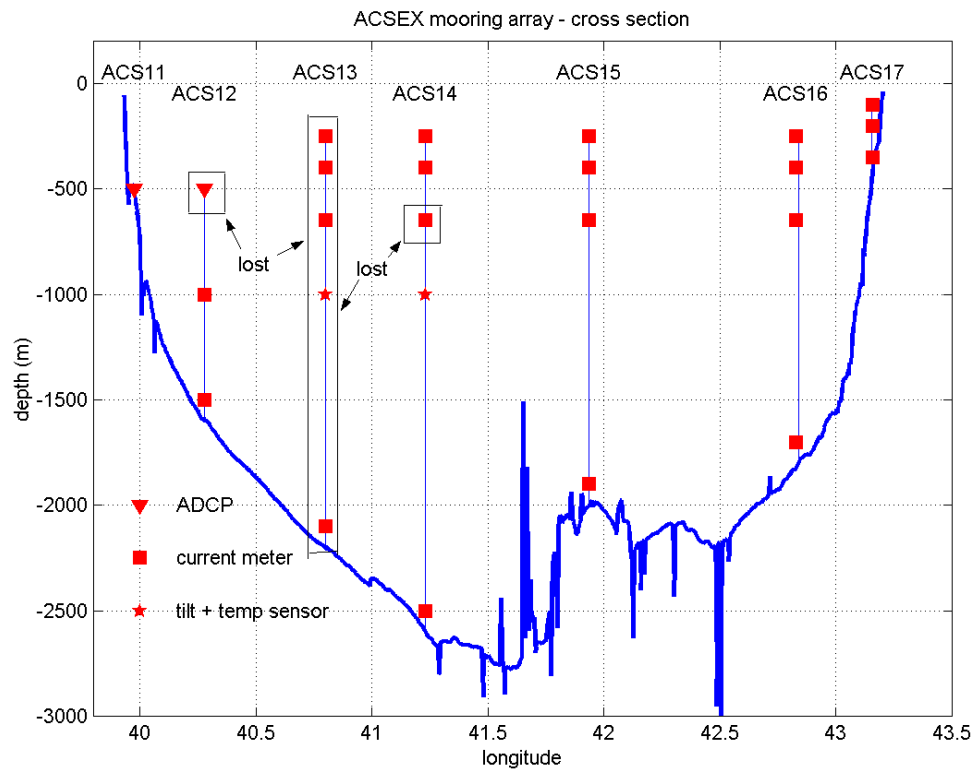


Figure 36. Cross section of the mooring array including the type and position of the instruments

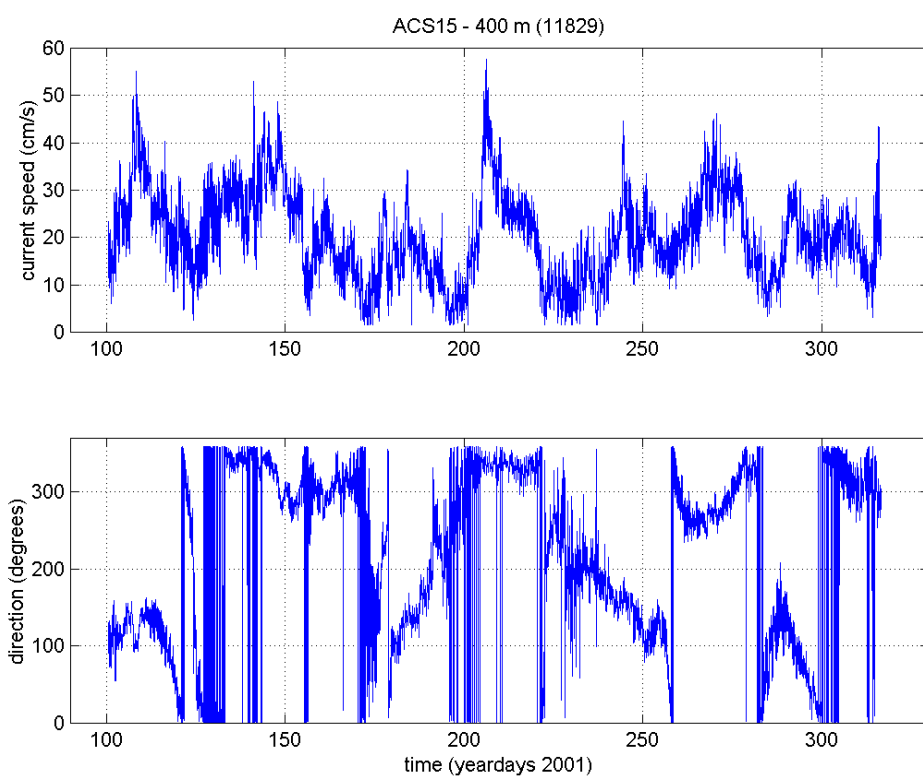


Figure 37. Current speed and direction of a current meter (400 m from surface) in mooring ACS15

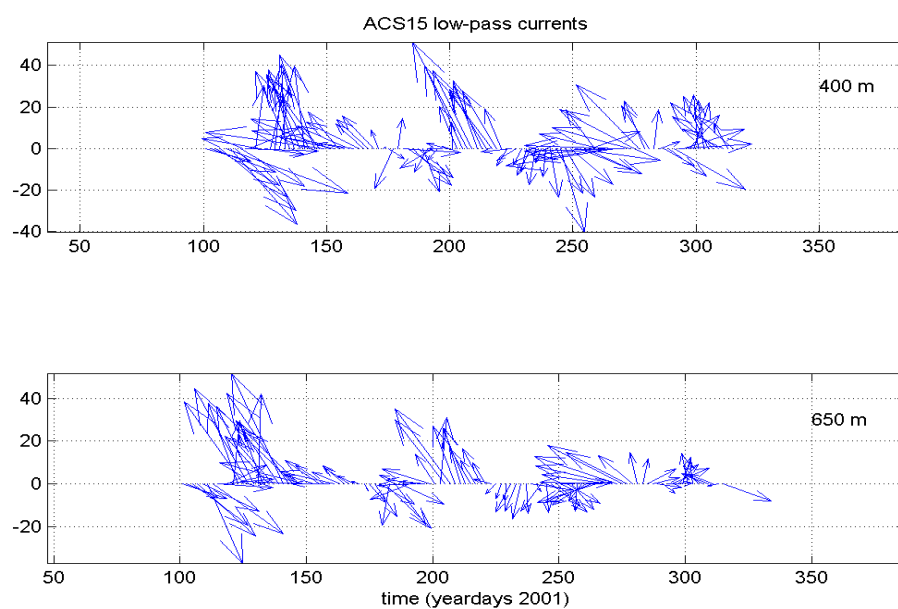


Figure 38. Low pass filtered currents from 2 current meters from mooring ACS15. Note the slight difference in horizontal scale

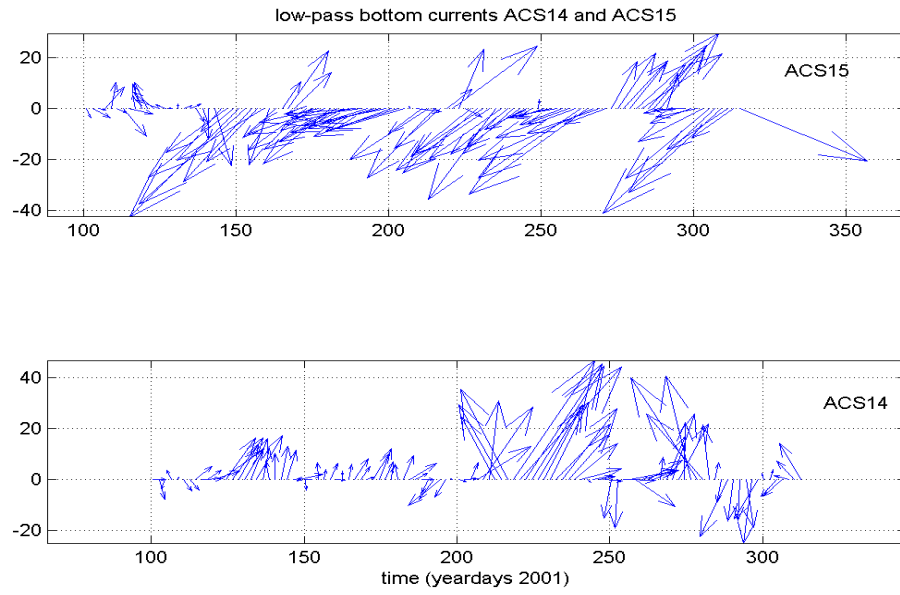


Figure 39. Low pass filtered currents from current meters at 100 m above the bottom at mooring ACS15 (top) and ACS14 (bottom). Note the difference in horizontal scale.